Substituted nickel pyrazole and palladium pyrazolyl complexes as catalyst precursors for ethylene polymerization

By

Simphiwe Maurice Nelana

A thesis submitted in partial fulfilment for the degree of Master of Science in the Department of Chemistry at the University of the Western Cape.

Supervisor: Prof. J. Darkwa (UWC)
Co-supervisor: Prof. S.F. Mapolie (UWC)
Date: May 2003

Declaration

I declare that **Substituted pyrazole nickel and pyrazolyl palladium complexes as catalyst precursors for ethylene polymerization** is my own work, that it has not been submitted before for any degree or examination in any other university and that all the sources I have used or quoted have been indicated and acknowledged by complete references.

SIMPHIWE MAURICE NELANA DATE

SM Nelana ..... 22-05-2003 .....

ACKNOWLEDGEMENTS

First of all I would like to thank God for protecting me all these years. Secondly I am grateful to my supervisor Prof. J. Darkwa for the support and encouragement. My since gratitude goes out to my co-supervisor Prof. S. F. Mapolie for guidance and for performing the high temperature NMR spectroscopy of the polymers. I would also like to thank my colleagues Mr. R. M. Moutloali, Ms. M. S. Mohlala, Mr. T. V. Segapelo and Mr. W. P. Swiggelaar. To the entire staff and postgraduate students of the Department of Chemistry at the University of the Western Cape thank you for everything.

Financial support from NRF and ESKOM is gratefully acknowledged. Thanks to Dr I.A. Guzei (University of Winsconsin, Madison, USA) for all the X-ray crystallography analyses. Thanks to Dr Ddamba (University of Botswana) and Mr W. Mhlongo (University of Cape Town) for thermal analyses. I would like to thank Mr S. de Goude (SASOL Technologies) and Dr V. Grumel (Institute for Polymer Science, University of Stellenbosch) for high temperature GPC analyses. I would like to thank my family especially my dad Mr. Buyekile Geza for believing in me. To my close friends Mr M.M. Ganto and Mr T. Ngenelwa thank you very much for encouraging me.

ABSTRACT

This study concerns the synthesis of pyrazole and substituted pyrazole nickel complexes of the type [(3,5-R,R'pz)$_2$NiBr$_2$ (pz = pyrazole; R = R' = CH_3 **(1)**, ^{t}Bu **(4)**] and of the type [(3,5-R,R'pz)$_4$NiBr$_2$ R = H, R' = CH_3, **(2)**; R = R' =H **(3)**]. These complexes were synthesized by reacting (DME)NiBr$_2$ and the appropriate pyrazole or substituted pyrazole in dichloromethane. The products were obtained in moderate to good yields. All the complexes isolated were characterized by a combination of IR spectroscopy, ^{1}H NMR spectroscopy and elemental analysis. Complexes **1** and **2** were further characterized by single crystal X-ray crystallography. Complex **1** was found to have a tetrahedral geometry and complex **2** has an octahedral geometry. In addition to the pyrazole nickel complexes, new pyrazolyl ligands with alkane-α,ω-dione linkers [RpzC(O)(CH$_2$)$_n$C(O)pzR); R = CH_3, n = 0 **(A1)**, n =2 **(A2)**, n =3 **(A3)** and R = ^{t}Bu, n = 3 **(A4)**] were synthesized. These new ligands were characterized by IR spectroscopy, ^{1}H NMR, ^{13}C NMR spectroscopy and elemental analysis. They were further reacted with $(CH_3CN)_2PdCl_2$ in attempts to obtain α,ω-bis(3,5-R$_2$pyrazolyl)alkane-α,ω-dione palladium chloride complexes. These ligands tend to undergo hydrolysis when they are reacted with $(CH_3CN)_2PdCl_2$ as confirmed by ^{1}H NMR spectral analysis. One complex, 1,5-bis(3,5-Me$_2$pz)pentane-1,5-dione palladium chloride was successfully prepared under very dry solvent conditions. The 1,5-bis(3,5-Me$_2$pz)pentane-1,5-dione palladium chloride complex was characterized by ^{1}H NMR spectroscopy.

The pyrazole nickel complexes **1** and **3** were used as catalysts for ethylene polymerization after activation with methylaluminoxane (MAO) to give high-density polyethylene (HDPE). Complex **3** was found to have a higher activity than complex **1**, since the metal centre is more accessible in **3** than **1**. In these polymerization reactions temperature, pressure and MAO concentration were varied. Activities ranging from 40 kg PE/mol Ni h to 3000 kg PE/mol Ni h were obtained with these catalysts depending on the conditions used. Polymers obtained were characterized by high temperature ^{1}H and ^{13}C NMR spectroscopy, high temperature gel permeation chromatography (GPC) and thermal analysis. Molecular weights between 0.84×10^{6} – 3.86×10^{6} g/mol and melting point range of 130 – 137 °C were observed for these polymers. All this data suggests that the polyethylene produced in this study is linear. Molecular weight of the polymers produced tends to decrease with increasing temperature and increasing pressure. This is due to the high rate of β-hydride elimination over chain propagation.

Another ethylene polymerization catalyst used in this study was 1,3,5-benzenetricarbonylpyrazolyl palladium complex **(4)**. Activities ranging from 440 kg PE/mol Pd h to 2497 kg PE/mol Pd h were observed for this catalyst. The effect of MAO concentration and temperature on the catalyst activity was investigated. At co-catalyst to catalyst ratio (Al:Pd) above 3000:1 catalyst activity decreases and at high temperatures (50-70 °C) low molecular polyethylene is produced. The polymers produced using **4** have melting points between 136 and 138 °C, which is indicative of linear polyethylene.

List of abbreviations

DFT	Density Functional Theory
DSC	Differential Scanning Calorimetry
Et_3N	Triethylamine
DME	1,2-dimethoxyethane
GPC	Gel Permeation Chromatography
HDPE	High Density Polyethylene
IR	Infrared
LDPE	Low Density Polyethylene
LLDPE	Linear Low Density Polyethylene
M	Transition metal
MAO	Methylaluminoxane
MeCN	Acetonitrile
M_n	Number-average molecular weight
M_w	Weight-average molecular weight
NMR	Nuclear magnetic resonance
PD	Polydispersity
PE	Polyethylene
R	Alkyl
TON	Turnover numbers
T_m	Melting point
X	Halogen

TABLE OF CONTENTS

List of Schemes

List of Figures

List of Tables

CHAPTER 1

Overview of olefin polymerization catalysis and coordination chemistry of pyrazole based ligands

1.1 General background

Catalysis has made a huge contribution to the chemical, petrochemical and oil refining industry. Catalysis is divided into three subdivisions namely: heterogeneous, homogeneous and bio-catalysis. Homogeneous catalysis is used in a number of industrial processes, such as hydrogenation, oxidation, oligomerization, polymerization and hydrocyanation and many more. For most industrial reactions, highly effective catalysts are required to accelerate these processes. For a catalyst to be effective, it has to combine high efficiency, high selectivity and total turnover with high durability.

Polymerization is a process whereby a monomer such as ethylene or propylene is converted to a large molecule called a polymer or a macromolecule. Polymer molecules consist of a restricted number of chemically different organic monomer residues: one for homopolymers, two in copolymers and three in terpolymers. The term polydispersity is used as a measure of polymer molecular weight distribution. In most cases polydispersity (PD) is measured as the weight average-molecular weight (M_w) divided by the number average molecular weight (M_n) (i.e. PD = M_w/M_n). Polydispersity imparts certain properties to the polymer like toughness, rigidity and

strength. The bulk of polyolefin (i.e. a product from the polymerization of olefins) production involves catalysis, either homogeneous or heterogeneous. Polyolefins are interesting polymers because they have diverse applications and are non toxic. For years, polyethylene (PE) has been used in food packaging, coatings, countless molded toys, and other household items, and it is now finding its way into the market to replace common materials such as glass, metal, paper and concrete.[1] Compared to other conventional materials, polyolefins require low energy in their production. Different transition metals are involved as catalysts in olefin polymerization. It is now possible to tailor the coordination environment of a metal centre in a catalyst to control molecular weight, molecular weight distribution, co-monomer incorporation, end groups and absolute stereochemistry of a polymer. Catalysts development has thus been and continues to be important to the polyolefin industry. This thesis combines the synthesis and testing of catalysts for polyethylene production. The following sections will focus on the structural details and catalysts development in this area of research.

1.1.1 Polyethylene structural details

Polyethylenes are olefinic polymers manufactured in the largest tonnage of all the thermoplastic materials.[1] They are produced by addition polymerization of ethylene to give the basic structure $-(CH_2\text{-}CH_2)_n-$. Polyethylene is classified according to density and the density of the polymer dictates its application. The first type of polyethylene is called low-density polyethylene (LDPE), which is a polymer with a density of 0.915-0.935 g/cm^3. It is a highly branched material. This polymer is

prepared by a free radical polymerization process at high temperatures (300-400 °C) and extremely high pressures (3000 atm). The second type is high-density polyethylene (HDPE), which has a density between 0.941-0.967 g/cm^3. This form of polyethylene contains moderate branches and is prepared using both conventional Ziegler-Natta and metallocene catalysts. Another form of HDPE, is called ultrahigh molecular weight polyethylene (UHMWPE), has a molecular weight (M_w) in the range 3-6 million, while the normal HDPE has molecular weight less than 3 million. The third type of polyethylene is linear low-density polyethylene (LLDPE), with density of 0.910-0.925 g/cm^3. Here the word 'linear' refers to the absence of long branches in the polymer chain. LLDPE is formed from the co-polymerization of ethylene with other olefins, such as 1-butylene and 1-hexene. The different types of polyethylene are shown schematically in Figure 1.1.

To identify the above types of polyethylene, certain properties are investigated. One of these properties is melting point, which is measured using differential scanning calorimetry (DSC). Each type of polyethylene has a characteristic melting point range as shown in Table 1.1. Another analytical technique that is used to characterize polyethylene is NMR spectroscopy. NMR spectroscopy can be used to distinguish between branched and linear polymers. Typical ^{13}C NMR spectra for linear and branched polyethylene are shown in Figure 1.2 and Figure 1.3 respectively.

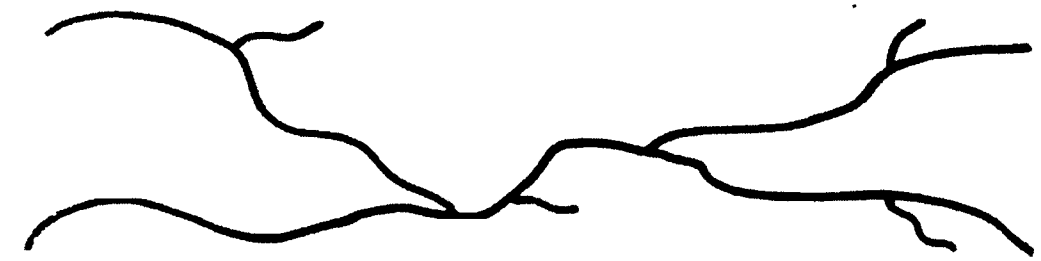

LDPE

HDPE

LLDPE

Figure 1.1: Schematic representation of the various types of polyethylene

Table 1.1: The melting point ranges characteristic of each type of polyethylene.

Type of polyethylene	Melting point range (°C)
LDPE	106-112
LLDPE	120-25
HDPE	130-133
UHMWPE	130-132

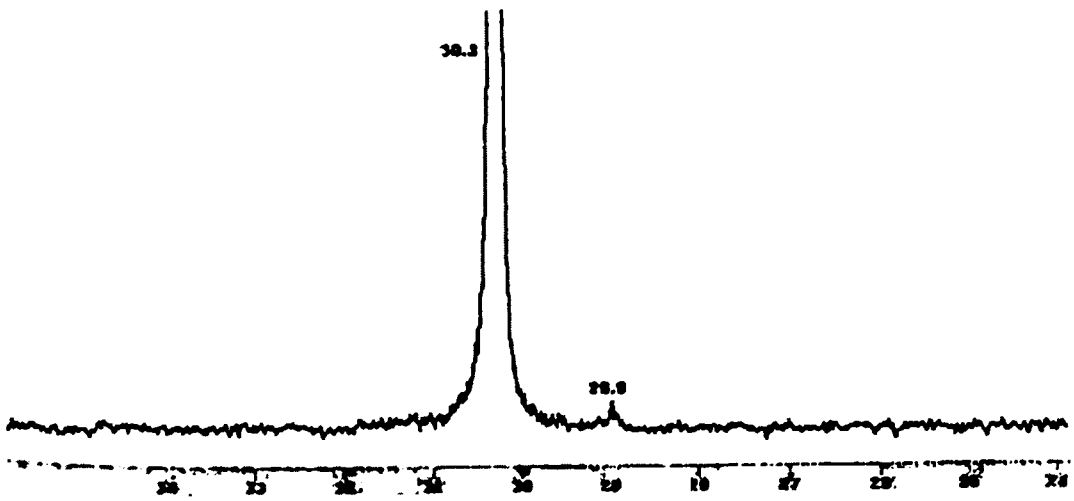

Figure 1.2: ^{13}C NMR spectrum of a linear polyethylene

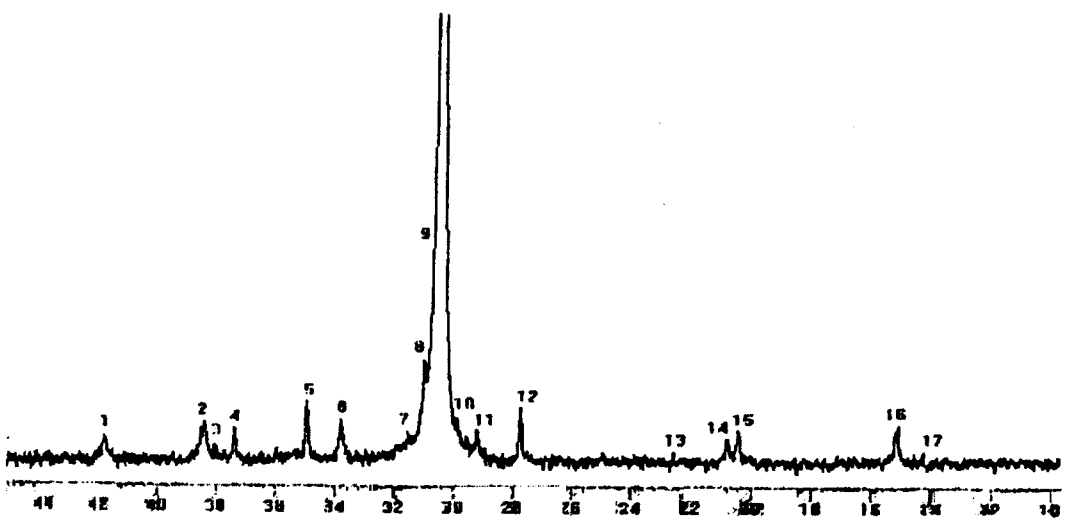

Figure 1.3: ^{13}C NMR spectrum of branched polyethylene

1.2 Early work on olefin polymerization catalysis

The discovery by Ziegler and Natta that transition metal complexes can catalyze polymerization of ethylene and other olefins is one of the great discoveries in the history of chemistry.[2] Prior to that free radical polymerization was the only process used for olefin polymerization reactions. The shortcoming of free radical polymerization is that harsh conditions that are needed for this process to take place, with pressures as high as 3000 atm and temperatures of 300 to 400 °C. Another shortcoming of free radical polymerization is that the process only gives low-density polyethylene. In 1955 Ziegler found that a $TiCl_4$–Et_3AlCl catalyst system could polymerize ethylene to high molecular weight polyethylene under mild conditions.[2] About the same time Natta independently showed that propylene can be stereo-selectively polymerized to stereo-regular polypropylene, using a catalyst system closely related to that of Ziegler.[3]

A few years after the findings by Ziegler and Natta, Hogan[4] at Philips Petroleum Co., reported that a mixture of oxides of chromium, supported on silica polymerizes ethylene to high-density polyethylene. The advantage of this catalyst over the Ziegler-Natta catalysts is that no co-catalyst is needed in the polymerization reaction. All the olefin polymerization catalysts described above are heterogeneous, they require a solid support for them to function effectively. The support system that makes $TiCl_4$-$AlEt_3$ catalysts highly active in olefin polymerization is $MgCl_2$. The catalyst is prepared by co-milling $TiCl_3$ and $TiCl_4$ with $MgCl_2$. Another widely used support for these catalysts is silica.[5] The mechanism by which olefins polymerize via

the Ziegler-Natta process was first proposed by Cossee.[5] After various modifications olefin polymerization is now generally accepted to proceed via what is known as the Cossee and Arlman mechanism (Scheme 1.1).[5] The mechanism involves chain growth by *cis*-insertion of the olefin into a Ti-C bond.

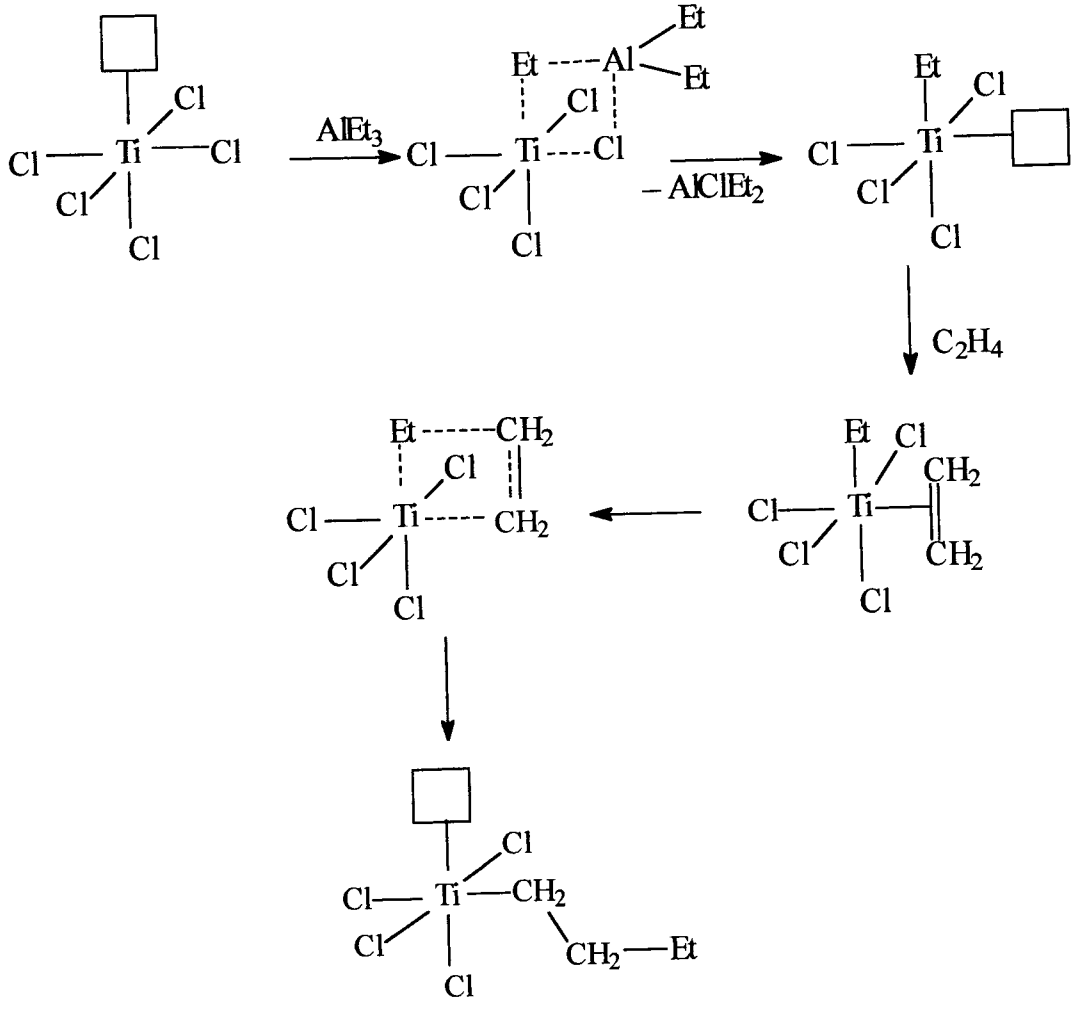

Scheme 1.1: Cossee-Arlman mechanism for olefin polymerization

1.3 Metallocenes as olefin polymerization catalysts

The active sites in heterogeneous catalyst systems are non-uniform. The non-uniformity of the active sites at times results in the formation of different products. It is thus difficult to have concrete evidence of the reaction mechanism in heterogeneous catalysis. It is believed that homogeneous catalyst systems can provide clues on the reaction mechanisms involved in catalytic processes in general and olefin polymerization in particular. In 1957 Breslow[7a] and Natta[7b] independently reported that homogeneous reaction mixtures of dicyclopentadienyltitanium dichloride (Cp_2TiCl_2) and diethylaluminium chloride (Et_2AlCl) polymerize ethylene with moderate activity, under conditions similar to those used for Ziegler-Natta catalysts.[2,3] These homogeneous catalyst systems could not polymerize propylene and other higher α-olefins. Mechanistic studies by Breslow[8] and Chien[9] led to a proposal that ethylene polymerization proceeds via olefin insertion into the Ti-C bond of the electron deficient species Cp_2TiRCl. The alkyl titanocene complex (Cp_2TiRCl) is formed by ligand exchange between titanium complex and aluminium compound. Coordination of the Lewis acid aluminium centre in Et_2AlCl to the chloride of the titanium complex polarizes the Ti-Cl bond to create an electron deficient Cp_2TiR species, which readily inserts ethylene. This mechanism is in line with the mechanism proposed by Cossee and Arlman.[5]

Overall metallocenes activated with alkylaluminium halides are unable to polymerize propylene and higher olefins, and that initially limited their utility in this field. The low activity of these metallocene-alkylaluminium halide based catalysts led to a new

search for more effective co-catalysts. Reichert and Meyer[10] reported that addition of water to the metallocene-alkyl aluminium system caused a surprising increase in the rate of ethylene polymerization by the catalyst system $Cp_2TiEtCl/AlEtCl_2$. Prior to this water was considered to be a poison for olefin polymerization catalysts. Subsequent studies by Long and Breslow showed that addition of water to the inactive system Cp_2TiCl_2/Me_2AlCl gives some activity.[11] They suggested that a dimeric aluminoxane with the structure ClMeAl-O-AlMe was formed, which was believed to be a stronger Lewis acid than Me_2AlCl. They also concluded that dimeric aluminoxane was a more efficient activator and was responsible for enhanced ethylene polymerization activity.

Sinn and Kaminsky also added water to the halogen free, polymerization inactive $Cp_2ZrMe_2/AlMe_3$ system and observed high activity for ethylene polymerization.[12] The combined effort of the above researchers led to the discovery of the highly effective activator, an oligomeric methylaluminoxane, (MAO).[12] For example metallocene catalysts **(A** and **B)** are now routinely activated with MAO and are capable of polymerizing propylene and other higher olefins, in contrast to aluminium halide activated systems.[13] Catalyst activities between 890 and 111900 kg of polyethylene per mol of metallocene per hour (kg/mol h) are achieved with these catalysts.[13] The discovery of MAO rejuvenated Ziegler-Natta catalysis and along with major advances achieved in controlling polymer stereochemistry and architecture, began what is called "single site" polymerization catalysis. These catalysts are called single site catalysts because they have a general formula L_nMR,

where L_n is an organic ligand part that remains bound and thus modifies the reactivity of the active metal center (M) during the entire chemical reaction and R is a growing polymer chain.

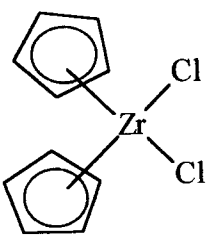

A

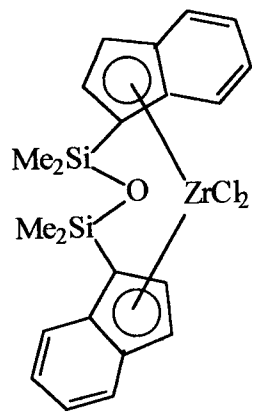

B

The polymers obtained from metallocene catalysts show different microstructures and properties compared to those produced by conventional Ziegler-Natta catalysts. Due to their efficiency, versatility and flexibility, metallocene/MAO catalysts have made possible the production of polyolefins, homopolymers and copolymers with narrow molecular weight distribution, raised degrees of density, low amount of extractables, high degree of tacticity and uniform co-monomer distribution.[14] One of the shortcomings of metallocene catalysts is their inability to polymerize polar olefins, because of the oxophilic nature of early transition metals used in metallocenes. To address this shortcoming, there has been a renewed focus on late

transition metal complexes as olefin polymerization catalysts, since these metals are less oxophilic.

1.3.1 Co-catalysts for ethylene polymerization by single site catalysts

The discovery of methylaluminoxane and the extent to which it is used as a co-catalyst has been described above. MAO as an activator is thought to (i) replace halides from a dihalide precursor complex with methyls, (ii) abstract a CH_3^- from a transition metal complex, forming a weakly coordinating counterion, and (iii) scavenge or scrub impurities. Even though the methylaluminoxane activated polymerization catalysts are promising future catalysts, they suffer from two shortcomings. Firstly, large amounts of MAO (Zr:Al , 1:3000) are required to obtain satisfactory catalytic activity. Secondly, the exact molecular composition and structure of MAO are not entirely clear, making it difficult to study its activation pathway. In metallocene olefin polymerization catalysis, MAO is the mostly used activator, but there are other co-catalysts based on perfluoroaryl boron compounds such as $B(C_6F_5)_3$ and $Ph_3C^+B(C_6F_5)_4^-$. The different types of olefin polymerization co-catalysts has recently been reviewed by Chen and Marks.[15] This review describes suitable co-catalysts for different catalysts from metallocene based to non-metallocene based catalysts. Hence it appears that the problem of larger amount of co-catalyst might be solved in the industrial process soon.

1.4 Late transition metals as olefin polymerization catalysts

1.4.1 Nickel complexes as olefin oligomerization and polymerization catalysts

One of the best known late transition metal catalyzed processes is the Shell High Olefin Process (SHOP) developed by Keim,[16,17] which uses nickel complexes as catalysts. This process involves the oligomerization of ethylene to linear α-olefins in the C_4-C_{20} range, which are converted to detergents, plasticizers, lubricants and a variety of fine chemicals. The nickel complex used in the SHOP process is a P-O anionic chelate complex that can be prepared *in situ* from the ligand and $(COD)_2Ni$ (Scheme 1.2). The scale in which this process is applied is about 1 million tons per year, and makes it one of the widely used process for the production of linear α-olefins.[18] The distribution of molecular weights is essentially a Schulz-Flory distribution.[19]

Oligomerization reactions industrially are mostly carried in polar solvents such as polyols, which are largely immiscible with the α-olefins formed,[20] a sign that late transition metals can tolerate polar solvents. In 1987 Klabunde[21] showed that using a nickel catalysts similar to those used by Keim[16,17] for olefin oligomerization, it was possible to prepare high molecular weight polymers by removing a phosphine with a phosphine sponge or phosphine scavenger. The removal of a phosphine in these complexes opens a vacant site for ethylene to coordinate and subsequently insert into a methyl alkyl bond. The effect of this is the transformation of a catalyst meant for the production of α-olefins, to a catalyst for the production of polyolefins, a development that showed late transition metal complexes could catalyze the

polymerization of olefins. The most useful phosphine scavengers used by Klabunde were $Rh(acac)(C_2H_2)$ and $Ni(COD)_2$. Although these catalysts are tolerant to polar substrates, they are still poisoned by water.

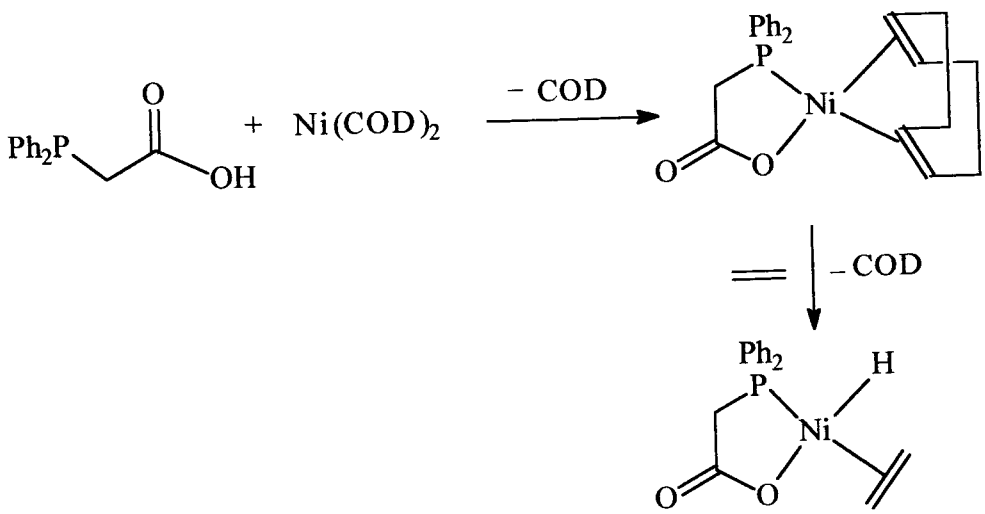

Scheme 1.2: Synthesis of P,O chelated nickel complexes

Another interesting α-iminocarboxamidato-nickel catalyst system has recently been reported by Bazan and coworkers,[22] for the production of branched polyethylene and treatment of this complex with $B(C_6F_5)_3$ results in high catalytic activity. This catalyst system can also be used for ethylene oligomerization[23] and copolymerization[24] with higher olefins under certain conditions. Recently Grubbs[25] and coworkers reported neutral Ni(II) salicylaldiminato complexes (Scheme 1.3), which are highly active catalysts for the polymerization of ethylene to high molecular weight polymers under moderate conditions. Catalyst activities of about

250 kg/mol Ni h are obtained using these catalysts and molecular weights of around 360 000 g/mol. They chose the salicylaldiminato ligands because they are easy to synthesize and simple modification of both steric and/or electronic effects is possible.

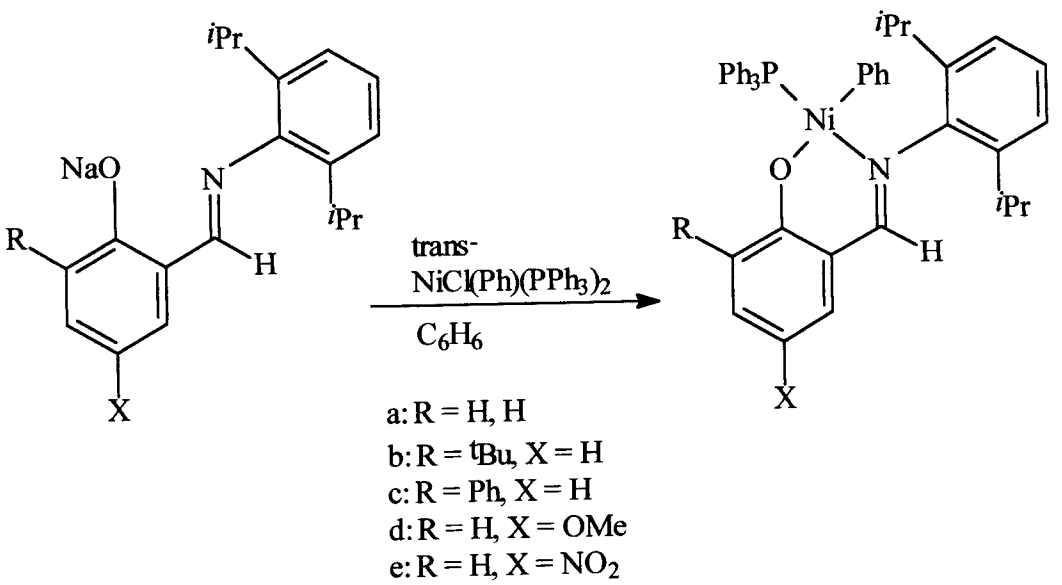

Scheme 1.3: Synthesis of Grubbs catalyst

But by far the single most important discovery for late transition metal olefin polymerization catalysts was made by Brookhart and co-workers in 1995.[26] The Brookhart catalyst system is based on α-diimine palladium and nickel complexes and will be discussed with other nitrogen ligand complexes in section 1.4.2. It is believed that the introduction of bulky substituents on the ketimine nitrogen and the phenolic ring of the salicylaldiminato ligand could block the axial faces of the metal centre, retarding the rate of associative displacement, similar to what is observed for

Brookhart[26] catalysts. Other neutral nickel(II) catalysts based on the pyridinecarboxylate ligand have been reported by Cavell[27] to be mildly active in both the polymerization and co-polymerization of ethylene and carbon monoxide without the addition of a co-catalyst. The use P,O chelated olefin polymerization catalysts is now competing with the fast growing nitrogen ligand based catalysts. The following sections will deal with recent developments in the use of nitrogen-based complexes as olefin polymerization catalysts.

1.4.2 Nitrogen based late transition metal complexes as olefin polymerization catalysts

Over the past decade, olefin polymerization by complexes of late transition metals has received increasing attention.[28] Catalysts based on early transition metals like zirconium and titanium dominate reported work on olefin polymerization catalysis.[29] Until recently there were few reports on late transition metals as catalysts for olefin polymerization.[27] This is due to the observation that in late transition complexes β-hydride elimination is faster than chain growth, so chain termination is faster leading to dimers and oligomers. In contrast to this, highly electrophilic early transition metals[29] have fast insertion rates and relatively slow β-hydride elimination rates. When compared to early transition metal complexes, late transition metals are less oxophilic and more tolerant to polar reagents. The tolerance of these complexes to functionalised monomers make the co-polymerization of these monomers with ethylene possible.[30] In addition to this, polyolefins with novel microstructures are accessible by varying temperature, pressure and ligand structure in these complexes.

The use of nickel and palladium complexes with sterically bulky α-diimine ligands by Brookhart[26] and coworkers in 1995 was a major advancement in this area of olefin polymerization catalysis. The olefin polymerization catalysts they discovered possess three features, first the highly electrophilic nickel and palladium centers depicted by structure **C**, secondly the use of sterically bulky diimine ligands and thirdly the use of non-coordinating counterions. Each of these features contributes to the high efficiency of these nickel and palladium catalysts. High electrophilicity in these cationic complexes leads to rapid rates of olefin coordination, an important step in the polymerization reaction, before olefin insertion. The use of bulky ligands dramatically lowers the rate of β-hydride elimination thus favouring chain growth. The use of non-coordinating counter ions opens a vacant site for the incoming olefin to coordinate and subsequently insert into a methyl alkyl bond. Activities of about 11000 kg of PE per mol of Ni per hour are obtained for these catalysts.

These nickel catalyst systems are unique because they produce highly branched polyethylene without addition of a co-monomer and also give high molecular weight polyethylene. The high degree of branching in the polymers obtained from these catalysts occurs by a process called "chain walking" or simply chain isomerisation.[31] In chain walking, branching occurs by a process whereby the growing site isomerizes to an internal position on the polymer backbone during propagation, so that the next monomer unit comes onto the polymer backbone instead of at the end. For coordination polymerization of ethylene and other olefins, reactions such as chain transfer by β-hydride elimination and chain isomerism (chain walking) compete with

chain propagation. For early transition metal catalysts, the chain-walking rate is usually very small compared to the insertion rate, and this leads to linear chain growth.

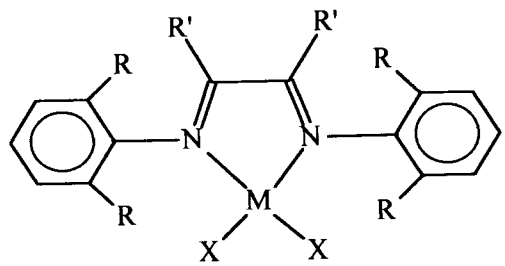

M = Ni, Pd
X = Br, Cl
R' = H, Me
R = ^{i}Pr, ^{t}Bu, Me

C

In their investigation Guan and coworkers[32] have shown that varying ethylene pressure can regulate the chain-walking process, and thus the polyethylene structure can be controlled from a linear structure to hyperbranched structure by simply changing the ethylene pressure. They observed that at high pressures linear polyethylene with short branches is obtained, while at low pressures highly branched polyethylene is obtained.

There are other classes of nitrogen-based ligands, which form complexes that are equally effective catalysts for olefin polymerization compared to the complexes used by Brookhart. Both Gibson[33] and Brookhart[34] have reported another class of non-metallocene catalysts highly active for olefin polymerization. These highly active

catalysts are based on iron and cobalt complexes **(D)** stabilized by arylimine ligands. When activated with MAO, these complexes have been found to be extremely active homogeneous catalysts for ethylene polymerization to linear polyethylene. Activities in the range 206-3750 kg/mol Fe h are observed for iron catalysts, while cobalt catalysts display activities in the range 450-1740 kg/mol Co h. The high activity of the Brookhart and Gibson catalysts for olefin polymerization led to an explosion of research activity to develop other late transition metal catalysts for this reaction. Most of this research activity is centered on nickel and palladium. The rest of this chapter is thus centered on a brief review of nitrogen ligand complexes of nickel and palladium that have relevance as olefin polymerization catalysts.

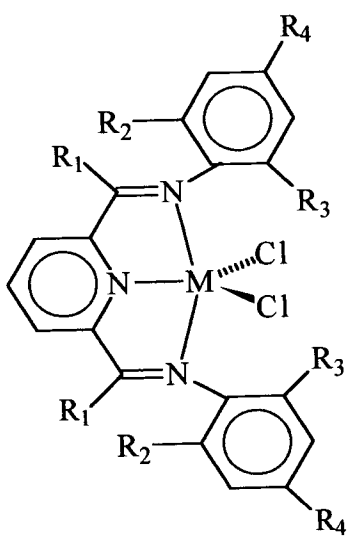

M = Fe, Co, X = Cl
R_1 = H, Me
$R_2 = R_3 = i$Pr, R_4 = H
$R_2 = R_3$ = Me, R_4 = H, Me
$R_2 = R_4$ = Me, R_3 = H

D

1.4.3 Synthesis of nitrogen based nickel and palladium complexes

Following a reported procedure, nickel complexes are readily obtained from the reaction of (1,2-dimethoxyethane)nickel(II) bromide (DME)$NiBr_2$ and an appropriate ligand. The characterization of these complexes was difficult because of their low solubility in organic solvents, and their paramagnetic nature made it impossible to obtain NMR data for these complexes. The paramagnetic nature of the nickel complexes is because they have tetrahedral geometry and not square planar. Hence the best way to characterize these nickel complexes is single crystal X-ray crystallography. The palladium complexes, on the other hand, are readily prepared from (COD)$PdCl_2$ or $(MeCN)_2PdCl_2$ starting materials. The structures are square planar and thus easily characterized by NMR spectroscopy, though structures are confirmed by X-ray crystallography too.

In another report Laine and coworkers[35] investigated pyridyl imino-based nickel and palladium complexes for their behavior as alkene polymerization catalysts. The nickel complexes were found to be dinuclear as depicted by structure **E** with nickel atoms bridged by two bromides and the analogous palladium complexes were found to be mononuclear **F**. As catalysts, both nickel and palladium complexes showed fairly good activity for ethylene and norbonene polymerization. Even though these catalysts show activity of 4800 kg/mol Ni h, the nickel catalysts loose activity at high temperatures. In comparison to the Brookhart[27] catalysts, the activity of these catalysts is low. Other contributors to this area of research are Koppl and coworkers[36] who reported nickel complexes with 1-(2-pyrilyl-2-azaethene) as

ligands **(G)**. These complexes can be used for the catalytic polymerization of ethylene, with MAO as a co-catalyst. The polyethylene prepared with these catalysts has a high degree of short chain branching with up to 240 branches per 1000 carbon atoms. All these nickel catalysts show high activity for ethylene polymerization but in most cases catalytic activity decreases above 60 °C. Decrease in catalytic activity of these catalyst systems is attributed to catalyst decomposition processes, which are not clearly understood.

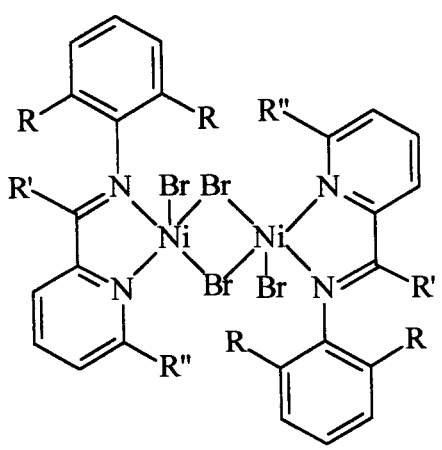

E

R = Me or *i*Pr
R' = H, *i*Pr, Ph
R" = H, Me

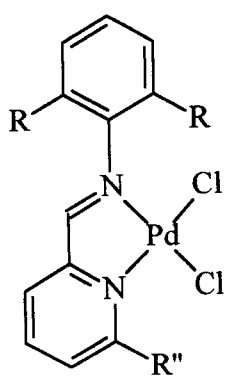

F

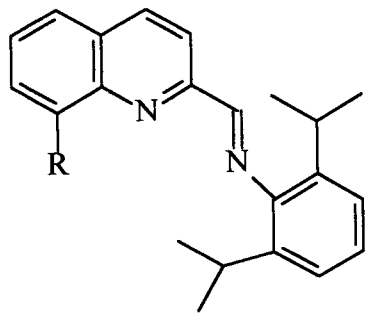

R = H, Me

G

Density functional theory (DFT) studies performed by Ziegler[37] and others[38] have been used to understand the mechanistic details of the Ni(II) and Pd(II)-catalyzed polymerization of ethylene and propylene. Although these studies are theoretical, they shed some light on the energetics and kinetics of late transition metal catalyzed polymerization. In a recent report using DFT, initial screening of late transition metal catalysts and N-containing polar monomers was performed in order to reveal potential future directions of research into co-polymerization of olefins with amines or nitriles.[39] All the synthetic and theoretical studies described above have resulted in fairly good understanding of the mechanism of olefin polymerization catalyzed by late transition metal complexes.

The mechanistic details of nickel and palladium diimine catalyzed ethylene polymerization have recently also been studied by Brookhart's group.[40] This reaction mechanism calls for a pre-catalyst (e.g. the dihalide complex) to be activated by a

co-catalyst, resulting in formation of a dimethyl complex (Scheme 1.4). Once activation has occurred, chain initialization proceeds via uptake of an olefin onto the free site of the metal centre. This is followed by the insertion of the coordinated olefin into the M-CH_3 (M = Pd, Ni) bond (**S1**). Chain propagation proceeds by coordination of free olefin and insertion into the M-R bond (R = growing chain (**S2**). Chain isomerization can then occur by β-hydride elimination of hydrogen from the growing chain and rotation of the chain by 180° around the M-olefin bond, followed by reattachment of the hydrogen to the terminal carbon atom (**S3**). Chain termination occurs by ethylene-assisted β-hydride elimination from the growing chain and transfer of the eliminated hydrogen to a coordinating olefin (**S4**). It is important to note that this mechanism is proposed for Brookhart type catalysts, and may be applied to explain the mechanistic details of ethylene polymerization catalyzed by related nitrogen based late transition complexes. This mechanism will thus be used to explain the formation of polyethylene produced in this project.

What is obvious from the mechanism in Scheme 1.4 is that high activity of a catalyst is promoted by a highly electrophilic metal centre. This observation suggests that new catalysts can make use of ligands that can enhance the electrophilicty of the catalyst. To do this we chose pyrazole and pyrazolyl compounds that have the carbonyl electron withdrawing group as nitrogen based ligands in this project. The last part of this Chapter will focus on the coordination chemistry of pyrazole-based complexes.

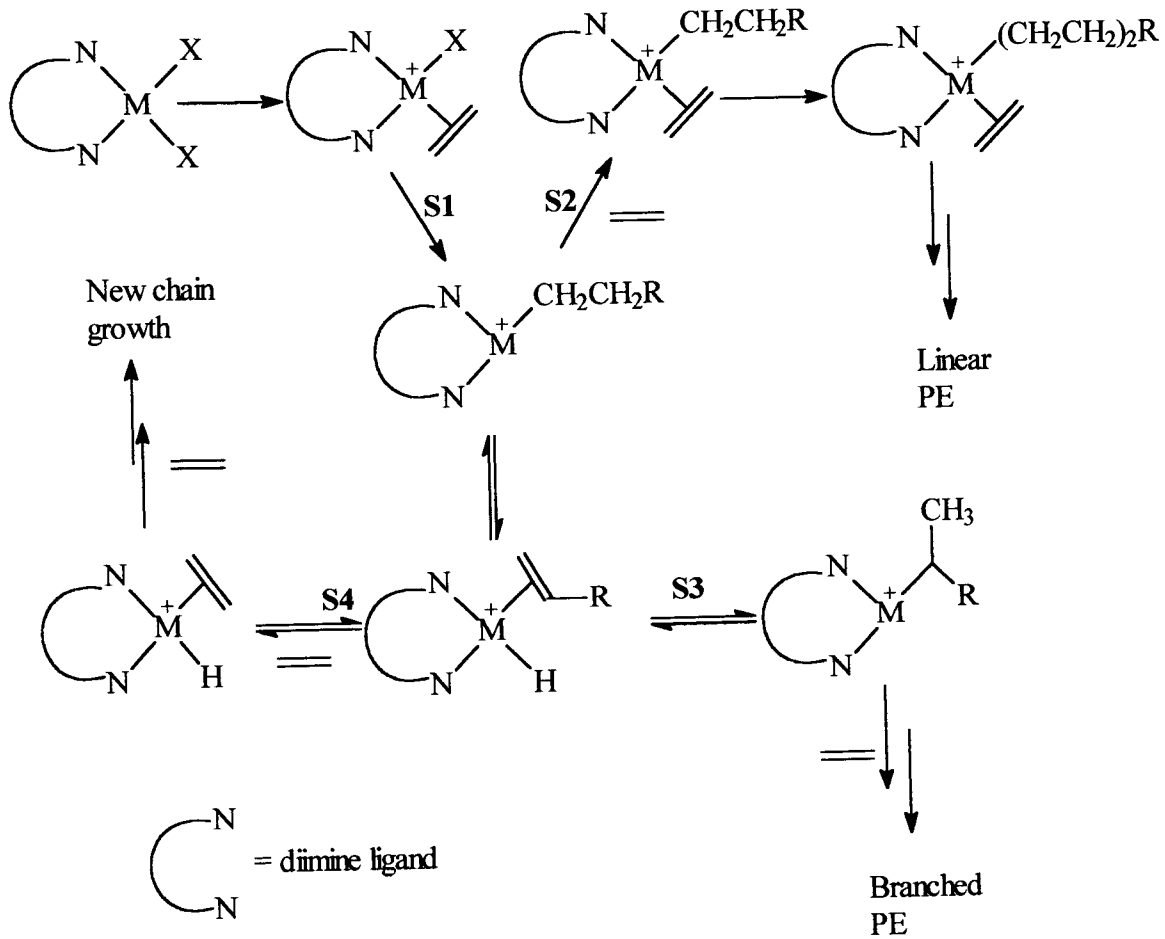

Scheme 1.4: General mechanism for ethylene polymerization for Brookhart catalysts

1.5 Pyrazole based ligands and complexes

1.5.1 Synthesis of substituted pyrazole ligands

Pyrazoles fall under a group of organic compounds called heterocyclic compounds. A heterocyclic compound is one which possesses a cyclic structure with at least two different kinds of atoms other than carbon in the ring.[41] Elements that are commonly found together with carbon in ring systems are nitrogen, oxygen and sulfur. Pyrazole (Fig.1.4) is a five membered heterocycle containing two nitrogen atoms bonded to each other, with one of the nitrogen atoms bonded to a hydrogen atom.

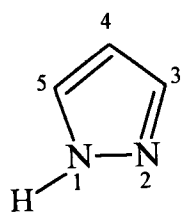

Figure 1.4: General structure of a pyrazole

Pyrazole derivatives have been used commercially as pharmaceuticals, pesticides and dyestuffs. The most general route to the synthesis of pyrazoles is the reaction of 1,3-dicarbonyl compounds with hydrazines.[42] For example 3,5-dimethylpyrazole is prepared from pentane-2,4-dione and hydrazine (eq.1). In this project we procured 3,5-dimethylpyrazole from commercial sources, but we used the procedure in equation (1) to prepare 3,5-ditertbutylpyrazole. The preparation of 3,5-ditertbutylpyrazole is thus described in the Chapter 2 of this thesis.

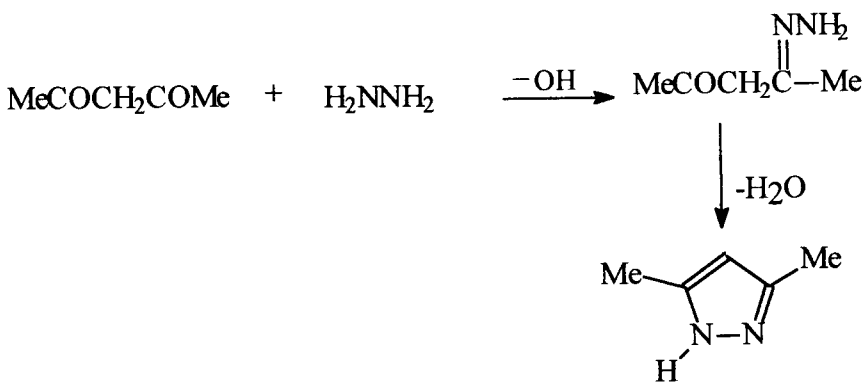

(1)

Pyrazoles are also prepared by cyclisation of acetylinic hydrazones or by electrocyclisation of unsaturated diazo compounds.[43] Pyrazole ligands are found in different fields of chemistry from synthetic inorganic chemistry or bioinorganic chemistry[44] to organometallic chemistry.[45] A unique feature of a pyrazole nucleus is that it is thermally and hydrolytically stable.[46] These two properties make pyrazoles suitable for complexation with metals without rigourously dried synthetic protocols.

1.5.2 The coordination chemistry of pyrazole ligands

As a ligand, pyrazole coordinates to metals and metalloids through the 2-N (Fig. 1.4) of the ring. The complexes formed are of the type $M(Hpz)_nX_m$, where M is a transition metal, Hpz is the pyrazole ligand, X is a non-coordinating anion, n is the coordination number of the metal and m is valence of the transition metal; usually 2.[46] In the case where the non-coordinating anion is NO_3, BF_4 or ClO_4, complexes of Mg, Mn, Ni, Fe, Co, Zn and Cd of the type $M(Hpz)_6X_2$ are known.[47] When X is a halide (Cl, Br), complexes of Ni, Co and Fe with formula $M(Hpz)_4X_2$ have been reported.[48] The $Ni(Hpz)_4X_2$ (X = Br or Cl) complexes have been studied by X-ray

crystallography and by spectroscopic techniques.[49] In contrast to other transition metals, copper does not form $M(Hpz)_6X_2$ type complexes; it only forms complexes of the type $Cu(Hpz)_4X_2$ irrespective of the nature of X (Cl, Br, BF_4, ClO_4, SO_4, NO_3).[50-52] When pyrazole ligand is 3-methylpyrazole, complexes of the type $M(H\text{-}3\text{-}Mepz)_7(ClO_4)_2$ are formed with transition metals like Mn, Fe, Co and Cd.[52] In the case of 3,5-dimethylpyrazole, complexes of the general formula $M(H\text{-}3,5\text{-}Me_2pz)_4X_2$ have been reported for most transition metals.[51]

The substituents on the pyrazole ring are not limited to the methyl group. Other interesting ligand systems are obtained when other nitrogen containing compounds are used as substituents. When pyridine is used as a bulky substituent at position 3 and 5, it forms 3,5-bis(2-pyridyl)pyrazole (Hbppypz). By changing the pyridine, different forms of this compound can be isolated. Ball and Blake reported this class of ligands in 1969, but it is only recently that these ligands have received attention.[53] Pons and coworkers have studied a series of Hbppypz complexes with divalent metal ions like Ni^{2+}, Co^{2+}, Zn^{2+} and Cu^{2+}.[54] The nickel complexes in particular show the formation of a dinuclear complexes in which the ligand itself exhibits a planar bridging mode.[54]

Because of the different bonding modes and modifications that can be made, pyrazole complexes have diverse applications from medicinal chemistry to catalysis. Sakai and coworkers have investigated the pyrazole platinum complexes with potential antitumour activity.[55] This is not the only report on the use of pyrazole

based ligands in bioinorganic chemistry, there is a lot of reported work on the use of pyrazole based complexes in this field.[56-58] Recently Cano et al.[59] have reported mesogenic Pd(II) complexes based on 3-substituted pyrazole ligands (Fig. 1.5). Cano and coworkers have also investigated the mesormophic properties of rhodium complexes of pyrazole ligands with alkyloxyphenyl substituents at the positions 3 and 5 of the pyrazole ring.[60] These compounds exhibit a smectic C mesophase, which is a form of a liquid crystal.

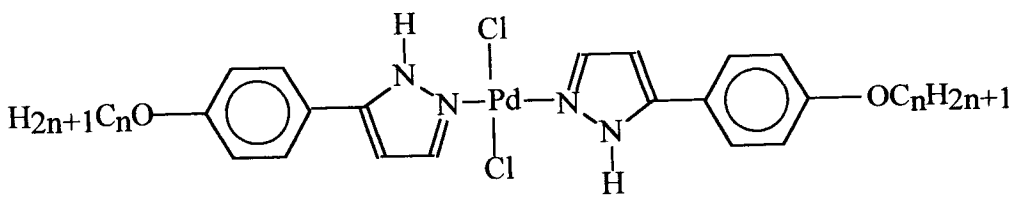

n = 6-18

Figure 1.5: Mesogenic pyrazole palladium complex

The oxidative coupling of 2,6-dimethylphenol results in polyphenylene ether, which is an important engineering plastic.[61] This reaction is mostly catalyzed by imine compounds of copper, but recently Driessen et al.[62] have shown that dinuclear copper macrocyclic pyrazole compounds can catalyze this reaction. The Mo complexes $[Mo(CO)_3(Hpz)_3]$ have been used as alkyne oligomerization catalysts and have been found to catalyze the cyclotrimerization of ethyl propiolate (EP, EtOOC-C≡C-C-H) and dimethyl acetylenedicarboxylate (DMAD, CH_3OOC-C≡C-C-$COOCH_3$).[63]

The choice of pyrazole ligands to prepare olefin polymerization catalysts is based on the fact that pyrazoles are weaker σ-donors than imine or pyridine ligands and therefore will form complexes that have more electrophilic metal centres. A high electrophilic metal centre is a requirement for an olefin polymerization catalyst to be highly active. This hypothesis has been tested with some work reported on lanthanide complexes. Ethylene polymerization activity in the presence of MAO of the cyclopentadienylterbium dibromides ($TbBr_2CpL$, L = Hpz and PPh_3) reported by De Oliviera and coworkers,[64] shows that catalytic activity is about 12 kg/mol Tb h at 70°C when the Al:Ln ratio is 2000. The presence of Hpz or PPh_3 ligands caused no steric or electronic effects on the metal centre that could modify catalytic activities. These activities are in the range of catalytic activities of other compounds containing pzA, where pz = pyrazole and A = Cl^-, $CH_3SO_3^-$. For the system $LnBr_2CppzA$ (where Ln is Nd or Sm there are reported activities of 13.2 and 19.2 kg/mol Ln h respectively.[65-67] A closely related system ($LnA_2Cp(pzA)$/MAO, Ln = Nd, Sm, Eu, Tb) has activities of about 20 kg/mol Ln h.

Motivated by the versatility of pyrazole complexes that can be used for diverse applications and renewed interest in the nitrogen based olefin polymerization catalysts, our group embarked on a project to synthesize substituted pyrazole palladium complexes. These complexes were evaluated as catalysts for ethylene polymerization (Scheme 1.5).[68] The results obtained have shown that pyrazole palladium complexes are effective catalysts in the polymerization of ethylene. Activities of about 1234 kg/mol Pd h at 5 atm were obtained for these catalysts. A

high average molecular weight of about 5.53×10^5 g/mol and low polydispersity polymers are obtained for these catalysts. The subtituents in the pyrazole ring are found to have some effect on the activity of these catalysts. High activities were obtained when R = R' = CH_3 compared to R = R' = ^{t}Bu. The reason for the difference in activity with the subtituent on the pyrazole is not clear at this stage.

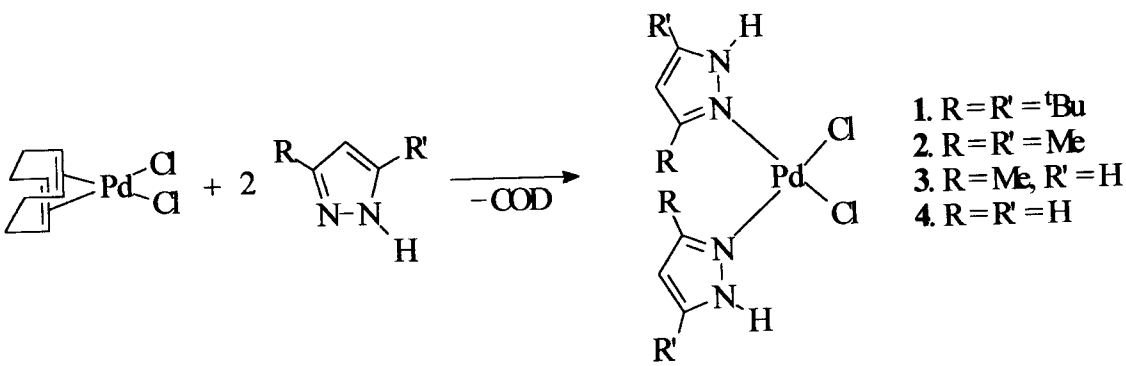

Scheme 1.5: Synthesis of substituted pyrazole palladium complexes

1.5.3 The coordination chemistry of pyrazolyl ligands

Most substituted pyrazoles can be derivatised through the 1-N hydrogen to form geminal poly(1-pyrazolyl) ligands.[69] In preparing poly(1-pyrazolyl) ligands, the substituents on the pyrazolyl units can be varied as well as the linkers that hold the pyrazolyl units. Hence the overall electrophilic nature of the metal complex can be fine-tuned by the choice of substituents, linkers or both. This leads to a variety of ligands with unique coordinating properties. Poly(1-pyrazolyl) substituted compounds are dominated by poly(1-pyrazolyl) borates[70] and to a lesser extent by poly(1-pyrazolyl) alkanes[71]. In this section poly(1-pyrazolyl) compounds will be

discussed in detail. The closely related pyrazolyl ligands are poly(pyrazolyl)benzenes and these compounds exhibit a variety of modes of coordination to transition metals.[72] For example the ability of these compounds to encapsulate metal ions and to form nanoscale metallosupramolecular cages have been reported by Hartshorn and Steel.[72c] Poly(pyrazolyl)benzenes can be used for the preparation of metallocycles, which are important organometallic compounds as shown in eq. 2.[72b]

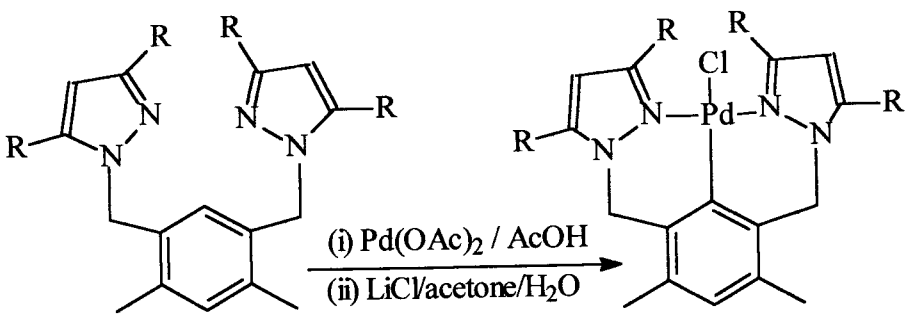

(2)

R = H or Me

1.5.3.1 Poly(1-pyrazolyl)borates or scorpionates

This class of compounds was first reported in 1967 by Trofimenko and has since found application in coordination chemistry.[70] Generally geminal poly(1-pyrazolyl)borate compounds are uninegative ligands with bonding modes ranging from bidentate to tetradentate. Poly(1-pyrazolyl)borate ligands are known to stabilize metals in both high and low oxidation states. Their complexes with most metals of the periodic table have been reported. The most studied ligands are of the form $[R_nB(pz)_{4-n}]^-$ where R = H, alkyl, aryl group and pz = pyrazole or substituted pyrazoles.[73] The ligands $[HB(pz)_3]^-$ **(H)** and $[HB(3,5\text{-}Mepz)_3]^-$ **(I)** are mostly used to

prepare complexes for most transition metals.[73] The chemistry of these ligands with first-row metals is dominated by the formation of the ML_2 complex, M = metal and L = ligand. There are few reports on the use of these complexes as catalysts in olefin polymerization. Kress[74] has reported vanadium(V) catalysts **(J)**, stabilized by imido and hydrotris(pyrazolyl)borato ligands, for ethylene and propylene polymerization. Moderate activity of 14 kg/mol h for ethylene polymerization have been reported for these catalysts. Propylene has also been polymerized but only to a low molecular weight material.

Several Ti and Zr complexes bearing hydrotris(pyrazolyl) borate ligands have been reported by Nakazawa et al. to be highly active ethylene polymerization catalysts.[75] Another example is that of the Nb complexes reported by Jaffart[76] and coworkers that polymerizes ethylene. Catalytic activity of these catalysts was about 125 kg/mol Tp h. The activity of the early transition metal pyrazolyl complexes is dependent on the size of the R substituents on the hydrido-tris(pyrazolyl)borate ligand. Activities up to 130 kg/mol Tp h have been achieved with R = CH_3, whereas lower activity is found with R = H. The activity of these catalysts also depends on the nature of the co-catalyst. The catalysts are active when activated with $B(C_6F_5)_3$ but are inactive when the cocatalyst is MAO. So far most of the olefin polymerization catalysts with pyrazolyl ligands are either early transition metals (V,Ti, Zr) or lanthanides (Tb, Sm, Nd). There are very few catalysts based on late transition metals; this was one of the motivating factors for undertaking this project.

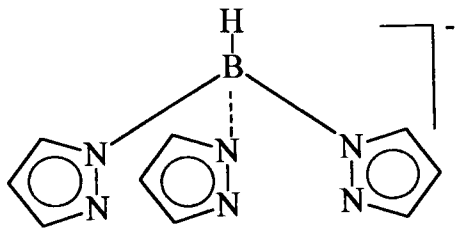

H

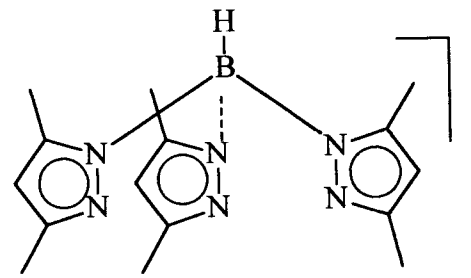

I

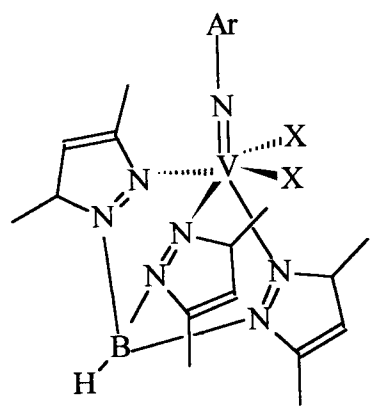

J

1.5.3.2 Poly(1-pyrazoly) alkanes

Poly(1-pyrazolyl)alkanes[71] have not been widely explored as ligands like the poly(1-pyrazolyl)borates. The poly(1-pyrazolyl)alkanes ligands are isosteric and isolectronic with poly(1-pyrazolyl)borates. The only difference between these compounds is that poly(1-pyrazolyl)alkanes are neutral while poly(1-pyrazolyl) borates are uninegative. Most of the published work on alkane analogues are on first row metals,[77] with a few ruthenium examples,[78] while coordination to metals having

d^8 (Ni, Pt, Pd) configuration is rare. In a report by Reedijk et al.[79] crystal and molecular structure of $[Ni(CH_2)_2(dmpz)_2Cl_2]$ are studied, in which (CH_2(dmpz) = bis(3,5-dimethylpyrazole)-methane). One interesting property about this nickel complex is that it is ferromagnetic, unlike other related compounds which are antiferromagenetic.[80] The studies were done to probe the cause of this exceptional magnetic property. Recently a paper that deals with the synthesis of the cationic precursors $[Pd(N\text{-}N)(CH_3CN)_2]^{2+}$ and $[Pd_2(N\text{-}N)_2(\mu\text{-}OH_2)_2]^2$ (where N-N = bis(pyrazol-1-yl)methane (bpzm) or bis(3,5-dimethylpyrazol-1-yl)methane (bpzm*)) was published.[81] These complexes can be used as catalysts for most polymerization reactions and other organic transformations, like hydrogenation. Jordan[82] and coworkers have reported neutral and cationic palladium complexes with bis(1-pyrazolyl) methane ligands ($Ph_2C(pz')$, pz' = 3-^{t}Bupz, pz) (Scheme 1.6), which when activated with MAO show very low activity for ethylene polymerization. Activity of about 1.8 kg-PE/mol. h is obtained for these catalysts, similar to the activity observed for $PdCl_2$/MAO. One possible explanation for this low activity is that the linker $Ph_2C(pz')_2$ is released upon reaction of these complexes with MAO. In a quest to find better pyrazolyl linkers, which do not dissociate upon activation, our group has reported a new class of linkers.[83] These linkers are 1,3-benzenedicarbonyl and 1,3,5-benzenetricarbonyl moieties and were used to synthesize palladium pyrazolyl complexes (Scheme 1.7 and 1.8). The electron withdrawing carbonyl group increases the electrophilic nature of the palladium centre and results in fast olefin coordination and insertion. When compared to the unlinked pyrazole palladium complexes we reported, these linked pyrazolyl palladium complexes were found to be more active

as ethylene polymerization catalysts. This proves that in order to increase the activity of oligomerization and polymerization catalysts with pyrazolyl ligands a strong electrophilic metal complex is imperative. The dissociation of the linker upon activation is not observed for these catalysts, as it was the case with bis(pyrazolyl)methane palladium complexes. This is based on the fact that the activities obtained were comparable to the known highly active ethylene polymerization catalysts. The work reported in this thesis is part of a project that is looking at nickel and palladium pyrazolyl compounds as olefin polymerization catalysts. The last section sets out the objectives for work reported in this thesis.

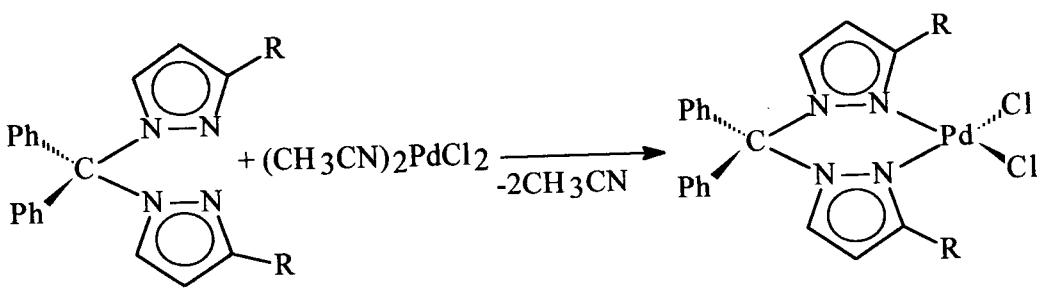

1. R = ^{t}Bu
2. R = H

Scheme 1.6: Activation pathway of bis(pyrazolyl)methane palladium complexes

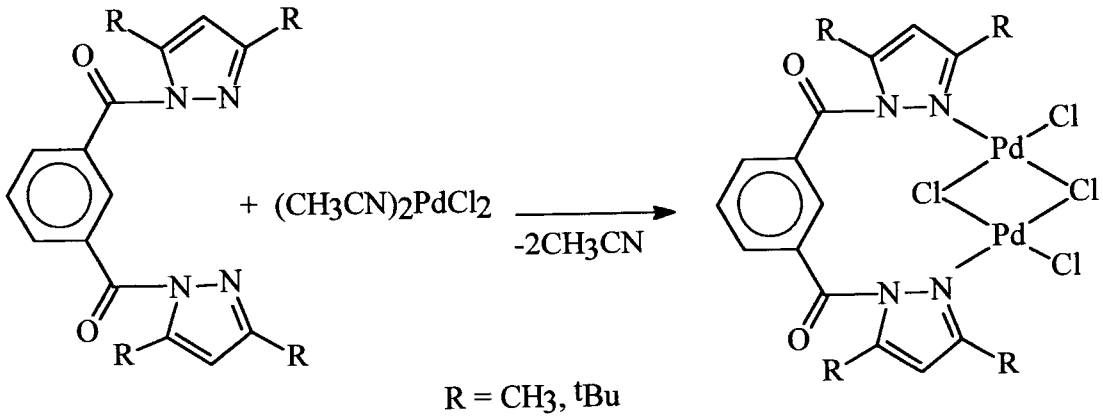

R = CH_3, ^tBu

Scheme 1.7: Synthesis of 1,3-benzenedicarbonylpyrazolylpalladium(II) chloride

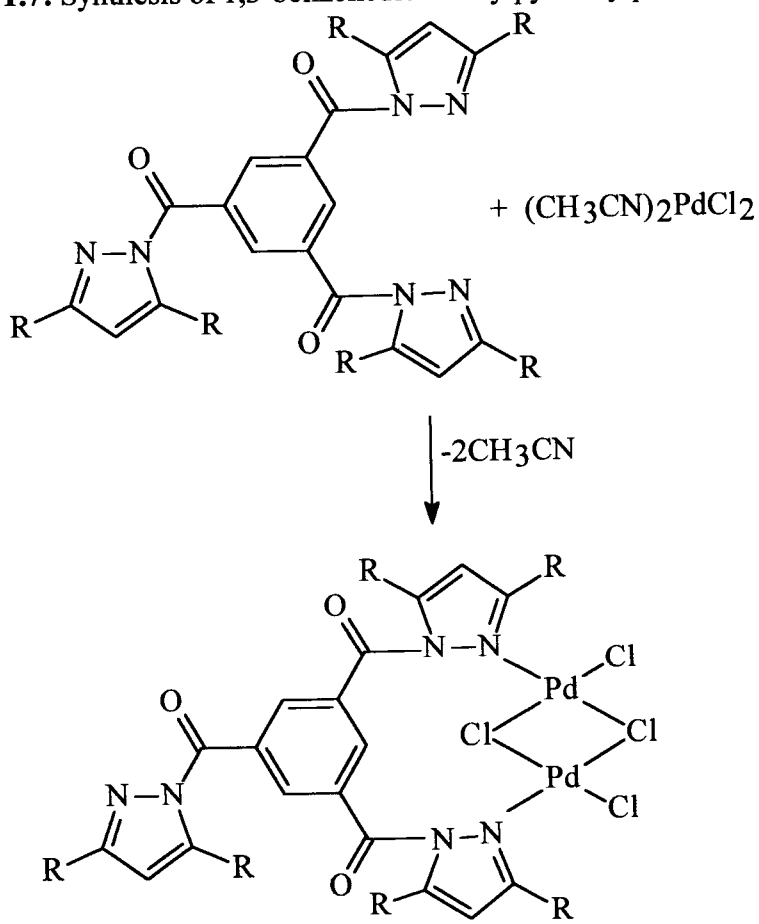

R = ^tBu

Scheme 1.8: Synthesis of 1,3,5-benzenetricarbonylpyrazolylpalladium(II) chloride

1.6 Objectives of this study

In our group we have for the past four years concentrated our research efforts on the synthesis of pyrazole and pyrazolyl palladium complexes. These studies have shown that pyrazole and pyrazolyl palladium complexes are effective catalysts for ethylene polymerization. This thesis deals firstly with the synthesis of nickel pyrazole complexes, as an extension to the successful chemistry done with substituted pyrazole palladium complexes.[68] These nickel complexes have been reported before, but in this thesis improved synthetic methodology for these complexes is described in Chapter 2. The behavior of these complexes as ethylene polymerization catalysts was investigated and compared to that of their palladium analogous and the results are summarized in Chapter 3.

Secondly, new alkanoyl pyrazolyl ligands and their palladium complexes were prepared and their synthesis is summarized in Chapter 2. Thirdly, this thesis deals briefly with the ethylene polymerization studies done with 1,3,5-benzenetricarbonyl pyrazolyl palladium catalyst. In this thesis the effect of MAO and temperature on the activity of this complex on ethylene polymerization is investigated. The polymerization data of this catalyst is summarized in Chapter 3 of this thesis.

References

1. (a) Levowitz I. L., *Morden Plastics Encyclopedia '99* (McGraw-Hill, New York, 1999), Vol. **75**, pp B3-B6. (b) Billmeyer F., *Textbook of Polymer Science, Interscience,* New York, 1962.

2. (a) Ziegler K., Holzkamp E., Breil H., Martin H., *Angew. Chem.* 1955, **67**, 541. (b) Natta G., *Angew. Chem.* 1956, **68**, 393.

3. Natta G., *Angew. Chem.* 1964, **76**, 533.

4. Hogan J. P., *J. Polym. Sci. A* 1970, **8**, 2637.

5. (a) Cossee P., *J. Catal.* 1964, **3**, 80. (b) Arlman E. J., *J. Catal.* 1964, **3**, 89. (c) Arlman E. J., Cossee P., *J. Catal.* 1964, **3**, 99.

6. A. Mayr, USP 4495338 and USP 4476289, *Montell Technology*

7. (a) Breslow D. S., Newburg N. R., *J. Am. Chem. Soc.* 1957, **79**, 5072. (b) Natta G., Pino P., Mazzanti G., Giannini U., *J. Am. Chem. Soc.* 1957, **79**, 2975.

8. (a) Breslow D. S., Newburg N. R., *J. Am. Chem. Soc.* 1959, **81**, 81. (b) Long W. P., Breslow D. S., *J. Am. Chem. Soc.* 1960, **82**, 1953.

9. Chien J. C. W., *J. Am. Chem. Soc.* 1959, **81**, 86.

10. Reichert K. H., Meyer K. R., *Makromol. Chem.* 1973, **169**, 163.

11. Long W. P., Breslow D. S., *Liebigs Ann. Chem.* 1975, 463.

12. (a) Andresen A., Cordes H. G., Herwig J., Kaminsky W., Merck A., Mottweiler R., Pein J., Sinn H., Volmer H. J., *Angew. Chem. Int. Ed. Engl.* 1976, **15**, 630. (b) Sinn H., Kaminsky W., Volmer H. J., *Angew. Chem. Int. Ed. Engl.* 1980, **19**, 396.

13. (a) Kaminsky W., *Nachr. Chem. Tech. Lab.* 1981, **29**, 373. (b) Herwig J., Kaminsky W., *Poly. Bull.* 1983, **9**, 464. (c) Kaminsky W., Miri M., Sinn H., Woldt R., *Makromol. Chem., Rapid. Commun.* 1983, **4**, 417.

14. Albizzati E., Galimberti M., *Catalysis Today* 1998, **41**, 159.

15. Chen E. Y., Marks T. J, *Chem. Rev.* 2000, **100**, 1391.

16. Keim W., *Angew. Chem. Int. Ed. Engl.* 1990, **29**, 235.

17. Keim W., Kowaldt F. H., Goddard, R., Krüger C., *Angew. Chem. Int. Ed. Engl.* 1978, **17**, 466.

18. Morse P. M., *Chem. Eng. News* 1999, March 15, 22.

19. Flory P. J., *J. Am. Chem. Soc.* 1940, **62**, 1561. (b) Schulz G. V. Z., *Phys. Chem., Abstr.* 1935, **B30**, 379. (c) Schulz G. V. Z, *Phys. Chem., Abstr.* 1939, **B43**, 25.

20 (a) O'Donnel A. E., Gum C. R., *U.S. Patent 4260844 to Shell Oil Co.*, April 7, 1981. (b) Lutz E. F., *U.S. Patent 4528416 to Shell Oil Co.*, July 9, 1985.

21. Klabunde U., Mülhaupt R., Herskovitz T., Janowicz A. H., Calabrese J., Ittel S. D., *J. Polym. Sci., Part A: Polym. Chem.* 1987, **25**, 1989.

22. Barnhart R. W., Bazan G. C., Mourey T., *J. Am. Chem. Soc.* 1998, **120**, 1082.

23. Komon Z. J. A., Bu X., Bazan G. C., *J. Am. Chem. Soc.* 2000, **122**, 12379.

24. Komon Z. J. A., Bu X., Bazan G. C., *J. Am. Chem. Soc.* 2000, **122**, 1830.

25. (a) Wang C., Friedrich S. K., Younkin T. R., Li R. T., Grubbs R. H., Bansleben D. A., Day M. W., *Organometallics* 1998, **17**, 3149. (b) Younkin T. R., Connor E. F., Henderson J. I., Friedrich S. K., Grubbs R. H., Bansleben D. A., *Science* 2000, **287**, 460.

26. Johnson L. K., Killian C. M., Brookhart M., *J. Am. Chem. Soc.* 1995, **117**, 6414.

27. (a) Desjardins S. Y., Cavell K. J., Hoare J. L., Skelton B. W., Sobolev A. N., White A. W., Keim W., *J. Organomet. Chem.* 1997, **544**, 163. (b) Jin H, Cavell K. J, Skelton B. W., White A. H., *J. Chem. Soc., Dalton Trans* 1995, 2159.

28. Ittel S. D., Johnson L. K., Brookhart M., *Chem Rev.* 2000, **100**, 1169.

29. (a) Kaminsky W., *J. Chem. Soc., Dalton Trans.* 1998, 1413. (b) Brintzinger H. H, Fischer D, Mülhaupt R., Rieger B., Waymouth R. M., *Angew. Chem Int. Ed. Engl.* 1995, **34**, 1143.

30. (a) Boffa L. S., Novak B. M., *Chem. Rev.* 2000, **100**, 1479. (b) Connor E. F., Younkin T. R., Henderson J. I., Hwang S., Grubbs R. H., Roberts W. P., Litzau J. J., *J. Polym. Sci., Part A, Polym. Chem* 2002, **40**, 2842.

31. Mohring V. M., Fink G., *Angew. Chem. Int. Ed. Engl.* 1985, **24**, 1001

32. Guan Z., Cotts P. M., McCord E. F., McLain S. J., *Science* 1999, **283**, 2059.

33. (a) Gibson V. C., Maddox P. J., Newton C., Redshaw C., Solan G. A., White A. J. P., Williams D. J., *J. Chem. Soc., Chem. Commun.* 1998, 1651. (b) Gibson V. C., Newton C., Redshaw C., Solan G. A., White A. J. P., Williams D. J., *J. Chem. Soc., Dalton Trans.* 1999, 827.

34. Small B. L., Brookhart M., *Macromolecules* 1999, 32, 2120.

35. Laine T. V., Piironen U., Lappalainen K., Klinga M., Aitola E., Leskela M., *J. Organomet. Chem.* 2000, **606**, 112.

36. Koppl A., Alt H. G., *J. Mol. Catal.A, Chem.* 2000, **154**, 45.

37. Deng L., Margl P., Ziegler T., *J. Am. Chem. Soc.* 1997, **119**, 1094.

38. (a) Musaev D. G., Froese R. D. J., Svensson M., Morokoma K., *J. Am. Chem. Soc.* 1997, **119**, 367.

39. Deuel D. V., Ziegler T., *Organometallics* 2002, **21**, 1603.

40. Johnson L. K., Mecking S., Brookhart M., *J. Am. Chem. Soc.* 1997, **119**, 1094.

41. Gilchrist T. L., *Heterocyclic Chemistry, 3 ed., Addison Wesley Longman Limited*, 1997, pp 304-308.

42. Wiley R. H., Hexner P. E., *Organic Synthesis* Vol. IV. pp 351 (1962)

43. Kost A. N., Grandberg I. I., *Adv. Heterocyl. Chem.*, 1966, **6**, 347.

44. (a) Sorrel T. N., Jameson D. L., *J. Am. Chem. Soc.* 1983, **105**, 6013. (b) Casella L., Gullotti M., Pallanza G., Rigoni L., *J. Am. Chem. Soc.* 1988, **110**, 4221.

45. Eichhorn D. M., Armstrong W. H., *Inorg. Chem.* 1990, **29**, 3607.

46. Trofimenko S., *Chem. Rev.* 1972, **72**, 497.

47. Daugherty N. A., Swisher J. H., *Inorg. Chem.* 1968, **7**, 1657.

48. Reedijk J., *Recl. Trav. Chim. Pays-Bas* 1969, **88**, 1451

49. (a) Reimann C. W., Santoro A., Mighell A. D., *Acta Cryst.* 1969, **B26**, 595. (b) Reimann C. W., Mighell A. D., Mauer F. A., *Acta Cryst.* 1967, **23**, 135.

50. Nichols D., Warburton B. A., *J. Inorg. Nucl. Chem.* 1971, **33**, 1041.

51. Reedijk J., *Recl. Trav. Chim. Pays-Bas* 1970, **89**, 605

52. Inoue M., Kishita M., Kubo M., *Inorg Chem.* 1965, **4**, 626.

53. Ball P. W., Blake A. B., *J. Chem. Soc. A*, 1969, 1415.

54. (a) Pons J., Lopez X., Benet E., Casabo J., *Polyhedron* 1990, **9**, 2839. (b) Pons J., Sanchez F. J., Labarta A., Casabo J., Teixidor F., Caubet A., *Inorg. Chim. Acta* 1993, **208**, 167. (c) Casabo J., Pons J., Siddiqi K. S., Teixidor F., Caubet, Molins E., Miravitlles C., *J. Chem. Soc., Dalton Trans.* 1989, 1401. (d) Pons J., Lopez X., Casabo J., Teixidor F., Caubet A., Rius J., Miravitlles C., *Inorg. Chim. Acta* 1992, **195**, 61.

55. Sakai K., Tomita Y., Ue T., Goshima K., Ohminato M., Tsubomura T., Matsumoto K., Ohmuro K., Kawakami K., *Inorg. Chim. Acta* 2000, **297**, 64.

56. Nivorozhkin A. L., Uraev A. I., Bondarenko G. I., Antsyskina A. S., Kurbatov V. P., Garnovskii A. D., Turta C. I., Brashoveanu N. D., *J. Chem. Soc., Chem. Commun.* 1997, 1711.

57. Sorrel T. N., Jameson D. L., *J. Am. Chem. Soc.* 1982, **104**, 2053.

58. Sorrel T. N., Vankai V. A., *Inorg. Chem.* 1990, **29**, 1687.

59. Torralba M. C., Cano M., Campo J. A., Heras J. V., Pinilla E., Torres M. R., *Inorg. Chem. Comm.* 2002, **5**, 887.

60. (a) Cano M., Heras J. V., Maeso M., Alvaro M., Fernandez R., Pinilla E., Campo J. A., Monge J., *J. Organomet. Chem.* 1997, **533**, 159. (b) Torralba M. C., Cano M., Campo J. A., Heras J.V., Pinilla E., Torres M. R., *J. Organomet. Chem.* 2001, **633**, 91.

61. Hay A. S., Stafford H. S., Endres G. F., Eustance J. W., *J. Am. Chem.* 1959, **81**, 6335.

62. Driessen W. L., Baesjou P. J., Bol J. E., Kooijman H., Spek A. L., Reedijk J., *Inorg. Chim. Acta* 2001, **324**, 16.

63. Ardizzoia G. A., Brenna S., LaMonica G., Maspero A., Masciocchi N., *J. Organomet. Chem.* 2002, **649**, 173.

64. de Souza Maia A., Paulino I. S., Oliveira W., *Inorg. Chem. Comm.* 2003, **6**, 304.

65. Lavini V., de Souza Maia A., Paulino I. S., Schuchardt U., Oliveira W., *Inorg. Chem. Comm.* 2001, **4**, 582.

66. Miotti R. D., de Souza Maia A., Paulino I. S., Oliveira W., *Quimica Nova* 2002, **25**, 762.

67. Miotti R. D., de Souza Maia A., Paulino I. S., Schuchardt U., Oliveira W., *J. Alloys Compd.* 2002, **344**, 92.

68. Li K., Darkwa J., Guzei I. A., Mapolie S. F., *J. Organomet. Chem.* 2002, **660**, 108.

69. Mani F., *Coord. Chem. Rev.* 1992, **120**, 325.

70. (a) Trofimenko S., *J. Am. Chem. Soc.* 1967, **89**, 3170. (b) Trofimenko S., Calabrese J. C., Thompson J. S., *Inorg. Chem.* 1987, **26**, 1507. (c) Trofimenko S., *Chem. Rev.* 1993, **93**, 943.

71. (a) Llobet A., Hodgson D. J., Meyer T. J., *Inorg. Chem.* 1990, **29**, 3760. (b) Llobet A., Curry M. A., Evans H. T., Meyer T. J., *Inorg. Chem.* 1989, **28**, 3131. (c) Llobet A., Doplet P., Meyer T. J., *Inorg. Chem.* 1988, **27**, 514.

72. (a) Hartshorn C. M., Steel P. J., *Aust. J. Chem.* 1995, **48**, 1587. (b) Hartshorn C. M., Steel P.J., *Angew. Chem. Int. Ed. Engl.* 1996, **35**, 2655. (c) Hartshorn C. M., Steel P. J., *Chem. Commun.* 1997, 541.

73. Roundhill S. G. N., Roundhill D. M., Bloomquist D. R., Landee C., Willet R. D., Dooley D. M., Gray H. B., *Inorg. Chem.* 1979, **18**, 831.

74. Scheuer S., Fischer J., Kress J., *Organometallics* 1995, **14**, 2627.

75. Nakazawa H., Ikal S., Imaoka K., Kai Y., Yano T., *J. Mol. Catal. A: Chem.* 1998, **132**, 33.

76. Jaffart J., Nayral C., Choukron R., Mathieu R., Etienne M., *Eur. J. Inorg. Chem.* 1998, 425.

77. Mani F., *Inorg. Chim. Acta* 1980, **38**, 97.

78. Farjardo M., de la Hoz A., Diez-Barra E., Jalón F. A., Otero A., Rodriguez J., Tejeda J., Belleti D., Lanfranchi M., Pellinghelli M. A., *J. Chem. Soc., Dalton Trans.* 1993, 1935.

79. Jansen J. C., Van Koningsveld H., Van Ooijen J. A. C., Reedijk J., *Inorg. Chem.* 1980, **19**, 170.

80. Butcher R. J., Sinn E., *Inorg. Chem.* 1977, **16**, 2334.

81. Sánchez G., Serrano J. L., Pérez J., de Arellano M. C. R., López G., Molins E., *Inorg. Chim. Acta* 1999, **295**, 136.

82. Tsuji S., Swenson D. C., Jordan R. F., *Organometallics* 1999, **18**, 4758.

83. Li K., Guzei I. A., Bikzhanova G. A., Darkwa J., Mapolie S. F., *J. Chem. Soc. ,Dalton Trans.* 2003, 715.

CHAPTER 2

Synthesis of substituted pyrazole nickel complexes and pyrazolyl ligands and their palladium complexes

2.1 INTRODUCTION

2.1.1 Synthesis of substituted pyrazole nickel complexes

The chemistry of pyrazole and substituted pyrazoles with most transition metals has been extensively reviewed by Trofimenko in his 1972 review.[1] The coordination chemistry of these ligands is interesting and includes several structural variations, and has been reported in section 1.5 of Chapter 1 of this thesis. Even though nickel complexes with substituted pyrazoles have been reported,[2-5] the current study shows new synthetic routes to these known complexes. Of particular interest are structures that had hitherto not been reported, which demonstrate the effect of substituents on the structure.

There are few reports on the application of these nickel complexes as catalysts for any organic transformation such as polymerization. It is in this regard that we were interested in synthesizing these complexes and to utilize them as catalysts for ethylene polymerization. By far the most extensive use of pyrazoles as ligands is when they are derivatised through 1-N hydrogen of the ring, to form geminal poly(1-pyrazolyl) compounds, that have been the subject of numerous studies.[5,6]

This section describes an improved synthesis for the substituted pyrazole nickel complexes and the synthesis of the new substituted α,ω-bis(3,5-R_2pyrazolyl)alkane-α,ω-dione; (R =CH_3, ^{t}Bu) ligands and attempted complexation with palladium. All the compounds prepared were characterized by NMR spectroscopy, IR spectroscopy, elemental analysis and in some cases by X-ray crystallography.

2.2 EXPERIMENTAL SECTION

2.2.1 Materials and Instrumentation.

All solvents were dried before use. Toluene and hexane were dried with sodium/benzophenone, by refluxing the solvent in a flask containing a mixture of sodium and benzophenone, under nitrogen, until a permanent blue colour was obtained. The solvent was then distilled and stored under nitrogen atmosphere. Dichloromethane was dried over phosphorus pentoxide by refluxing under nitrogen for 12 h, distilled and stored under nitrogen atmosphere. The starting materials 3,5-ditertbutylpyrazole[7] (3,5-^{t}Bu$_2$pz), (1,2-dimethoxyethane)nickel(II) bromide[8] [(DME)$NiBr_2$] and bis(acetonitrile)palladium(II) chloride[9] [$(MeCN)_2PdCl_2$] were synthesized according to literature procedures. Other starting materials such as 3,5-dimethlypyrazole (3,5-Me_2pz), 3-methylpyrazole (3-Mepz), pyrazole (pz), oxalyl chloride, malonyl chloride, succinyl chloride, glutaryl chloride, were purchased from Sigma-Aldrich and used as received. All manipulations that are air and/or moisture-sensitive were performed under a dry, deoxygenated nitrogen atmosphere using standard high vacuum or Schlenk tube techniques. IR spectra were recorded as nujol mulls on a PERKIN ELMER, paragon 1000 PC FT-IR spectrometer. NMR spectra

were recorded on a Varian Gemini 2000 instrument (^{1}H at 200 MHz, ^{13}C at 50 MHz). Chemical shifts are reported in ppm and referenced to residual protons (7.26 ppm) and carbon signals (77.0 ppm) of $CHCl_3$ in $CDCl_3$. Elemental analysis was performed in-house on a Carlo Erba NA analyzer in the Department of Chemistry at the University of the Western Cape.

2.2.2 Preparation of Nickel complexes

2.2.2.1 Preparation of (3,5-Me$_2$pz)$_2$NiBr$_2$ (1)

To an orange suspension of (DME)$NiBr_2$ (1.00 g, 3.25 mmol) in 20 ml CH_2Cl_2 was added 3,5-dimethylpyrazole (0.62 g, 6.50 mmol) in 20 ml CH_2Cl_2. The colour of the mixture immediately changed to dark blue. The mixture was stirred for 10 minutes, filtered and solvent removed to give a dark blue powder. Crystals suitable for X-ray analysis were obtained by slow diffusion of hexane into a CH_2Cl_2 solution of the compound, which was kept at –15 °C. Yield = 1.05 g (78%). Anal. Calcd. for $C_{10}H_{16}Br_2N_4Ni$: C, 29.24; H, 3.93; N, 13.64. Found: C, 29.14; H, 3.86; N, 13.23%. IR (nujol mull, cm^{-1}): ν(N-H) = 3328, 3225; ν(C=C) = 1612; ν(C=N) = 1564.

2.2.2.2 Preparation of (5-Mepz)$_4$NiBr$_2$ (2)

The preparation of **2** followed the same procedure as described for **1** in 2.2.2.1 starting with (DME)$NiBr_2$ (0.50 g, 1.62 mmol) and 3-methylpyrazole (0.27 g, 0.26 ml, 0.81 mmol). Light green crystals were obtained by slow evaporation of a CH_2Cl_2/ hexane (1:1) solution of the product. Yield = 0.45 g (72%). Anal. Calcd. for

$C_{16}H_{24}Br_2N_8Ni$: C, 35.14; H, 4.42; N, 20.49. Found: C, 35.32; H, 4.21; N, 20.07%. IR (nujol mull, cm^{-1}): ν(N-H) = 3291; ν(C=C) = 1653; ν(C=N) = 1561.

2.2.2.3 Preparation of $(pz)_4NiBr_2$ (3)

The preparation of **3** followed the same procedure as for **1** in 2.2.2.1 starting with $(DME)NiBr_2$ (1.00 g, 3.25 mmol) and pyrazole (0.44 g, 6.50 mmol). A pale blue powder was isolated and was insoluble in most organic solvents. Yield = 0.80 g (69%). Anal. Calcd. for $C_{12}H_{16}Br_2N_8Ni$: C, 29.37; H, 3.29; N, 22.83. Found: C, 28.98; H, 2.73; N, 21.92%. IR (nujol mull, cm^{-1}): ν(N-H) = 3230; ν(C=C) = 1622, ν(C=N) = 1574.

2.2.2.4 Preparation of $(3,5\text{-}^tBu_2pz)_2NiBr_2$ (4)

The preparation of **4** followed the same procedure as for **1** in 2.2.2.1 starting with $(DME)NiBr_2$ (0.90 g, 2.92 mmol) and 3,5-ditertbutylpyrazole (0.52 g, 5.84 mmol). A dark blue powder was isolated. Yield = 0.76 g (44%). Anal Calcd. for $C_{22}H_{40}Br_2N_4Ni$: C, 45.64; H, 6.96; N, 9.68. Found: C, 46.58; H, 8.32; 9.89%.

2.2.3 Preparation of alkanoyl pyrazolyl ligands

2.2.3.1 1,2-bis(3,5-dimethylpyrazolyl)ethane-1,2-dione, A1

A mixture of oxalyl chloride (0.66 g, 5.20 mmol) and 3,5-dimethylpyrazole (1.00 g, 10.40 mmol) were dissolved in degassed toluene (60 ml). To this mixture was added Et_3N (1 ml) and mixture was refluxed for 24 h. A white precipitate of Et_3NHCl began to form after refluxing the mixture for about 2 h. Upon filtration, the filtrate

was evaporated to dryness to give the crude product as a dirty white solid, which was purified by column chromatography using silica gel CH_2Cl_2/hexane (4:1). Yield = 0.54 g (41%). Anal. Calcd. for $C_{12}H_{14}O_2N_4$: C, 58.53; H, 5.73; N, 22.75. Found: C, 58.02; H, 5.58; N, 21.98%. ^{1}H NMR ($CDCl_3$): δ 6.05 (s, 2H, 4-Pz), 2.66 (s, 6H, 5-CH_3), 2.19 (s, 6H, 3-CH_3). $^{13}C\{^1H\}$ NMR ($CDCl_3$): δ 154.14, 143.11, 111.65, 30.34, 12.75.

2.2.3.2 1,4-bis(3,5-dimethylpyrazolyl)butane-1,4-dione, A2

The preparation of **A2** followed the same procedure as for **A1** in 2.2.3.1 and a white solid was obtained after purification. Yield = 1.05 g (75%). Anal Calcd for $C_{14}H_{18}O_2N_4$: C, 61.29; H, 6.61; N, 20.42. Found: C, 61.34; H, 6.73; N, 19.88%. ^{1}H NMR ($CDCl_3$): δ 5.96 (s, 2H, 4-Pz), 3.54 (s, 4H, CH_2, -$OC(CH_2)_2CO$-), 2.53 (s, 6H, 5-CH_3), 2.42 (s, 6H, 3-CH_3). $^{13}C\{^1H\}$ NMR ($CDCl_3$): δ 172.11, 151.55, 143.59, 110.52, 29.40, 27.83, 13.89, 13.27. IR (nujol mull, cm^{-1}): ν(C-H) = 2854; ν(C=O) = 1715; ν(C=N) = 1586.

2.2.3.3 1,5-bis(3,5-dimethylpyrazolyl)pentane-1,5-dione, A3

The preparation of **A3** followed the same procedure as for **A1** in 2.2.3.1 and a white solid was isolated after purification. Yield = 1.16 g (78%). Anal Calcd. for $C_{15}H_{20}O_2N_4$: C, 62.48; H, 6.99; N, 19.43. Found: C, 62.18; H, 7.19; N, 19.07%. ^{1}H NMR ($CDCl_3$): δ 5.93 (s, 2H, 4-Pz), 3.23 (t, 4H, CH_2, -$OC(CH_2)_3CO$-), 2.52 (s, 6H, 5-CH_3), 2.23-2.16 (m, 2H, CH_2, -$OC(CH_2)_3CO$-), 2.20 (s, 6H, 3-CH_3). $^{13}C\{^1H\}$

NMR ($CDCl_3$): δ 173.36, 151.77, 143.97, 110.91, 34.39, 18.93, 14,47, 13.72. IR (nujol mull, cm^{-1}): ν(C-H) = 2856; ν(C=O) = 1725; ν(C=N) = 1579.

2.2.3.4 1,5-bis(3,5-ditertbutylpyrazolyl)pentane-1,5-dione, A4

The preparation of **A4** followed the same procedure as for **A1** in 2.2.3.1 and a white solid was isolated after purification by column chromatography using silica gel CH_2Cl_2/diethyl ether (8:1). Yield = 0.84 g (64%). ^1H NMR ($CDCl_3$): δ 6.06 (s, 2H, 4-Pz), 2.45 (t, 4H, CH_2, $-OC(CH_2)_3CO-$), 1.95 (m, 2H, CH_2, $-OC(CH_2)_3CO-$), 1.43 (s, 18H, 5-CH_3), 1.36 (s, 18H, 3-CH_3). $^{13}C\{^1H\}$ NMR ($CDCl_3$): δ 177.79, 157.21, 97.98, 33.88, 31.46, 30.32, 20.56.

2.3 Synthesis of pyrazolyl palladium complexes

2.3.1 Reaction of 1,5-bis(3,5-dimethylpyrazolyl)pentane-1,5-dione (A3) and $(CH_3CN)_2PdCl_2$ (5)

The following synthetic method was followed for most of the attempted reactions between the α,ω-bis(3,5-R_2pyrazolyl)alkane-α,ω-dione ligands and bis(acetonitrile)palladium(II) chloride. To a solution of $(CH_3CN)_2PdCl_2$ (0.10 g, 0.38 mmol) in 20 ml CH_2Cl_2 was added (0.12 g, 0.38 mmol) of 1,5-bis(3,5-dimethylpyrazolyl)pentane-1,5-dione **(A3)**. The mixture was stirred for 24 h. The solvent was evaporated to give an orange-red residue, which was recrystallised from CH_2Cl_2/hexane. Yield = 0.057 g (34%). ^1H NMR ($CDCl_3$): δ 6.10 (s, 2H, 4-pz), 4.48 (s, 4H, CH_2, $-OC(CH_2)_3CO-$), 2.89-3.09 (m, 2H, CH_2, $-OC(CH_2)_3CO-$), 2.80 (s, 6H, 5-CH_3), 2.45 (s, 6H, 3-CH_3).

2.4 X-ray crystal structure determination of (3,5-dimethylpyrazole)$_2$NiBr$_2$ (1), and (5-methylpyrazole)$_2$NiBr$_2$ (2).

A representative crystallographic experiment is described below for (5-Mepz)$_4$NiBr$_2$ (2):

Data collection

A green-blue crystal with approximate dimensions 0.3 × 0.3 × 0.2 mm^3 was selected under oil under ambient conditions and attached to the tip of a nylon loop. The crystal was mounted in a stream of cold nitrogen at 100(2) K and centred in the X-ray beam by using a video camera. The crystal evaluation and data collection were performed on a Bruker CCD-1000 diffractometer with Mo K_α (λ = 0.71073) radiation and diffractometer to crystal distance of 0.49 cm. The initial cell constants were obtained from three series of ω scans at different starting angles. Each series consisted of 20 frames collected at intervals of 0.3° in a 6° range about ω with the exposure time of 5 seconds per frame. A total of 52 reflections were obtained.

The reflections were successfully indexed by an automated indexing routine built in the SMART program. The final cell constants were calculated from a set of 1469 strong reflections from actual data collection. The data was collected by using the hemisphere data collection routine. The reciprocal space was surveyed to the extent of full sphere to a resolution of 0.80. A total of 4414 data were harvested by collecting three sets of frames with 0.3° scans in ω with an exposure time of 15 seconds per frame. These highly redundant datasets were corrected for Lorentz and

polarization effects. The absorption correction was based on fitting a function to the empirical transmission surface as sampled by multiple equivalent measurements.[10]

Structure resolution and refinement

The systematic absences in the diffraction data were consistent for the space groups $P\bar{1}$ and $P1$. The E-statistics strongly suggested the centrosymmetric space group $P\bar{1}$ that yielded chemically reasonable and computationally stable results of refinement.[11] A successful solution by the direct methods provided mostly non-hydrogen atoms from the E-map. The remaining non-hydrogen atoms were located in an alternating series of least-squares cycle and difference Fourier maps. All non-hydrogen atoms were refined with anisotropic displacement coefficients. All hydrogen atoms were included in the structure factor calculation at idealized positions and were allowed to ride on the neighbouring atoms with relative isotropic displacement coefficients. The molecule occupies a crystallographic inversion centre with the independent portion of the crystal labeled in the attached ORTEP diagram.

The final least squares refinement of 126 parameters against 2133 data resulted in residuals R (based on F^2 for $1>2\sigma$) and wR (based on F^2 for all data) of 0.0244 and 0.0651 respectively. The final difference Fourier map was featureless. The ORTEP diagram is drawn with 50% probability ellipsoids.

2.5 Results and discussions

2.5.1 Synthesis of substituted pyrazole complexes

The complexes $(3,5\text{-}Me_2Pz)_2NiBr_2$ **(1)**, $(5\text{-}MePz)_4NiBr_2$ **(2)**, $(Pz)_4NiBr_2$ **(3)** and $(3,5\text{-}{}^tBu_2pz)_2NiBr_2$ **(4)** were prepared according to Scheme 2.1. In this synthetic route, $(DME)NiBr_2$ is suspended in dichloromethane and to this suspension the appropriate pyrazole ligand in dichloromethane is added. In the case of **1** a dark blue solution formed immediately on addition of the ligand and reaction was complete in 10 minutes. The dark blue reaction mixture was filtered off to remove any unreacted residues and the filtrate was recrystallised in dichloromethane/hexane solution at -15°C.

Complex **2** behaved the same way as complex **1** during synthesis, and the light green crystals were obtained after recrystallisation. Complex **3** on the other hand was isolated as a pale blue powder and found to be insoluble in most organic solvents. The presence of the substituents on the pyrazole ring improves the solubility of the solubility of these complexes in most organic solvents. When reaction time for the synthesis of complex **1** was longer than 15 minutes, an insoluble pale blue solid was isolated. The elemental analysis data suggested that the insoluble solid could be formulated as compound **1B** shown in Scheme 2.1. This insoluble product form because this complex polymerize if the reaction times are very long. Because of the above problems reaction times were kept to 10 minutes. The reported procedure for the preparation of these substituted pyrazole nickel complexes (**1**, **2**, **3**) uses

alcoholic or aqueous solution as a solvent medium and has been reported by Reedjik[2] and others.[4]

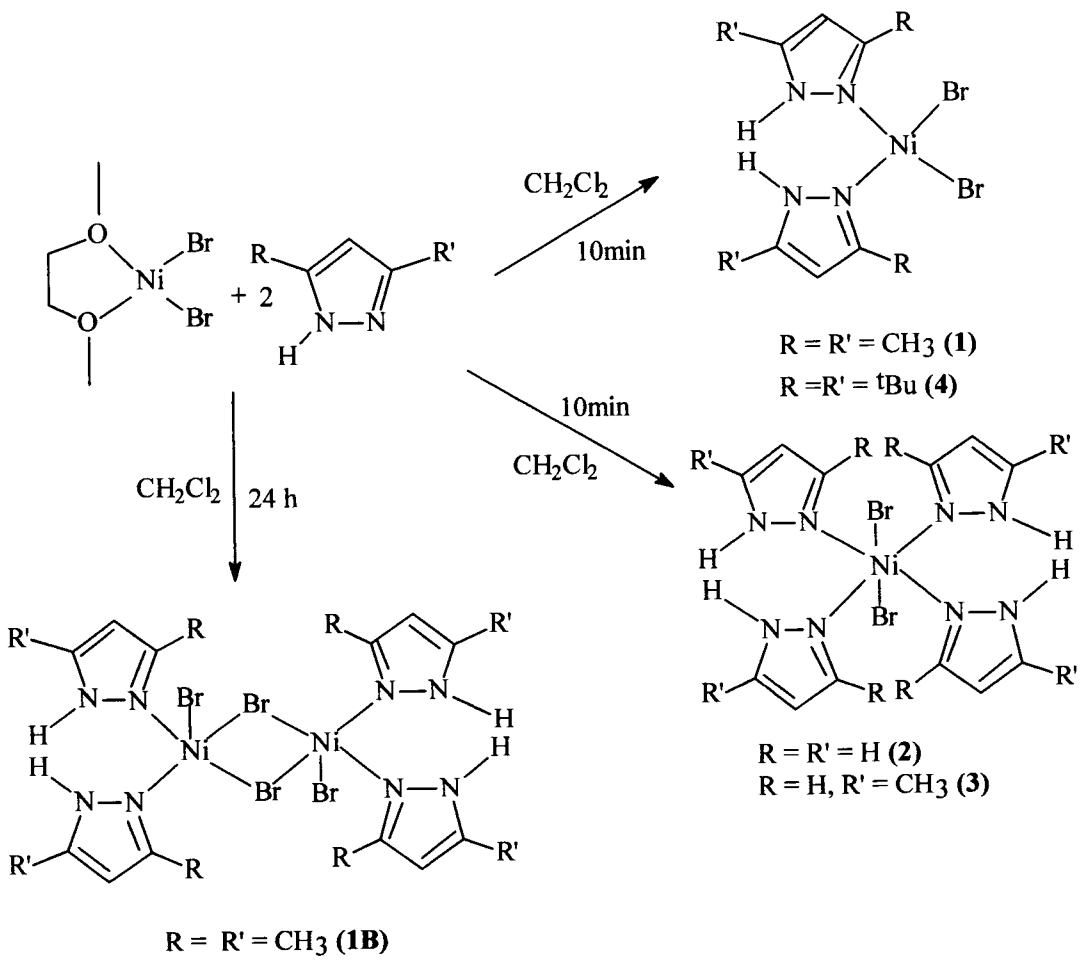

Scheme 2.1: Synthetic route to substituted pyrazole nickel complexes

The ^{1}H NMR spectra of these complexes were at best very broad or in most cases showed no peaks other than the NMR solvent, for example a spectrum of complex **1** (Figure 2.1). This is typical of paramagnetic compound. Literature reports show that **3** is soluble in water. Hence the ^{1}H NMR of **3** was run in D_2O. The spectrum showed three broad peaks (Fig. 2.2). Again this suggests the presence the presence of a paramagnetic material. From the single crystal structure of **1** discussed in the next section of this Chapter, it is clear why **1** is paramagnetic. With a tetrahedral structure, this d^8 system is expected to have two unpaired electrons in its HOMO, hence the paramagnetism. However the solid structures of **2** and **3** are six coordinate and hence octahedral. The single X-ray structure of **2** is shown in Figure 2.5. Both **2** and **3** show paramagnetic behavior, which suggests that, some equilibrium between a four coordinate, tetrahedral form (paramagnetic) and a six coordinate octahedral form (diamagnetic) of these compounds exists in solution.

As far as we know complex **4** ($3,5\text{-}^t\text{Bu}_2\text{pz})_2\text{NiBr}_2$) has never been reported before. The synthetic route for **4** is similar to that of **1**. This complex is highly unstable in solution when kept longer than 2 h. The reason for the high instability of **4** may due to the steric bulk of the tertbutyl substituents on the pyrazole ring which crowd the nickel centre. Elemental analysis data shows that in **4** there are two 3,5-ditertbutylyrazole rings around the nickel centre and two Br atoms. This complex is expected to have a distorted tetrahedral geometry around the nickel centre similar to that of complex **1**. Efforts to grow single crystals of this complex were unsuccessful due to its lack of stability. Characterization of complex **4** by ^{1}H NMR spectroscopy

showed this complex to be paramagnetic. This is because in most cases when nickel is surrounded by bulky substituents, tetrahedral geometry is preferred over a square planar geometry. Hence the formation of a six coordinate complexes for **2**, **3** and four coordinate complexes for **1**, **4** is explained in terms of steric bulk of the pyrazole ligands. In **2**, **3** pyrazole rings do not have bulky substituents, so the coordination of four rings around the nickel centre is possible. One interesting observation that relates steric bulk with geometry is the solid-state structure of **2.** Even though **3**-methylpyrazole was used as a starting material for the synthesis of **2**, the structure shows the ligand to be 5-methylpyrazole in the complex. It is well known that 3-methylpyrazole readily tautomerizes to 5-methylpyrazole,[4] hence to avoid steric crowding in **2** the ligand undergoes this tautomeric process. Because of the paramagnetism found in solutions of complexes **1-4**, the best characterization of these complexes was done by IR spectroscopy, elemental analysis and single X-ray diffraction studies. The IR spectra of all complexes prepared in this study displayed peaks around 3200 cm^{-1} ν(N-H). Other characteristic peaks associated with pyrazole rings were observed at 1612 cm^{-1} ν(N-C) and 1590 cm^{-1} ν(C-H). An IR spectrum (Fig. 2.3) of $(pz)_4NiBr_2$ is representative of all the nickel pyrazole complexes.

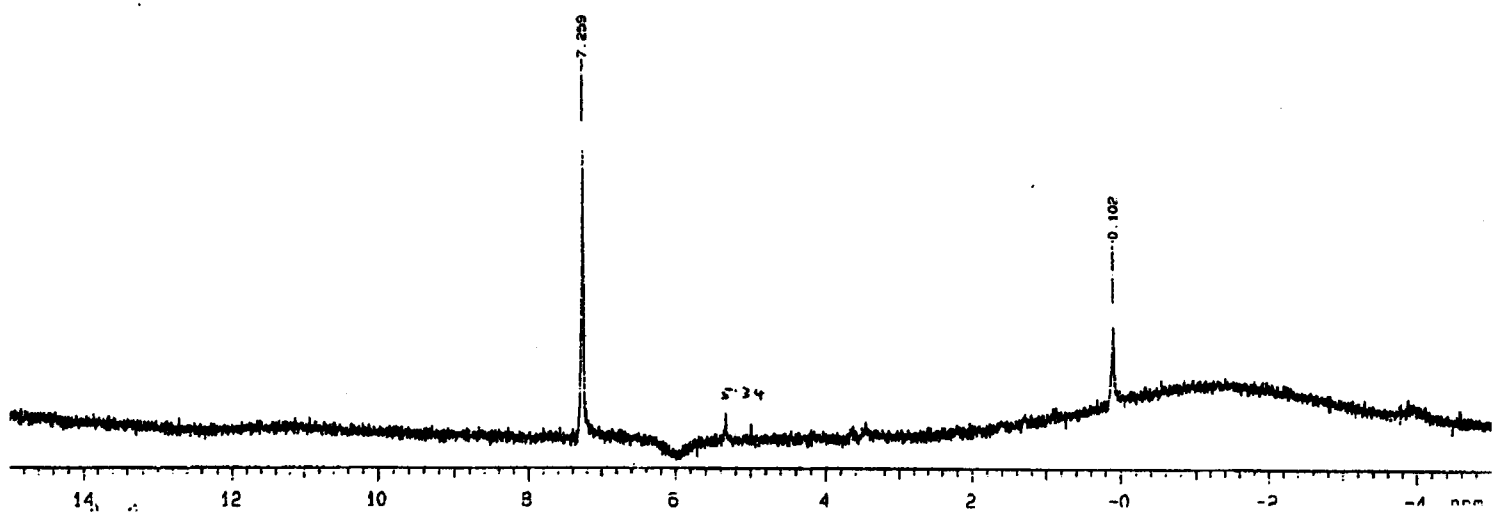

Figure 2.1: ^{1}H NMR spectrum of complex **1** in $CDCl_3$

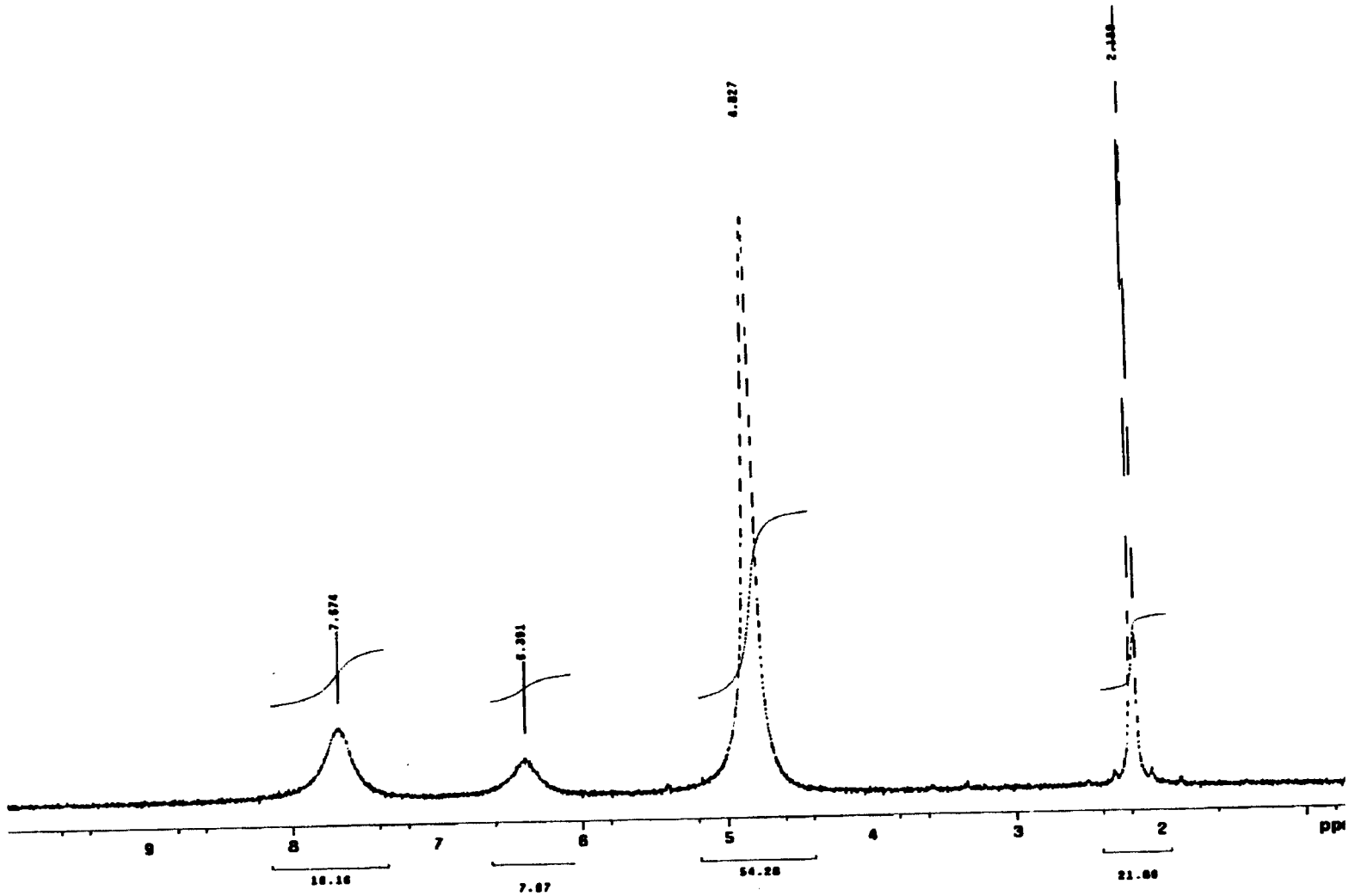

Figure 2.2: ^{1}H NMR spectrum of complex **3** in D_2O

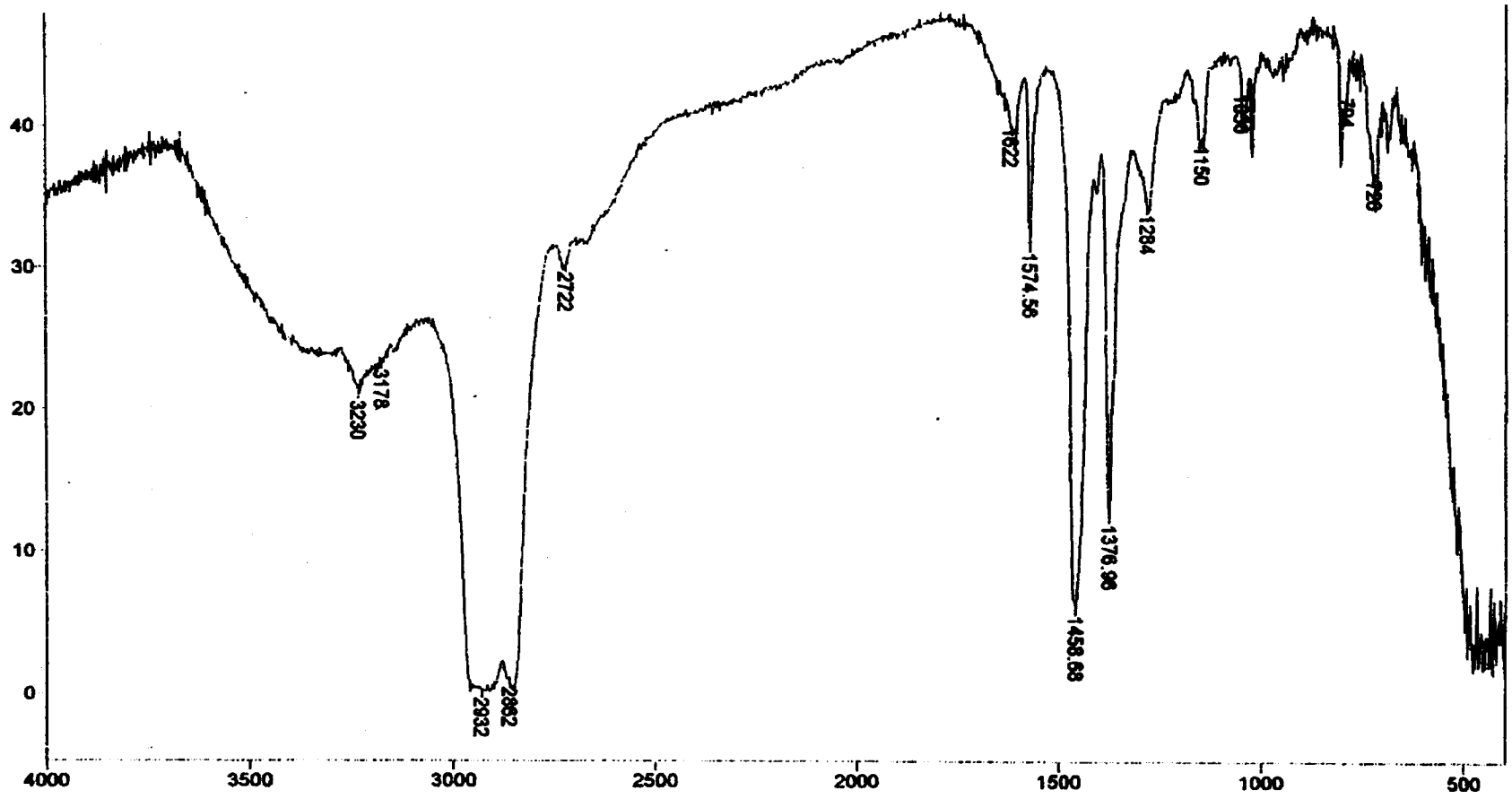

Figure 2.3: IR spectrum of complex **3**

2.5.2 Molecular structure of 1

Crystals of **1** suitable for X-ray analysis were grown from CH_2Cl_2/hexane at -15°C. Table 2.1 summarizes the experimental crystal data for **1**, and Table 2.2 gives selected bond distances and angles. An ORTEP diagram of molecule **1** including the atom-numbering scheme is shown in Figure 2.4. The 3,5-dimethylpyrazole ligand behaves as a monodentate ligand and coordinates to the metal through the N2 of the ring. The Ni atom in this complex is in a distorted tetrahedral environment with two substituted pyrazole ligands trans to each other and two Br atoms completing the coordination sphere. Poddar et al.[12] has proposed an octahedral complex from spectroscopic data consisting of four pyrazole and two bromo ligands around the metal centre. This octahedral complex looses two moles of the ligand to form a tetrahedral complex on heating at 130-150°C for 8 h. In contrast to Poddar's observation, complex **1** was not formed on heating. The product formed did not show any change of geometry in solid state or in solution. As can be seen in the ORTEP diagram of **1** the pyrazole NH groups are trans to each other and H atoms point away from the Br atoms. The bond angles around the metal centre are 98.90(12)°, 113.45(12)°, 115.14(12)°, 99.73(12)° corresponding to N(1)-Ni-Br(2), N(3)-Ni-Br(2), N(1)-Ni-Br(1), N(3)-Ni-Br(1) respectively. These bond angles are evident of a distorted tetrahedral geometry around the metal centre. The Ni-Br bond distances (2.366(9) and 2.379(8) Å) are shorter compared to those reported for Ni-Br bond distances 2.682(1) Å in $(pz)_4NiBr_2$ and $(CH_2Me_2pz)_2Ni_2Br_4$ complexes.[2,13] The Ni-N bond distances are 1.971(4) and 1.975(4) Å for Ni-N(3) and Ni-N(4) respectively.

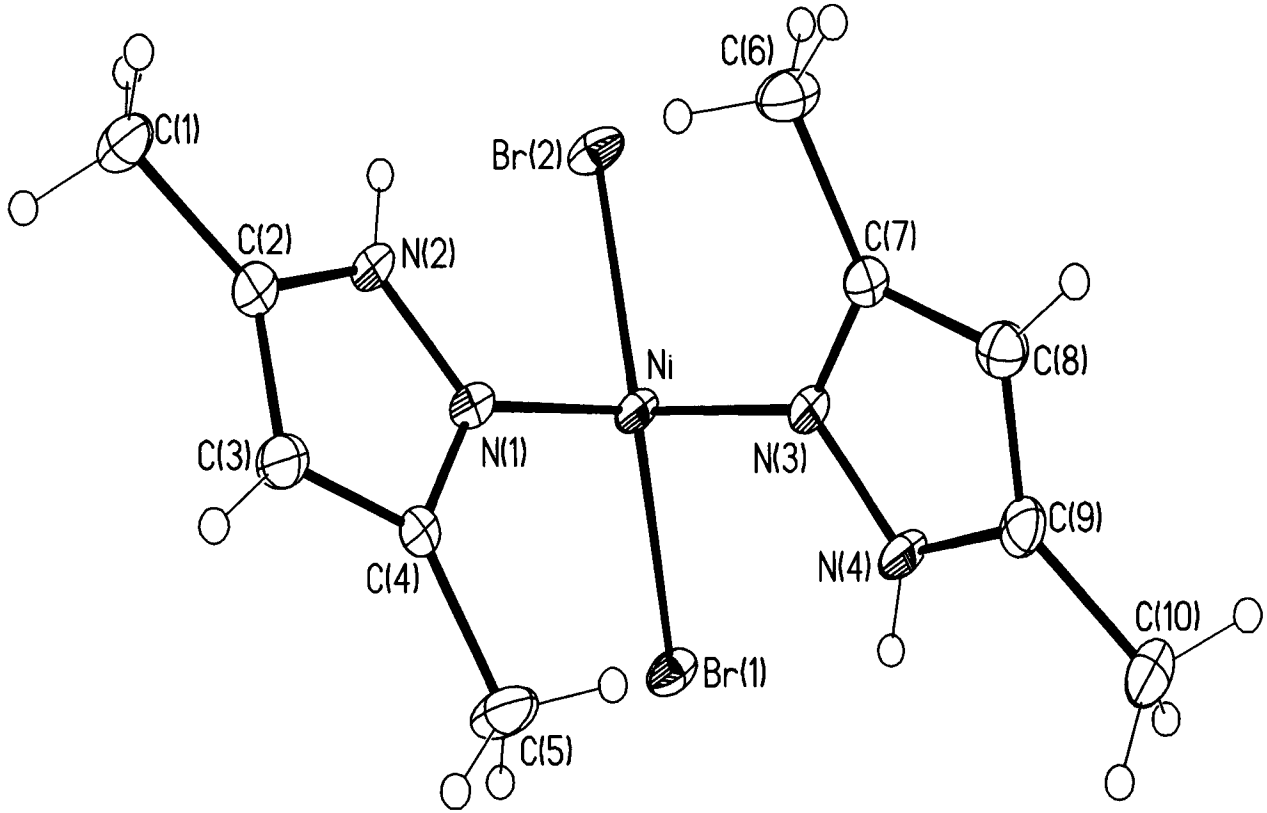

Figure 2.4: ORTEP diagram of complex **1**

Table 2.1: Crystal data and structure refinement for **1**

Empirical formula:	$C_{10}H_{16}Br_2N_4Ni$	
Formula weight:	410.8	
Temperature:	173(2) K	
Wavelength:	0.71073	
Crystal system:	Monoclinic	
Space group:	$P2_1/n$	
Unit cell dimensions:	a = 8.3441(11) Å	$\alpha = 90°$
	b = 14.261(2) Å	$\beta = 97.721°$
	c = 12.4449(16) Å	$\gamma = 90°$
Volume:	1467.5(3) $Å^3$	
Z:	4	
Density (calculated):	1.859 Mg/m^3	
Absorption coefficient:	6.753 mm^{-1}	
F(000):	808	
Crystal size:	0.40 × 0.30× 0.20 mm^3	
Theta range for data collection:	2.18 to 26.41°	
Index ranges:	-10<=h<=10, 0<=k<=17, 0<=l<=15	
Reflections collected:	6973	
Independent reflections:	2900 [R(int) = 0.0400]	
Completeness to theta =26.41°:	96.1%	
Absorption correction:	Empirical with SADABS	
Max. and min. transmission:	0.3453 and 0.1731	
Refinement method:	Full-matrix least-squares on F^2	
Data/restraints/parameters:	2900/0/159	
Goodness-of-fit on F^2:	1.000	
Final R indeces[1>2sigma(1)]:	R1 = 0.0403, wR2 = 0.0938	
R indeces (all data):	R1 = 0.0787, wR2 = 0.1065	
Largest diff. Peak and hole:	0.773 and – 0.565 $e.Å^{-3}$	

Table 2.2: Bond lengths [Å] and angles [°] for **1**

Bond lengths [Å]			
Ni-N(1)	1.971(4)	N(4)-C(9)	1.356(7)
Ni-N(3)	1.975(4)	C(1)-C(2)	1.505(6)
Ni-Br(2)	2.3662(9)	C(2)-C(3)	1.366(7)
Ni-Br(2)	2.3791(8)	C(3)-C(4)	1.384(7)
N(1)-N(2)	1.354(5)	C(4)-C(5)	1.484(7)
N(1)-N(4)	1.358(6)	C(6)-C(7)	1.495(7)
N(2)-C(2)	1.348(7)	C(7)-C(8)	1.390(7)
N(3)-C(7)	1.335(6)	C(8)-C(9)	1.360(7)
N(3)-N(4)	1.367(5)	C(9)-C(10)	1.492(7)

Bond angles [°]			
N(1)-Ni-N(3)	101.78(18)	N(2)-C(2)-C(3)	105.6(5
N(1)-Ni-Br(2)	98.90(12)	N(2)-C(2)-C(1)	121.8(5)
N(3)-Ni-Br(2)	113.45(12)	C(3)-C(2)-C(1)	132.6(5)
N(1)-Ni-Br(1)	115.14(12	C(2)-C(3)-C(4)	107.9(5)
N(3)-Ni-Br(1)	99.73(12)	N(1)-C(4)-C(3)	109.0(4)
Br(2)-Ni-Br(1)	125.94(12)	N(1)-C(4)-C(5)	120.6(5)
N(2)-N(1)-C(4)	105.1(4)	C(3)-C(4)-C(5)	130.4(5)
N(2)-N(1)-N	122.9(3)	N(3)-C(7)-C(8)	109.5(5)
C(4)-N(1)-Ni	132.0(3)	N(3)-C(7)-C(6)	121.4(5)
C(2)-N(2)-N(1)	112.4(4)	C(8)-C(7)-C(6)	129.0(5)
C(7)-N(3)-N(4)	105.9(4)	C(9)-C(8)-C(7)	107.4(5)
C(7)-N(3)-Ni	132.1(3)	N(4)-C(9)-C(8)	106.3(5)
N(4)-N(3)-Ni	122.0(3)	N(4)-C(9)-C(10)	121.1(5)
C(9)-N(4)-N(3)	110.9(4)	C(8)-C(9)-C(10	132.6(5)

2.5.3 Molecular structure of 2

Table 2.3 summarizes the experimental crystal data for complex **2**. Bond lengths and bond distances are shown in Table 2.4 and the ORTEP diagram is shown in Fig. 2.5. An earlier report on a proposed structure by Reedijk[4] was based on elemental analysis, magnetic moment measurements and powder X-ray data. They proposed a six coordinate complex, suggesting that the complex has an octahedral geometry. Our single crystal X–ray crystallographic data agrees with the proposed structure by Reedjik and a detailed description of the structure will be discussed in this section.

The structure has Ni coordinated to four substituted pyrazoles through the nitrogen atom in position 2 of the pyrazole ring and two bromo atoms. The methyl group has also moved from position 3 in the ligand to position 5. This rearrangement makes it possible for the four 3(5)-methylpyrazole rings to be accommodated around the nickel. The reason for this observation is that the methyl groups in the 5 position of the ring are pointing away from the metal centre, so there is more coordination space. In this complex there are two rings above and below the nickel plane, in other words the complex has slightly different halves. The angle between opposite pyrazole rings in different planes, N(2)-Ni-N(2) and N(4)-Ni-N(4) is exactly 180°, which is typical of an octahedral geometry. The N(2)-Ni-N(4) bond angles are 88.87(7) and 91.13(7)°, which are assigned to both halves of the complex. The Ni-N bond distances, Ni-N(2); 2.0996(18) Å and Ni-N(4); 2.1004(18) Å differ slightly, which means that complex is close to being symmetrical. These bond distances are longer compared to that of **1**, Ni-N(1); 1.971(4) Å and Ni-N(3); 1.975(4) Å. The

longer bond distances prevent the interaction of neighbouring pyrazole rings around the nickel centre. The bromide ions are located trans to each other and the Ni-Br(1) bond distance is 2.6617(2) Å which is longer compared to that of complex **1** (2.3727(8) Å). This Ni-Br bond distance is a bit shorter in comparison to that of octahedral pyrazole nickel $(pz)_4NiBr_2$ which is 2.682(1) Å.[2] In general the Ni-Br bond distance is long compared to other related nickel complexes, these bond distances between 2.331(1) and 2.515(1) Å.[13] This complex was found to contain hydrogen bonds between N-H and Br; (N(1)-H(1)....Br(1) = 2.54(3) Å and N(3)-H(3)....Br(1) = 3.10 Å as shown in Table 2.5.

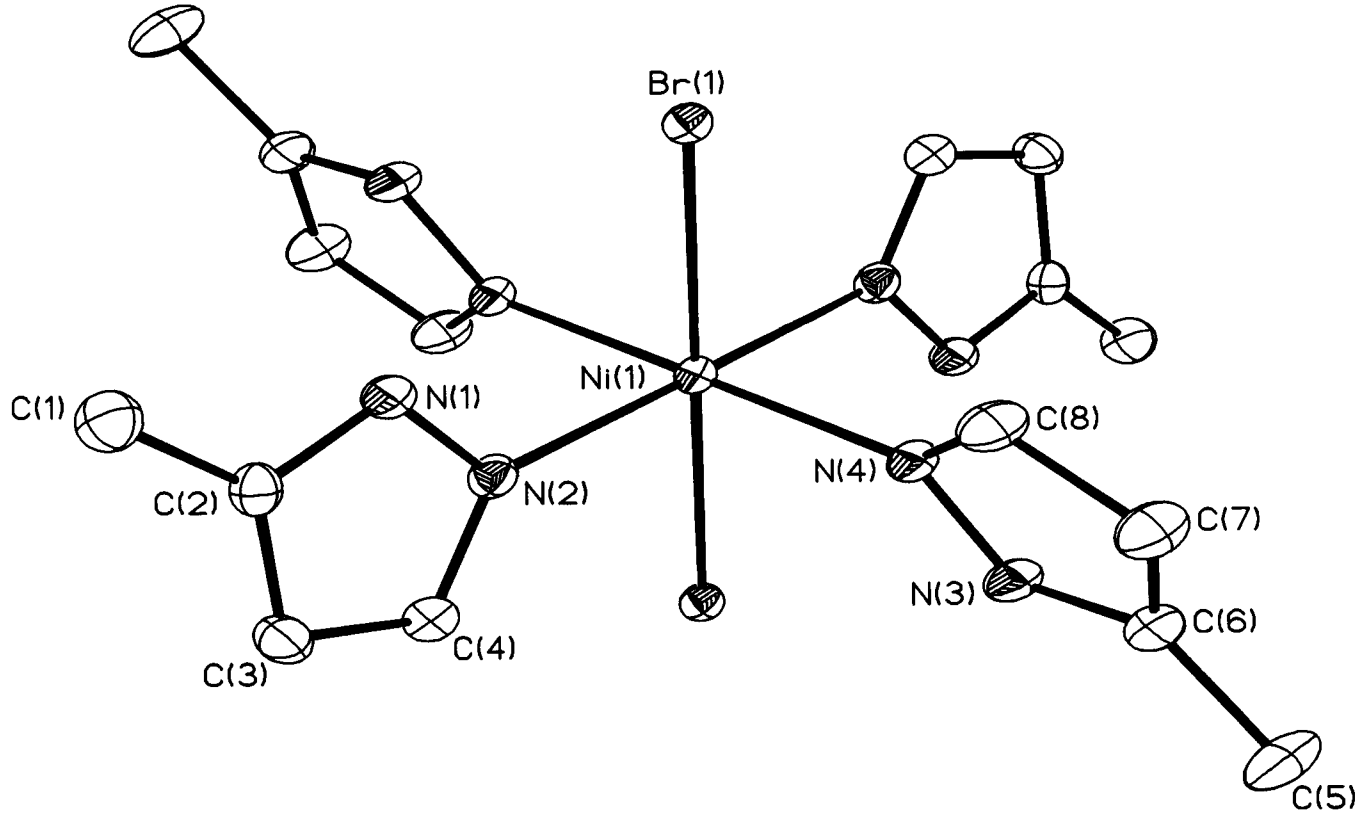

Figure 2.5: ORTEP diagram of **2**. The labeled atoms comprise the asymmetric portion of the unit cell with Ni(1) located at the crystallographic inversion center. All atoms are shown with 50% thermal probability ellipsoids.

Table 2.3: Crystal data and structure refinement for **2**

Empirical formula:	$C_{16}H_{24}Br_2N_8Ni$
Formula weight:	546.96
Temperature:	100(2) K
Wavelength:	0.71073 Å
Crystal system:	Triclinic
Space group:	P1
Unit cell dimensions:	a = 7.5408(4) Å α = 92.086(1)°
	b = 8.5615(4) Å β = 105.470(1)°
	c = 9.3947(4) Å γ = 114.453(1)°
Volume:	524.62(4) $Å^3$
Z:	1
Density (calculated):	1.731 Mg/m^3
Absorption coefficient:	4.751 mm^{-1}
F(000):	274
Crystal size:	0.30 × 0.30× 0.20 mm^3
Theta range for data collection:	2.28 to 26.37°
Index ranges:	-9<=h<=9,-10<=k<=10, -11<=l<=11
Reflections collected:	4414
Independent reflections:	2133 [R(int) = 0.0181]
Completeness to theta =26.41°:	99.5%
Absorption correction:	Empirical with SADABS
Max. and min. transmission:	0.4500 and 0.3298
Refinement method:	Full-matrix least-squares on F^2
Data/restraints/parameters:	2133/0/160
Goodness-of-fit on F^2:	1.042
Final R indeces[1>2sigma(1)]:	R1 = 0.0244, wR2 = 0.0648
R indeces (all data):	R1 = 0.0249, wR2 = 0.0651
Largest diff. Peak and hole:	0.792 and –0.489 $e.Å^{-3}$

Table 2.4: Bond lengths [Å] and angles [°] for **2**

Bond lengths [Å]			
Br(1)-Ni	2.6617(2)	N(3)-C(6)	1.345(3)
Ni-N(2)	2.0996(18)	N(3)-N(4)	1.357(3)
Ni-N(2)	2.0996(18)	N(4)-C(8)	1.333(3)
Ni-N(4)	2.1004(18)	C(1)-C(2)	1.498(3)
Ni-N(4)	2.1004(18)	C(2)-C(3)	1.378(3)
Ni-Br(1)	2.6617(2)	C(3)-C(4)	1.398(3
N(1)-C(2)	1.343(3)	C(5)-C(6)	1.496(3)
N(1)-N(2)	1.360(3)	C(6)-C(7)	1.375(3)
N(2)-C(4	1.335(3)	C(7)-C(8	1.399(3)

Bond angles [°]			
N(2)-Ni-N(2	180	C(4)-N(2)-Ni	133.72(15)
N(2)-Ni-N(4	88.87(7)	N(1)-N(2)-Ni	121.92(14)
N(2)-Ni-N(4)	91.13(7)	C(6)-N(3)-N(4)	112.70(19)
N(2)-Ni-N(4	91.13(7)	C(8)-N(4)-Ni	104.38(18)
N(2)-Ni-N(4)	88.87(7)	C(8)-N(4)-N(3)	133.18(15)
N(4)-Ni-N(4)	180.0	N(3)-N(4)-Ni	122.39(14)
N(2)-Ni-Br(1)	89.79(5)	N(1)-C(2)-C(3)	106.12(19)
N(2)-Ni-Br(1)	90.21(5)	N(1)-C(2)-C(1)	121.1(2)
N(4)-Ni-Br(1	89.81(5)	C(3)-C(2)-C(1)	132.7(2)
N(4)-Ni-Br(1)	90.19(5)	C(2)-C(3)-C(4)	105.6(2)
N(2)-Ni-Br(1)	89.79(5)	N(2)-C(4)-C(3)	111.2(2)
N(4)-Ni-Br(1)	90.19	N(3)-C(6)-C(7)	106.24(19)
N(4)-Ni-Br(1)	132.1(3)	N(3)-C(6)-C(5)	122.0(2)
Br(1)-Ni-Br(1)	180.0	C(7)-C(6)-C(5)	131.7(2)
C(2)-N(1)-N(2)	112.85(18)	N(6)-C(7)-C(8)	105.5(2)
C(4)-N(2)-N(1)	104.27(18)	C(4)-C(8)-C(7)	111.2(2)

Table 2.5: Hydrogen bonds for **2** [Å and °].

D-H...A	d(D-H)	d(H...A)	d(D...A)	<(DHA)
N(1)-H(1)...Br(1)	0.87(3)	2.54(3)	3.2198(19)	136(2)
N(3)-H(3)...Br(1)	0.87(3)	2.62(3)	3.225(2)	128(2)
N(1)-H(1)...Br(1)	0.87(3)	3.10(3)	3.7320(19)	131(2)
N(3)-H(3)...Br(1)	0.87(3)	2.95(3)	3.650(2)	139(2)

2.5.4 Synthesis of α,ω-bis(3,5-R$_2$pyrazolyl)alkane-α,ω-dione ligands

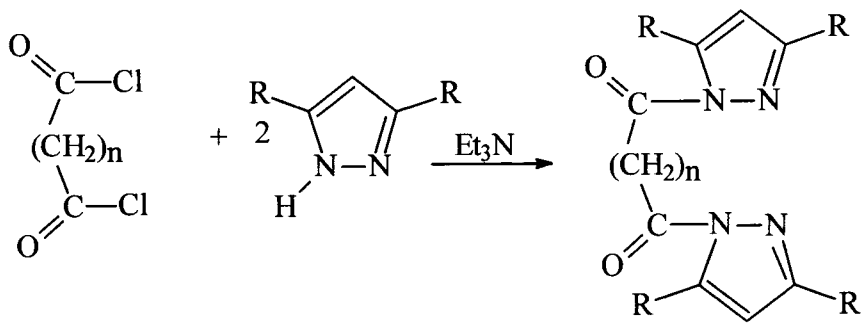

R = CH_3; n = 0 **(A1)**, n = 2 **(A2)**, n = 3 **(A3)**

R = ^tBu; n = 3 **(A4)**

Scheme 2.2: α,ω-bis(3,5-R_2pyrazolyl)alkane-α,ω-dione ligands

Pyrazolyl ligands with alkane-α,ω-dione linkers were prepared by reacting the appropriate substituted pyrazole ligand and the alkanoyl chloride according to Scheme 2.2. The ligands are distinguished by the number of CH_2 units in the linker. Their synthesis involves dissolving both reactants in toluene, followed by the addition of the base triethylamine (Et_3N). Toluene was used as a solvent in these reactions because the by-product Et_3NHCl is not soluble in toluene, but the product is soluble in toluene. The by-product could therefore be filtered off fairly easily. The reactions were found to take place only after addition of the base as evidenced by the colour changes and precipitate formation that occurred immediately after the addition of the base. The role of the base in these reactions was to deprotonate the acidic protons of pyrazole compounds and to remove the chloride from the carbonyl chloride, thereby forming the amine salt $Et_3NH^+Cl^-$ as the by-product. The colour

'changes varied from dirty white to dark brown and the resultant products were found to be white after purification by column chromatography (silica gel, CH_2Cl_2/hexane, 4:1 for **A1-A3** and CH_2Cl_2/diethyl ether, 8:1 for **A4**). These compounds were found to be soluble in most organic solvents, which made their characterization easy.

All the ligands were fully characterized by elemental analysis, IR spectroscopy and NMR spectroscopy. The IR spectra of these ligands were not significantly different and the spectrum of **A3** in Figure 2.6 was chosen as the representative spectrum for all the ligands. It is observed in the spectrum that a peak at around 3200 cm^{-1} ν(N-H) disappears in these ligands, which proves linkage of the alkane-α,ω-dione moiety to the pyrazole through the 1-H. A broad peak between 2856-2900 cm^{-1} which is assignable to the CH_2 units of the linker is observed in the spectrum. A sharp peak around 1700 cm^{-1} which is assignable to the carbonyl group is observed in this spectrum. This peak is not observed in the spectrum of the unlinked substituted pyrazole ligand. The peaks at 1612 cm^{-1} ν(C-C) and around 1590 cm^{-1} ν(C-H) are also observed. These peaks have shifted slightly due to the presence of the carbonyl group. The ^1H NMR spectrum (Fig. 2.7) of **A3** is chosen as a representative spectrum for all the ligands and ^{13}C NMR spectrum of **A3** is shown in Fig. 2.8. The absence of a peak around 11.80 ppm belonging to N-H proton shows that the pyrazole is linked to this alkane-α,ω-dione moeity. A closer look at the ^1H NMR spectra of these ligands shows that the presence of carbonyl group shifts the peaks slightly downfield. In most cases in the spectrum of the unlinked substituted pyrazole ligand, the proton at position four of the ring appears around 5.50 ppm, but in these new

ligands the peaks are between 5.90-6.06 ppm. A peak assignable to the protons in the CH_2 unit is observed at 3.22 ppm in the spectrum. These ligands were also characterized by ^{13}C NMR, and the peaks observed in the spectra are as expected. A peak around 173 ppm in the **A3** ligand spectrum which belongs to carbonyl group carbon is obeserved. The peak at 151 ppm which is assignable to the carbon of the two terminal CH_2 units appear as a singlet because the two CH_2's in **A3** ligand closer to the carbonyl group are equivalent. The carbon from the CH_2 unit which is sandwiched between the two terminal CH_2 units appear as a singlet at 143 ppm. The peaks (110, 34, 18, 14, 13) which belong to the pyrazole ring carbons have shifted downfield due to the carbonyl group in the linker.

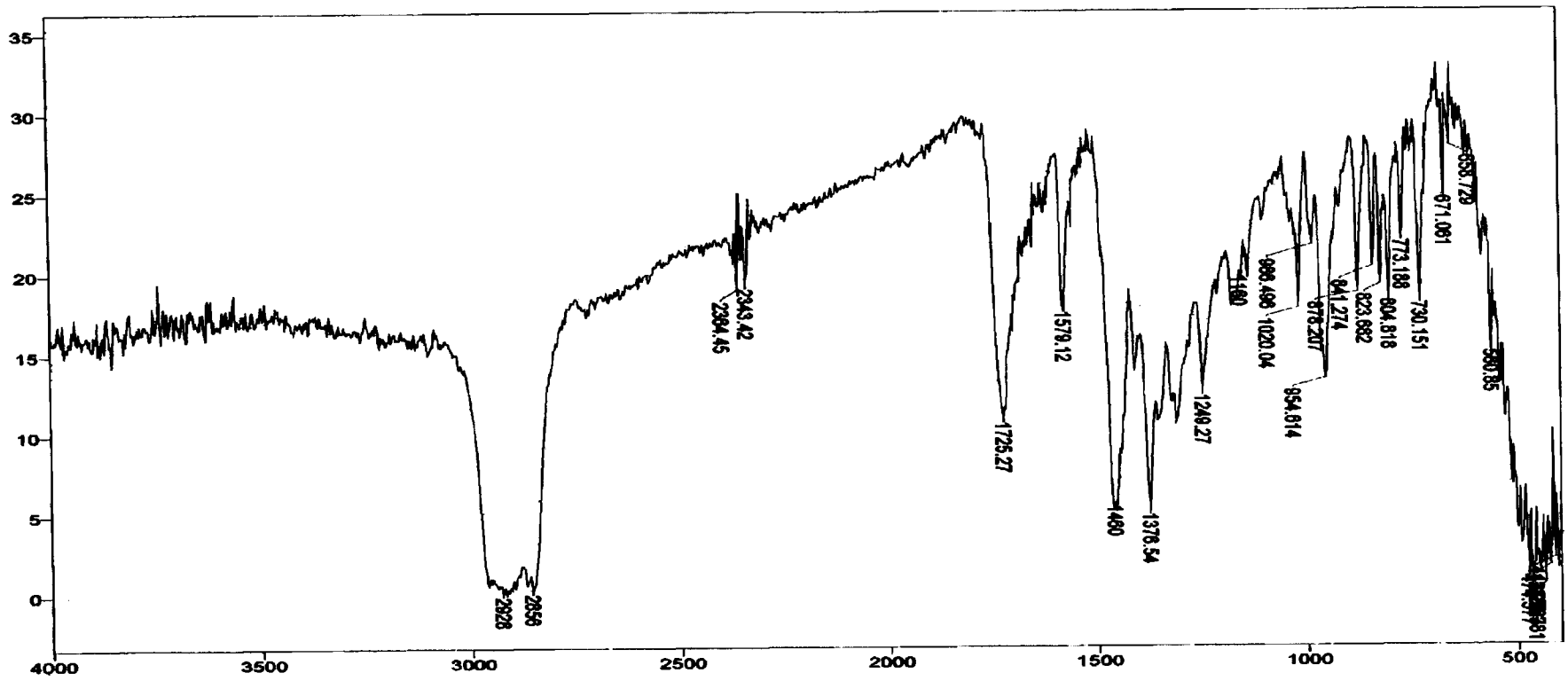

Figure 2.6: IR spectrum of ligand **A3**

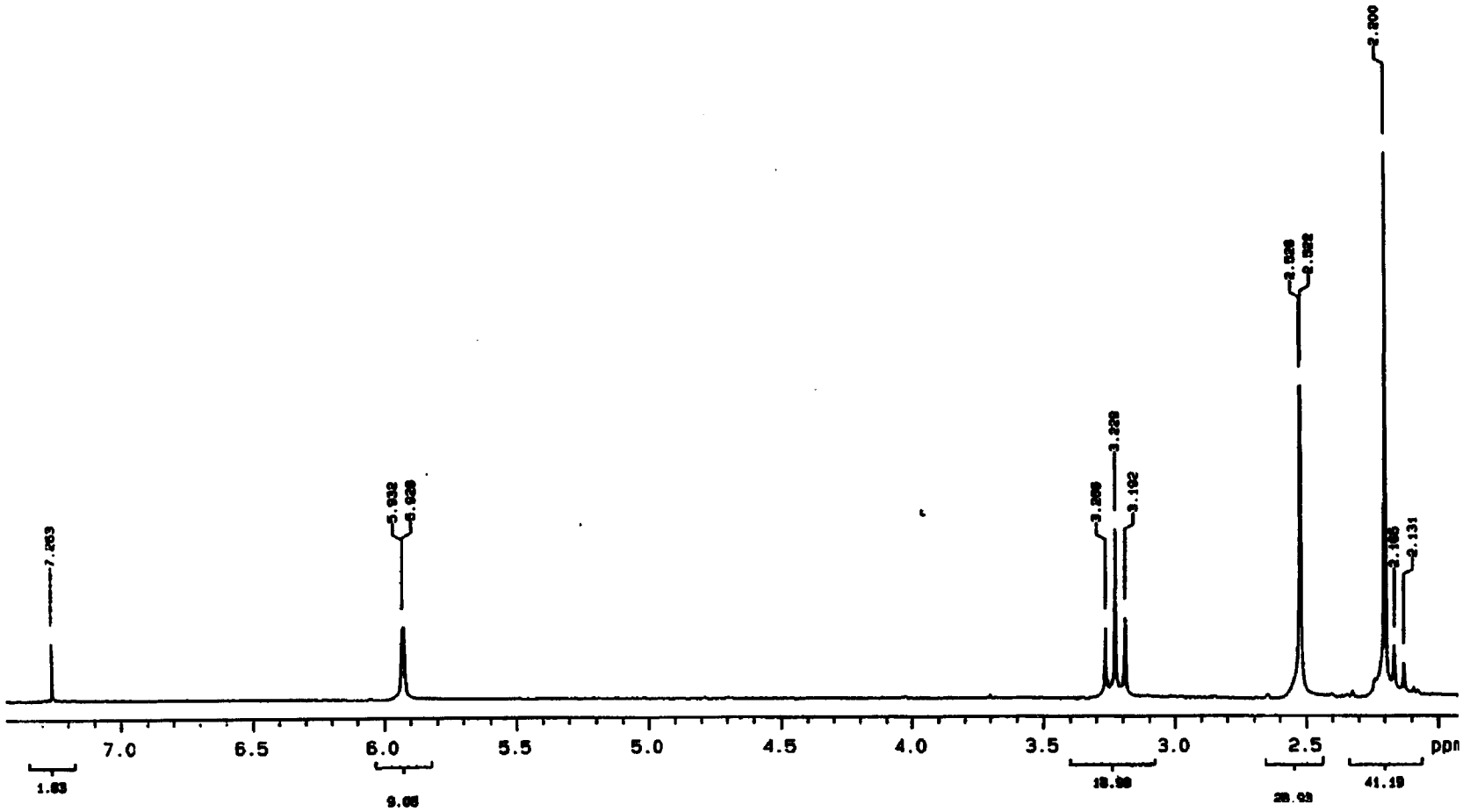

Figure 2.7: ^{1}H NMR spectrum of ligand **A3**

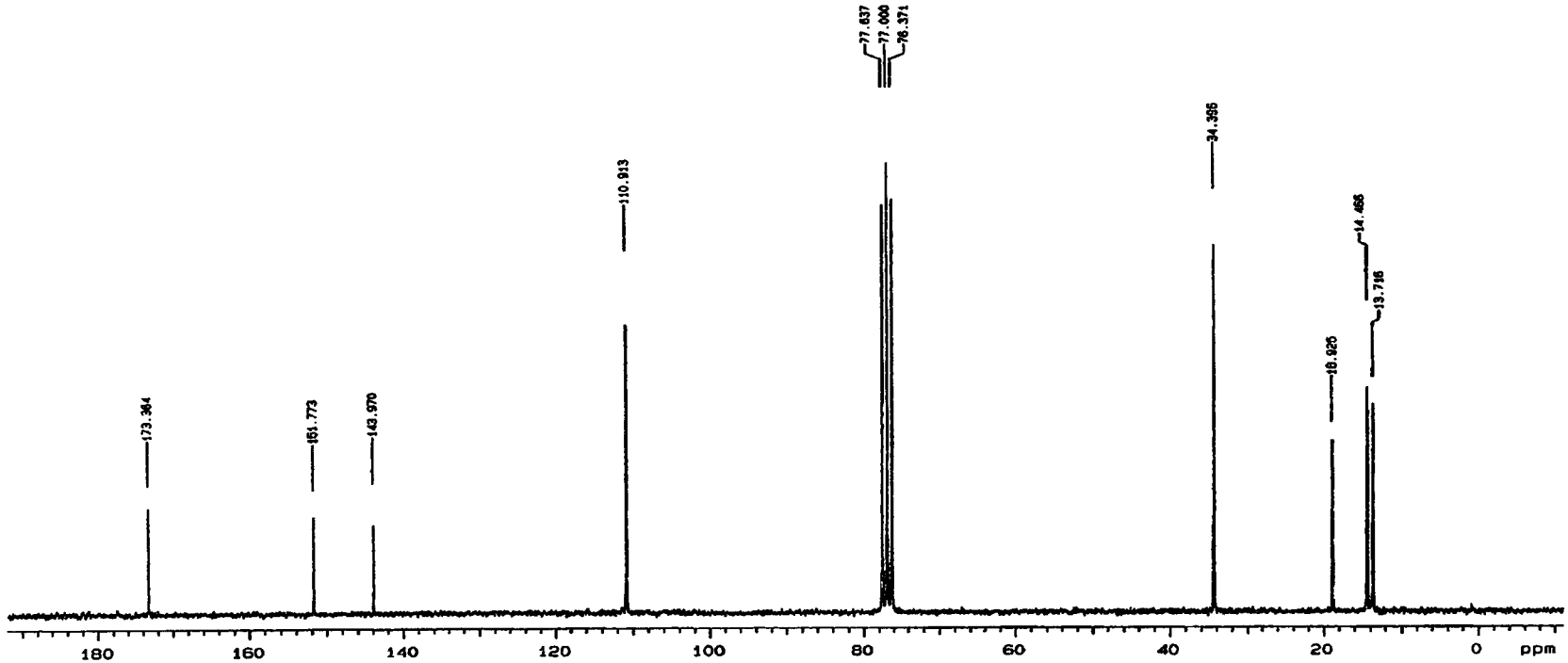

Figure 2.8: ^{13}C NMR spectrum of **A3** ligand

2.5.5 Synthesis of α,ω-bis(3,5-R_2*pyrazolyl)alkane-*α,ω*-dione palladium complexes*

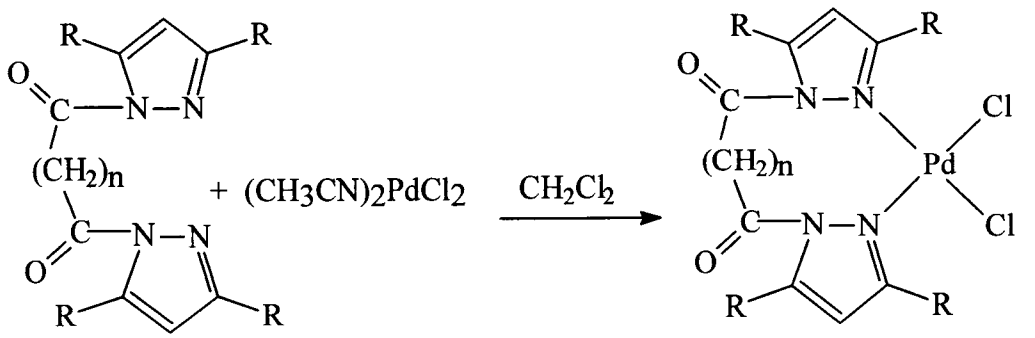

R = CH_3; n = 0 **(A1)**, n = 2 **(A2)**, n = 3 **(A3)**
R = ^{t}Bu; n = 3 **(A4)**

Scheme 2.3: Synthesis of α,ω-bis(3,5-R_2pyrazolyl)alkane-α,ω-dione palladium complexes

Complexes of the ligands prepared in Scheme 2.2 were performed by a reaction between an appropriate ligand and $(MeCN)_2PdCl_2$ as described in Scheme 2.3. Generally synthesis of these complexes is supposed to be simple, but from the reactions attempted this generalization does not hold. The complexes expected to be obtained are of the form $(pz(O)C(CH_2)_nC(O)pz)PdCl_2$; (n =0, 2, 3) with structures similar to those obtained for poly(1-pyrazolylmethane) palladium complexes[16], described in Chapter 1. The colour of the products formed from these reactions varied from orange to red depending on the ligand used. The characterization of the products was mainly done by elemental analysis and ^{1}H NMR spectroscopy.

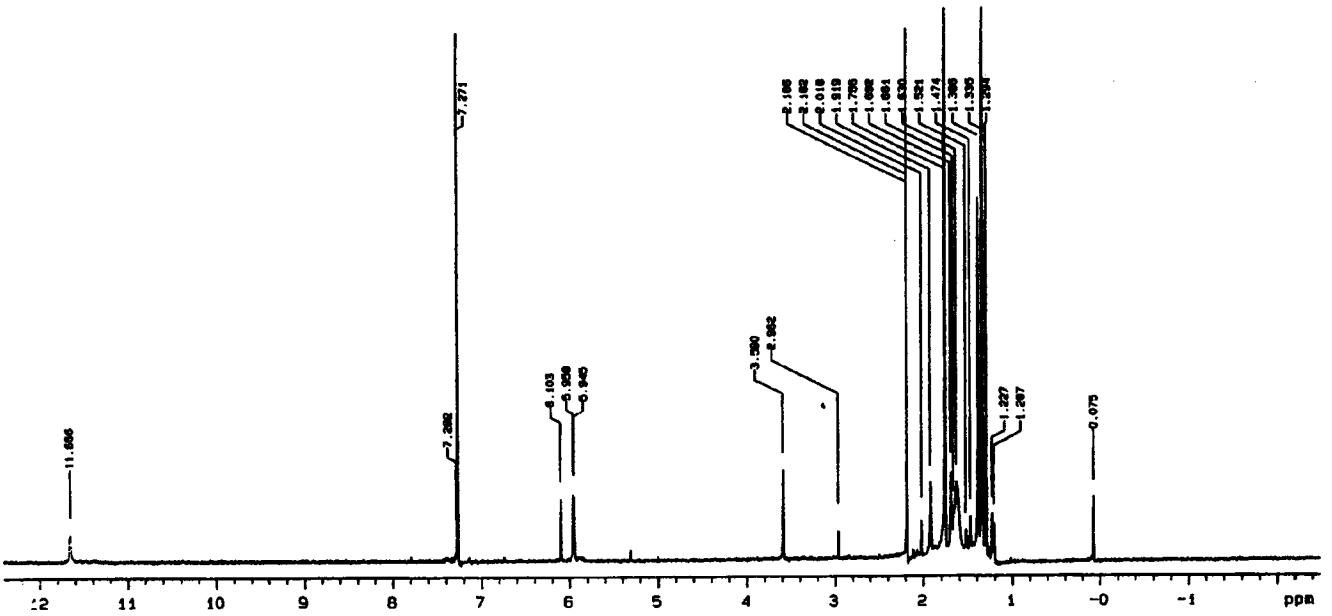

Figure 2.9: ^{1}H NMR of mixture of **A2** ligand complex and $(3,5\text{-}Me_2pz)_2PdCl_2$

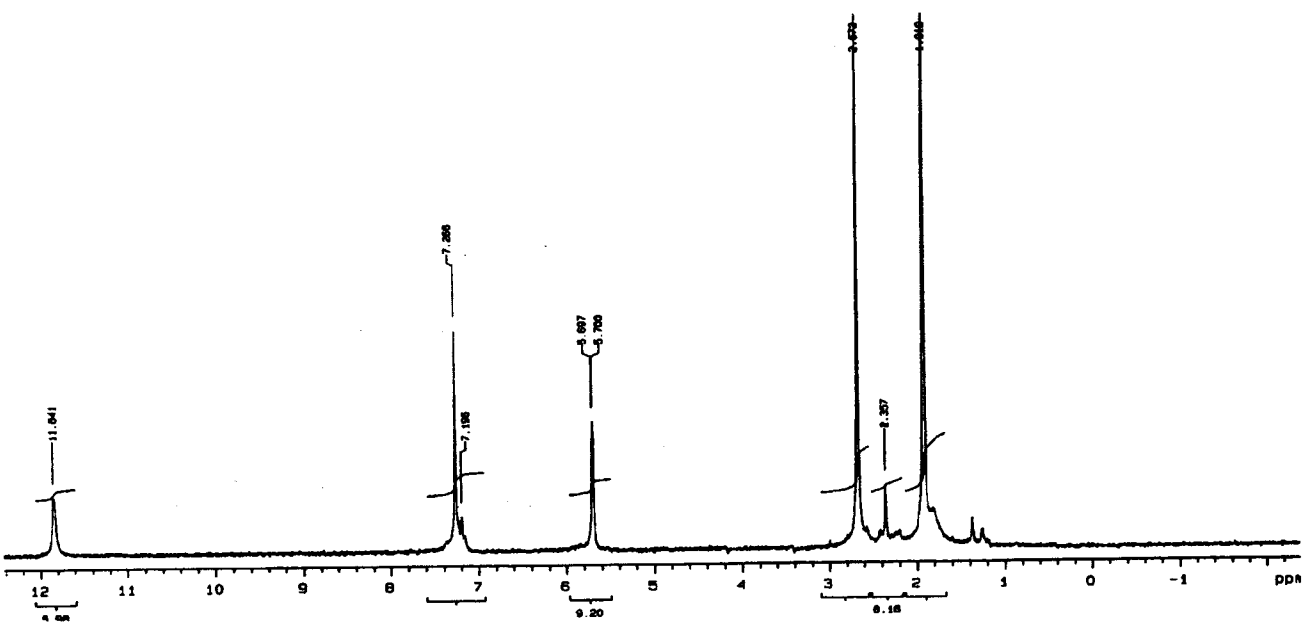

Figure 2.10: ^{1}H NMR spectrum of $(3,5\text{-}Me_2pz)_2PdCl_2$

The ^{1}H NMR spectrum (Fig. 2.9) obtained for complex of the ligand **A2**; n =2 (Scheme 2.2), showed a mixture of two products, the expected product and the presence of an unlinked substituted pyrazole palladium complex ($(3,5\text{-}Me_2pz)_2PdCl_2$) reported by Darkwa and coworkers.[15] This was verified by comparing the ^{1}H NMR spectrum (Fig.2.9) of this mixture and that of the pure unlinked pyrazole complex (Fig. 2.10). As can be observed in both spectra there is a peak around 11.80 ppm which belongs to the N-H proton. The presence of this peak in the spectrum of $(3,5\text{-}Me_2pz)_2PdCl_2$ (Fig. 2.10) is expected, but in the 1,4-bis(3,5-Me_2pyrazolyl)butane-1,4-dione palladium complex spectrum (Fig. 2.9) this shows decomposition of the linker. There are two peaks for a proton in position 4 of the pyrazole ring in the spectrum in Figure 2.9, one at 5.95 ppm for the unlinked palladium complex and at 6.10 ppm for the linked pyrazolyl palladium complex. There are peaks at 3.59 and 2.96 ppm that appear in the spectrum of the mixture of the compounds (Fig. 2.9), which are not observed in the spectrum in Fig. 2.10. These peaks belong to protons of the CH_2 unit of the linker, and show that the product isolated is a mixture. This observation in the ^{1}H NMR spectrum (Fig. 2.9) of this mixture suggests that some decomposition of ligand **A2** occurs, leading to the formation of unlinked pyrazole ligand and subsequently react with $(CH_3CN)_2PdCl_2$ to form two products, the unlinked pyrazole palladium complex and an 1,4-bis(3,5-Me_2pyrazolyl)butane-1,4-dione palladium complex. In other reactions performed with some of the ligands, notably **A1** and **A4,** there was not even a sign of a linked pyrazolyl palladium complex in the ^{1}H NMR spectra. The spectra obtained were identical to those of an unlinked pyrazole palladium complexes. The mode of decomposition of these ligands upon complexation is not clear at this stage. There are reports in literature where pyrazolyl linker compounds

decompose to form free substituted pyrazole complex. One such report is the work by Hamon and coworkers,[18] where they observed an unexpected deboronation of *tert*-butyl-tris(3-tert-butylpyrazol-1-yl)borate [^{t}BuB(3-^{t}BuC$_3$H$_2$N$_2$)$_3$]$^-$ when the ligand reacts with iron(II) chloride. The only isolable product they obtained was $FeCl_2(^tBuC_3H_3N_2)_4$, with no sign of a boron linker. The structure of the product they obtained was characterized by X-ray crystallography and was found to be a complex without a linker. These authors attribute this puzzling observation to possible fragility of these ligands. They also concluded that the formation of this complex results from the complete degradation of [^{t}BuB(3-^{t}BuC$_3$H$_2$N$_2$)$_3$]$^-$. In another report by Barszcz and coworkers,[19] 1-hydroxymethyl-3.5-dimethylpyrazole ligand decomposes during coordination to hydrated $Cu(BF_4)_2$. This ligand decomposes into two fractions; one fraction that contains HCOH and 3,5-dimethylpyrazole and other fraction gives 1-methoxy-3,5-dimethylpyrazole. The crystal structure reveals that the copper complex contains the 3,5-dimethylpyrazole, 1-methoxy-3,5-dimethylpyrazole and BF_4 ligands. It is hard to explain why this ligand decomposes upon coordination.

Comparing the above observation with the ligands we prepared, we suspect that hydrolysis might be involved in the decomposition of alkane-α,ω-dione linkers upon complexation. We envisaged that this hydrolysis is brought about by the use of wet solvents. To see the influence of wet solvents on these reactions, we performed one reaction with dichloromethane that was dried over P_2O_5 for 3 days. The reaction we performed was between the 1,5-bis(3,5-dimethylpyrazolyl)pentane-1,5-dione ligand (**A3**) and $(CH_3CN)_2PdCl_2$. The ^{1}H NMR spectrum (Fig. 2.11) shows that the reaction has taken

place when compared to the free ligand spectrum (Fig 2.12). The peak at 11.80 ppm for N-H proton does not appear in this spectrum and peaks belonging to the linker were observed in this spectrum. The peak at position 4 of the pyrazole ring has shifted from 5.93 ppm in the free ligand (Fig. 2.12) to 6.10 ppm (Fig. 2.11) in the 1,5-bis(3,5-Me_2pyrazolyl)pentane-1,5-dione palladium complex. There was a broad peak around 4.50 ppm, which integrates for four protons of the terminal CH_2's on the linker. This is a significant shift for these protons compared to their assignment in the ligand, which was found to be around 3.20 ppm. A multiplet between 2.90 and 3.01 ppm is assignable to the two protons on the sandwiched CH_2 of the linker. The peaks for these two protons appear around 2.10 ppm in the ligand, so there is downfield shift of about 0.79 ppm in the spectrum of the complex. This downfield shift of these methylene protons on the linker is a sign that the complex has formed. The peaks for the protons on the methyl group were slightly affected by the complexation reaction. Unfortunately this synthetic approach was only successful for the complexation of ligand **A3**. Attempts to apply it to the complexation of other pyrazolyl ligands were unsuccessful. It is not clear as to why the other ligands do not form clean complexes under stringently dry condition. It is possible that **A3** ligand has the right bite angle for complexation, which explains why a complex was obtained for this ligand. However, when attempts were made to grow crystals of the palladium complex formed by **A3** there were visible signs of decomposition which indicates that the complex is not stable in solution over prolong periods.

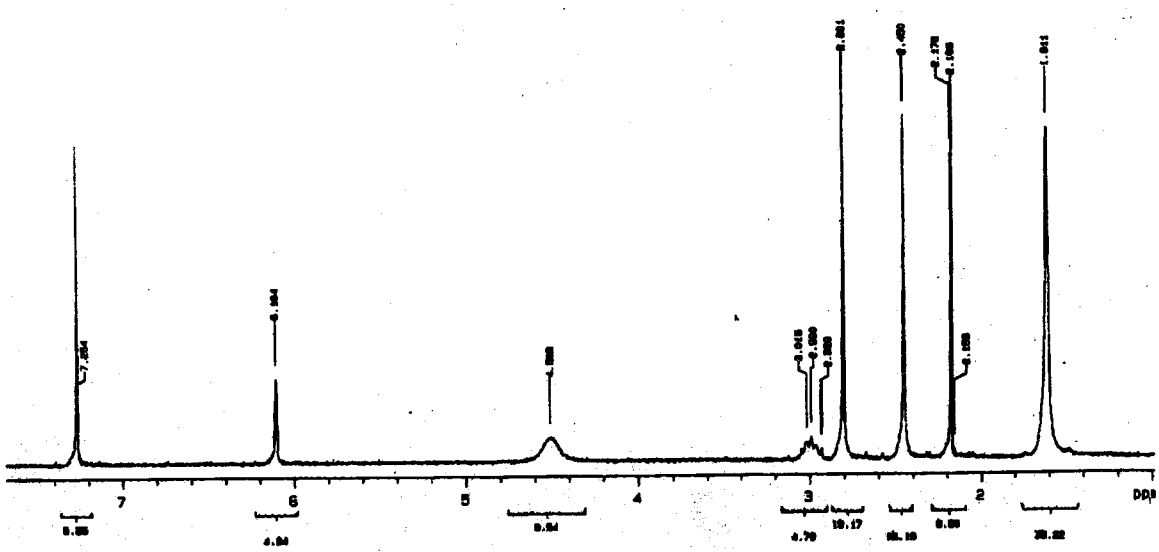

Figure 2.11: ^{1}H NMR spectrum of **A3** ligand complex

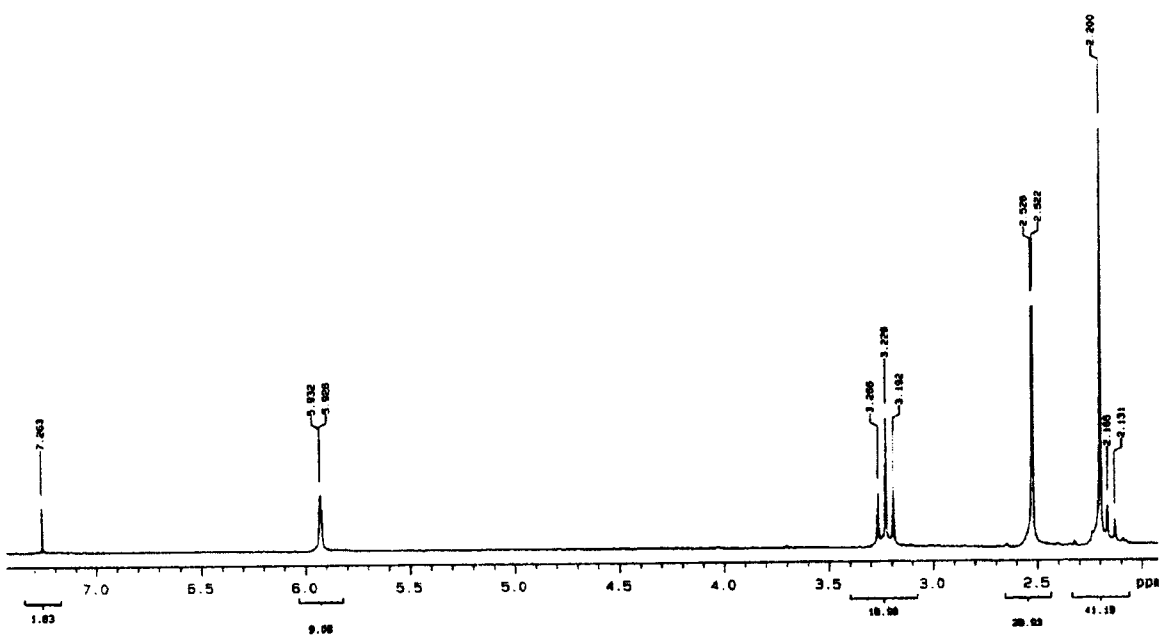

Figure 2.12: ^{1}H NMR spectrum of **A3** ligand

2.6 Summary

Two types of pyrazole complexes were prepared in this project. These include the well-characterized pyrazole and substituted pyrazole nickel complexes. They formed four coordinate, tetrahedral complexes **(1, 4)**, which are paramagnetic and could only be characterized by elemental analysis, IR spectroscopy and single crystal X-ray crystallography. The other nickel complexes **(2, 3)** are six coordinate octahedral complexes, also characterized by elemental analysis, IR spectroscopy and X-ray crystallography. Two of the complexes namely **1** and **3** were subsequently used as catalysts for ethylene polymerization and their full catalytic behavior is discussed in Chapter 3 of this thesis.

The second type of complexes, though not fully characterized, was pyrazolyl palladium complexes. New pyrazolyl ligands, with alkane-α,ω-dione linkers, were prepared and well characterized. However, attempts at using these ligands to form palladium complexes had mixed success. Future work ought to include investigating why these ligands do not readily form complexes with palladium.

References

1. Trofimenko S., *Chem. Rev.* 1972, **72**, 497.

2. Reedijk J., *Recl. Trav. Chim. Pays-Bas* 1969, **88**, 1451.

3. Reimann C. W., Santoro A., Mighell A. D., *Acta Cryst.* 1969, **B26**, 595. (b) Reimann C. W., Mighell A. D., Mauer F. A., *Acta Cryst.* 1967, **23**, 135.

4. Reedijk J., *Recl. Trav. Chim. Pays-Bas* 1970, **89**, 605.

5. (a) Mani F., *Coord. Chem. Rev.* 1992, **120**, 325. (a) Trofimenko S., *J. Am. Chem. Soc.* 1967, **89**, 3170. (c) Trofimenko S., Calabrese J. C., Thompson J. S., *Inorg. Chem.* 1987, **26**, 1507. (d) Trofimenko S., *Chem. Rev.* 1993, **93**, 943.

6. (a) Hartshorn C. M., Steel P. J., *Aust. J. Chem.* 1995, 48, 1587. (b) Hartshorn C. M., Steel P. J., *Angew. Chem. Int. Ed. Engl.* 1996, **35**, 2655. (c) Hartshorn C. M., Steel P. J., *Chem. Commun.* 1997, 541.

7. Elguero J., Jacquier E. G. R., *Bull. Soc. Chim. Fr.* 1968, **2**, 707.

8. Ward L. G. L., *Inorg. Synth.* 1972, **13**, 154.

9. Drew D., Doyle J. R., *Inorg. Synth.* 1972, **12**, 47.

10. Blessing R. H., *Acta Cryst.* 1995, **A51**, 33.

11. Sheldrick G., Bruker *SHELXTL (Version 5.1), Analytical X-ray Systems, Madison,WI*, 1997.

12. Poddar S. N., *Sci. Cult.* 1969, **35**, 28.

13. Butcher R. J., Sinn E., *Inorg. Chem.* 1977, **16**, 2334.

14. (a) Llobet A., Hodgson D. J., Meyer T. J., *Inorg. Chem.* 1990, **29**, 3760. (b) Llobet A., Curry M. A., Evans H. T., Meyer T. J., *Inorg. Chem.* 1989, **28**, 3131. (c) Llobet A., Doplet P., Meyer T. J., *Inorg. Chem.* 1988, **27**, 514.

15. Li K., Darkwa J., Guzei I. A., Mapolie S. F., *J. Organomet. Chem.* 2002, **660**, 108.

16. Graziani O., Toupet L., Hamon J., Tilset M., *Inorg. Chim. Acta* 2002, **34**, 127.

17. Barszcz B., Glowiak T., Jeziarska J., Kurdziel K., *Inorg. Chem. Commun.* 2002, **5**, 1055.

CHAPTER 3

Ethylene polymerization catalyzed by nickel pyrazole and palladium pyrazolyl catalysts

3.1 INTRODUCTION

3.1.1 Nitrogen based late transition metal complexes as ethylene polymerization catalysts

The use of late transition metal complexes as catalysts in olefin polymerization has attracted tremendous attention.[1-4] Although olefin polymerization catalysis is dominated by metallocene catalysts,[5-8] late transition metal catalysts based on nitrogen ligands have been widely explored since the report by Brookhart and coworkers[9] in 1995. Brookhart and coworkers have shown that bulky α-diimine ligands enhance the activity of late transition metal catalysts. This leads to polyethylene with different microstructures and high molecular weight. One of the features of late transition metals is that they are less oxophilic compared to early transition metals. The lack of oxophilicity of these catalysts allows co-polymerization of ethylene with polar monomers.[10] Generally, alkylaluminum compounds are used as co-catalysts to the late transition catalysts with methylaluminoxane (MAO) being the most extensively used co-catalyst.[11]

The behavior of late transition metal catalysts and their co-catalysts was fully discussed in Chapter 1 of this thesis. A report on simple substituted pyrazole

palladium complexes as catalyst precursors for ethylene polymerization recently appeared in the literature.[12] In this Chapter ethylene polymerization activity of pyrazole nickel and pyrazolyl palladium complexes will be discussed. Comparison of the nickel catalysts to their reported palladium analogues forms part of this Chapter. The polyethylene produced was characterized by a combination of NMR spectroscopy, high temperature gel permeation chromatography (GPC) and thermal analysis.

3.2 GENERAL PROCEDURE FOR ETHYLENE POLYMERIZATION

Polymerization was carried out in a 300 ml stainless steel autoclave, which was loaded with the catalyst and co-catalyst, methylaluminoxane (MAO) in a nitrogen purged glove box. This was done by charging the autoclave with a nickel or palladium complex in dry toluene (150 ml), and the appropriate amount of MAO (10% in toluene) at a co-catalyst to catalyst ratio ranging from 250-1000. The reactor was sealed and removed from the glove box and then flushed three times with ethylene after which it was heated to the polymerization temperature. Ethylene was continuously supplied to maintain a constant pressure during the polymerization reaction. After the set reaction time, excess ethylene was vented and the polymerization quenched by adding ethanol. The polymer was filtered, washed with 2M HCl, followed by ethanol and dried in an oven overnight at 50 °C under vacuum. NMR spectra of polyethylene were recorded in 1,2,4-trichlorobenzene/benzene-d^6 at 115 °C. The number- (M_n) and weight-average (M_n) molecular weights and polydispersity (M_w/M_n) of the polymers were determined by high temperature gel

permeation chromatography (GPC) (1,2,4-trichlorobenzene, 145 °C, rate = 1.000 mL/min) at the Group Technologies Research and Development laboratory of SASOL polymers and the Institute of Polymer Science at the University of Stellenbosch. Thermal analyses were performed on Universal V2.3H TA instrument at the University of Botswana and on a Perkin Elmer PC Series 7 system at the University of Cape Town.

3.3 RESULTS AND DISCUSSIONS

3 3.1. Polymerization results using nickel catalysts

Two nickel complexes were extensively investigated for their ability to catalyze ethylene polymerization when activated with MAO. The polymerization reactions were performed under various reaction conditions. These include varying co-catalyst to catalyst ratio, temperature and pressure. These variations allowed the catalytic activities of complex **1** and **2** to be compared. The catalytic behavior of these pyrazole nickel complexes was compared to that of pyrazole palladium complexes $(pz)_2PdCl_2$ and $(3,5\text{-}Me_2pz)_2PdCl_2$ and $(3,5\text{-}^tBu_2pz)_2PdCl_2$.

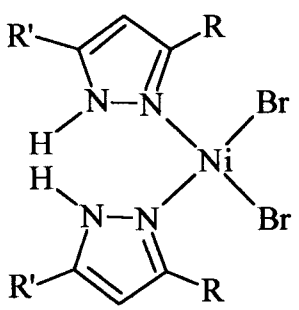

1. R = R' = CH_3

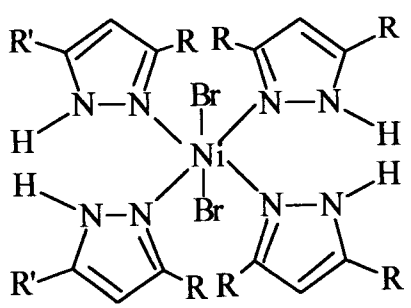

2. R = R' = H

Figure 3.1: Nickel catalysts used in this project

3.3.1.1 Comparison between 1 and 2 in ethylene polymerization

Complex **1**, $(3,5\text{-}Me_2Pz)_2NiBr_2$ (Fig. 3.1) was used as a catalyst precursor for most of the polymerization reactions, but for comparison purposes preliminary polymerization reactions were performed using complex **2**, $(pz)_4NiBr_2$ (Fig. 3.1). The synthesis and full characterization of these catalysts were described in Chapter 2 of this thesis. To understand the effectiveness of the ethylene polymerization catalyst, reaction parameters were varied during the investigation. In this study the parameters that were investigated for their role in the polymerization reaction were temperature, pressure and co-catalyst concentration. The nickel pyrazole complexes act as ethylene polymerization catalysts in the presence of co-catalyst methylaluminoxane (MAO), in the rest of this chapter the term catalyst will refer to a metal complex activated with MAO.

In this section a comparison of the activity of catalysts **1** and **2** is discussed. The polymerization data using catalyst **1** and **2** are summarized in Table 3.1. Most of the polyethylene produced in this study was found to be a fibrous polymer. Catalyst **2** shows higher activity compared to catalyst **1**, in actual fact the turnover number (TON) is nearly doubled under the same reaction conditions (entry 2, TON is 249.48 kg/mol Ni h vs entry 5, TON is 481 kg/mol Ni h, Table 3.1). TON refers to the amount in kg of polyethylene produced per mol catalyst per hour and is used as a measure of the activity of the catalyst. The difference in activity between catalyst **1** and **2** can be explained by looking at the geometry around the metal centre in both complexes. Catalyst **1** is a four coordinate, tedrahedral system[13] and catalyst **2** is a

six coordinate, octahedral system.[14] As was alluded to in Chapter 2 it is believed that catalyst **2** converts from a six coordinate octahedral geometry to a four coordinate geometry in solution in order to catalyze the polymerization reaction. Even though these catalysts are both tedrahedral, the active site is more accessible in **2** than in **1**, because there are less bulky substituents around the metal centre in **2**. In other words ethylene coordination and insertion to the metal alkyl bond is more efficient in **2** than in **1**, leading to high yields of polyethylene. The influence of the concentration of MAO on catalyst activity was investigated for catalyst **2**. This system produces a polymer even at low Al:Ni ratio of 250:1, even though catalyst activity is low (entry 3, 40.83 kg/mol Ni h). This was not the case with catalyst **1** where at Al:Ni ratio of 250:1 only a trace amount of polymer was obtained (entry 1). Catalyst activity is nearly tripled when Al:Ni ratio was increased from 500 to 1000 (164 to 481 kg/mol Ni h) for catalyst **2** entries 4 and 5. Compared to its reported palladium analogue $(pz)_2PdCl_2$[12] which has activity of 1131.90 kg/mol Pd h at 30°C, catalyst **2** has a lower activity. This difference in activity between palladium and nickel pyrazole catalysts may be due to the square planar geometry of the palladium pyrazole catalysts, which is more suitable for olefin coordination and subsequent insertion for chain growth. This seems to indicate that a square planar geometry around the metal centre is vital for the catalyst to be active in olefin polymerization. Theoretical studies on the binding of ethylene to Pd(II) and Ni(II) complexes reveal that ethylene binds more strongly to a highly square planar Pd(II) complex than the distorted square planar Ni(II) complex.[15]

Table 3.1: Ethylene polymerization data and conditions[a] for catalyst **1** and **2.**

Entry	Catalyst	Ni:Al ratio	Press. (atm)	Temp. (°C)	TON[b]	($M_w \times 10^6$)[c]	M_w/M_n[d]	T_m[e] (°C)
1	**1**	250	5	25	Trace			
2	**1**	1000	5	25	249.48	1.44	2.43	136.76
3	**2**	250	5	25	40.83	1.62	2.27	135.45
4	**2**	500	5	25	164.01	1.59	2.43	134.08
5	**2**	1000	5	25	481.23	1.61	2.78	133.83

[a]Reaction conditions: [Ni] = 4.5×10^{-5}M, toluene = 150 ml, 25 ° C, polymerization time = 3 h

[b]TON = kg/mol Ni h

[c]Determined by GPC, 1,3,5-trichlorobenzene

[d]Polydispersity determined by GPC

[e]Melting point determined by DSC

There is no significant difference in molecular weights of the polymers produced using catalyst **1** and **2** under similar reaction conditions (1.44×10^6 for **1**, entry 2 and 1.61×10^6 for **2**, entry 5). The polydispersity indeces of polymers produced by these catalysts are around 2.

3.3.1.2 Effect of temperature on ethylene polymerization by catalyst 1

In this section the influence of temperature on ethylene polymerization using catalyst **1** is discussed and the polymerization data are summarized in Table 3.2. The ratio of Al:Ni used for most of these reactions is 1000:1, since the highest catalyst activity is obtained at this concentration of MAO. From the polymerization data in Table 3.2 it can be seen that as the temperature increases, catalyst activity increases. This is also shown graphically in Fig. 3.2. There is an exponential increase in catalyst activity

with increasing temperature. At 25 °C catalyst activity is low (entry 6, TON = 249.48 kg/mol Ni h) and increases up to 1170.32 kg/mol Ni h at 70 °C (entry 10).

Table 3.2: Effect of temperature on ethylene polymerization by catalyst **1**

Entry	Press. (atm)	Temp. (°C)	TON[a]	$(M_w \times 10^6)$[b]	M_w/M_n[c]	T_m[d] (°C)
6	5	25	249.48	1.44	2.43	136.76
7	5	40	336.98	1.62	1.51	135.95
8	5	50	409.87			134.88
9	5	60	811.63	0.74	2.07	135.42
10	5	70	1170.32	0.39	2.46	131.54
11	2	70	734.86	1.06	2.26	133.61
12	5	80	1439.86	0.74	1.74	
13	1	90	1295.90	0.19	2.34	
14	5	100	2363.95	0.48	1.69	

Reaction conditions: [Ni] = 4.5×10^{-5} M, toluene = 150 ml, polymerization time = 3 h

[a]TON = kg/mol Ni h

[b]Determined by GPC, 1,3,5-trichlorobenzene

[c]Polydispersity determined by GPC

[d]Melting points determined by DSC

Darkwa and co-workers[12] also observed this increase in activity with increasing temperature when they used the analogous substituted pyrazole palladium catalysts. Their catalyst $(3,5\text{-}^tBu_2pz)_2PdCl_2$, gave a TON of 1034.50 kg/mol Pd h at 5 atm, 70 °C, compared to 174 kg/mol Pd h at 25 °C. This phenomenon of increasing activity with increasing temperature has also been reported by others.[16-21] The first few minutes of the polymerization reaction are envisaged to be vital in the polymerization reaction, since ethylene diffusion is higher before the catalyst decomposes with time. Most of the reported catalysts based on late transition metals

tend to loose activity at temperatures above 60 °C, due to catalyst decomposition. It is not known how these catalysts deactivate during ethylene polymerization. One possible mode of decay is through C-H activation of an *ortho* alkyl substituent in the case of α-diimine ligands, but there is no evidence to support this.[22] To probe the thermal stability of catalyst **1,** reactions were performed at temperature as high as 90 °C, 1 atm and at 100 °C, 5 atm for one hour. Under these conditions high amounts of polyethylene were obtained (entry 13, TON = 1296 kg/mol Ni h and entry 14, 2364 kg/mol Ni h). In another report, Brookhart et al.[22] performed a polymerization reaction using a α-diimine nickel catalyst [ArN=C(R)C(R)=NAr]$NiBr_2$ (R = Ph, ^{i}Pr) at 85°C and 1 atm and there was no polymer obtained due to catalyst decomposition. This shows that our catalyst is more thermally stable at elevated temperatures compared to other related nitrogen based late transition catalysts.

The polymers produced in this study were characterized by gel permeation chromatography (GPC) to obtain their molecular weights and molecular weight distribution. The weight average-molecular weights (M_w) of the polyethylene produced by catalyst **1** decrease with increasing temperature. The M_w decreases from 1.44×10^6 g/mol at 25 °C (entry 6, Table 3.2) to 0.74×10^6 g/mol at 60 °C (entry 9, Table 3.2). As the temperature is increased from 60 °C to 70 °C, M_w decreases from 0.74×10^6 g/mol to 0.39×10^6 g/mol (entry 9 and 10).

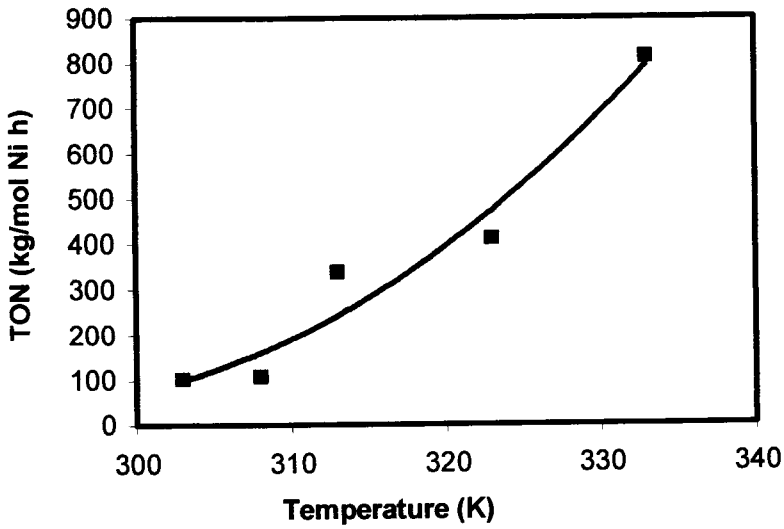

Figure 3.2: A graph that shows the effect of temperature on ethylene polymerization

Generally molecular weights of the polyethylene produced by late transition metal catalysts at low temperatures are higher than those produced at high temperatures.[17,18] This is due to the high rate of chain transfer and chain termination over chain propagation at high temperatures. From the GPC traces of the polyethylenes obtained from the reactions performed at 25 °C and 70 °C (Fig. 3.3 and Fig. 3.4 respectively), it can be seen that unimodal molecular weight distribution curves are obtained. This shows that there is only one type of active species in the polymerization reactions. Polydispersity indices for all these cases are around 2, similar to those reported for other late transition metals.[16-22]

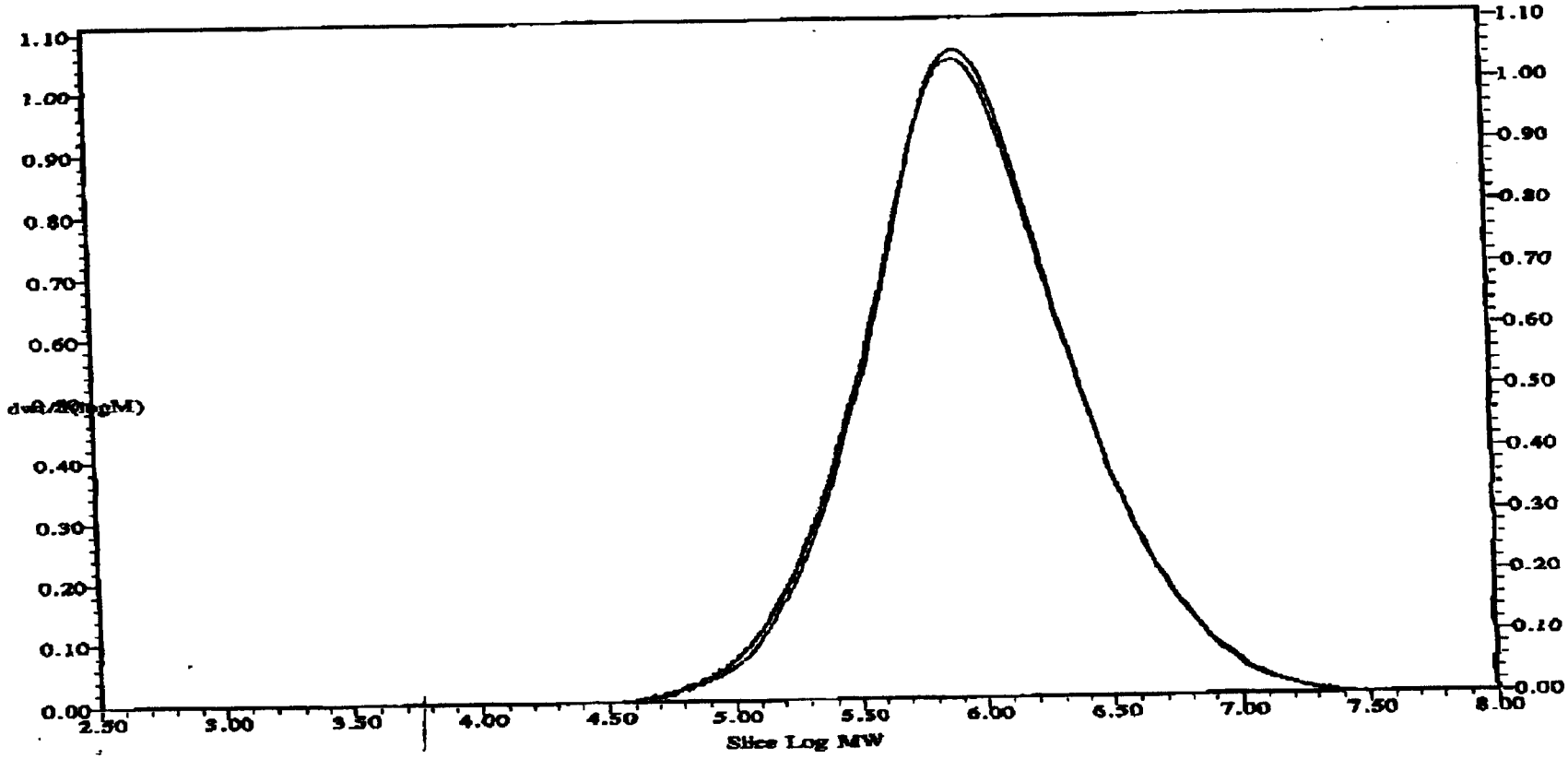

Figure 3.3: A GPC curve of polyethylene produced at 25 °C

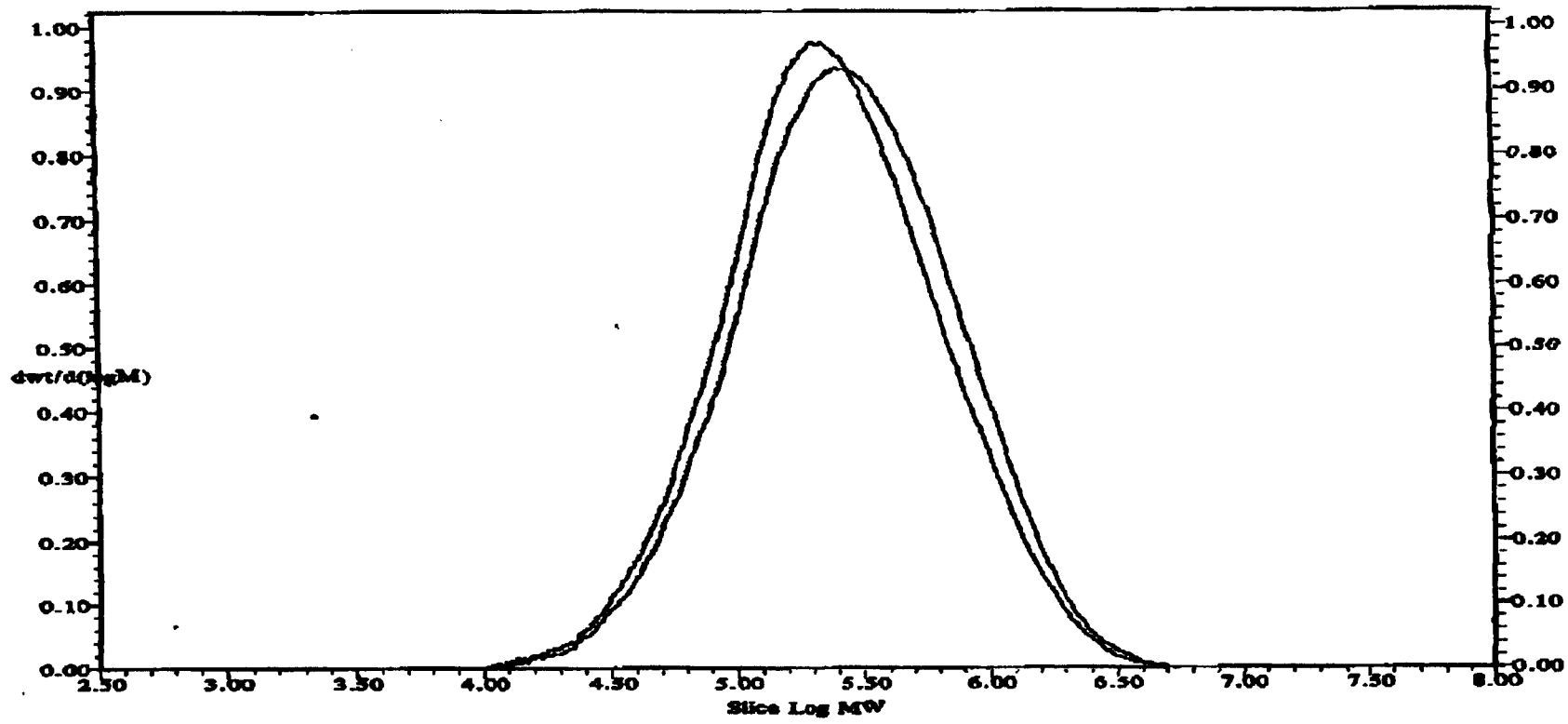

Figure 3.4: A GPC curve of polyethylene produced at 70 °C

It is also interesting to note that temperature does not seem to have any significant influence on polydispersity indices. Even at 90 °C the polydispersity is 2.34, entry 13, Table 3.2. The polyethylene produced was found to be linear as determined by high temperature ^{1}H NMR, since only one peak was observed in the spectrum (Fig. 3.5). From this NMR spectral data, it can be concluded that the polyethylene formed in our reactions is high-density polyethylene (HDPE). The formation of linear polyethylene indicates that there is no "chain walking" during polymerization reactions. Hence using our catalyst system there was no branching observed as suggested in ethylene polymerization mechanism catalyzed by some other late transition metals which is described fully in Chapter 1.[22,23] Most nickel catalysts form highly branched polyethylene, because the process of chain walking is dominant in these catalyst systems.

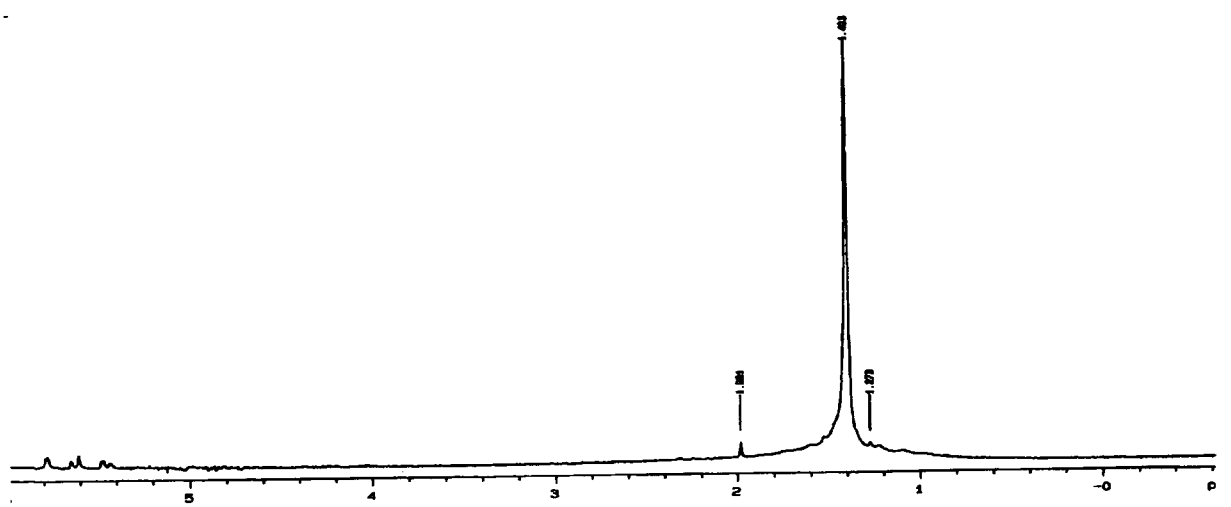

Figure 3.5: ^{1}H NMR spectrum of polyethylene produced at 25 °C using **1**

To probe the thermal properties of these polymers, they were subjected to differential scanning calorimetry (DSC) as well as thermogravimetric analysis-differential thermal analysis (TGA-DTA). DSC data of the polyethylene isolated in this study and the reaction conditions are listed in Table 3.2. Melting points from the DSC measurements were found to be between 131 °C and 136 °C which is typical of high density polyethylene (HDPE), which has a melting point around 135 °C.[24] There was no change in DSC melting point ranges with change in reaction temperature, at both low temperatures (25 °C and 40 °C, T_m =136.76 °C and 135.95 °C respectively, Table 3.2) and high temperatures (60 °C and 70 °C, T_m = 135.42 °C and 131.54 °C).

The DSC data shows that the microstructure of the polymer is independent of the polymerization temperature. In general, as is evident from the thermograms the polyethylene undergoes decomposition from 449 °C to 498 °C as can be seen in Fig. 3.6. This decomposition pathway was also observed for polyethylene produced by analogous palladium catalysts $(3,5\text{-}Me_2pz)_2PdCl_2$[12] and related catalysts.[16-23]

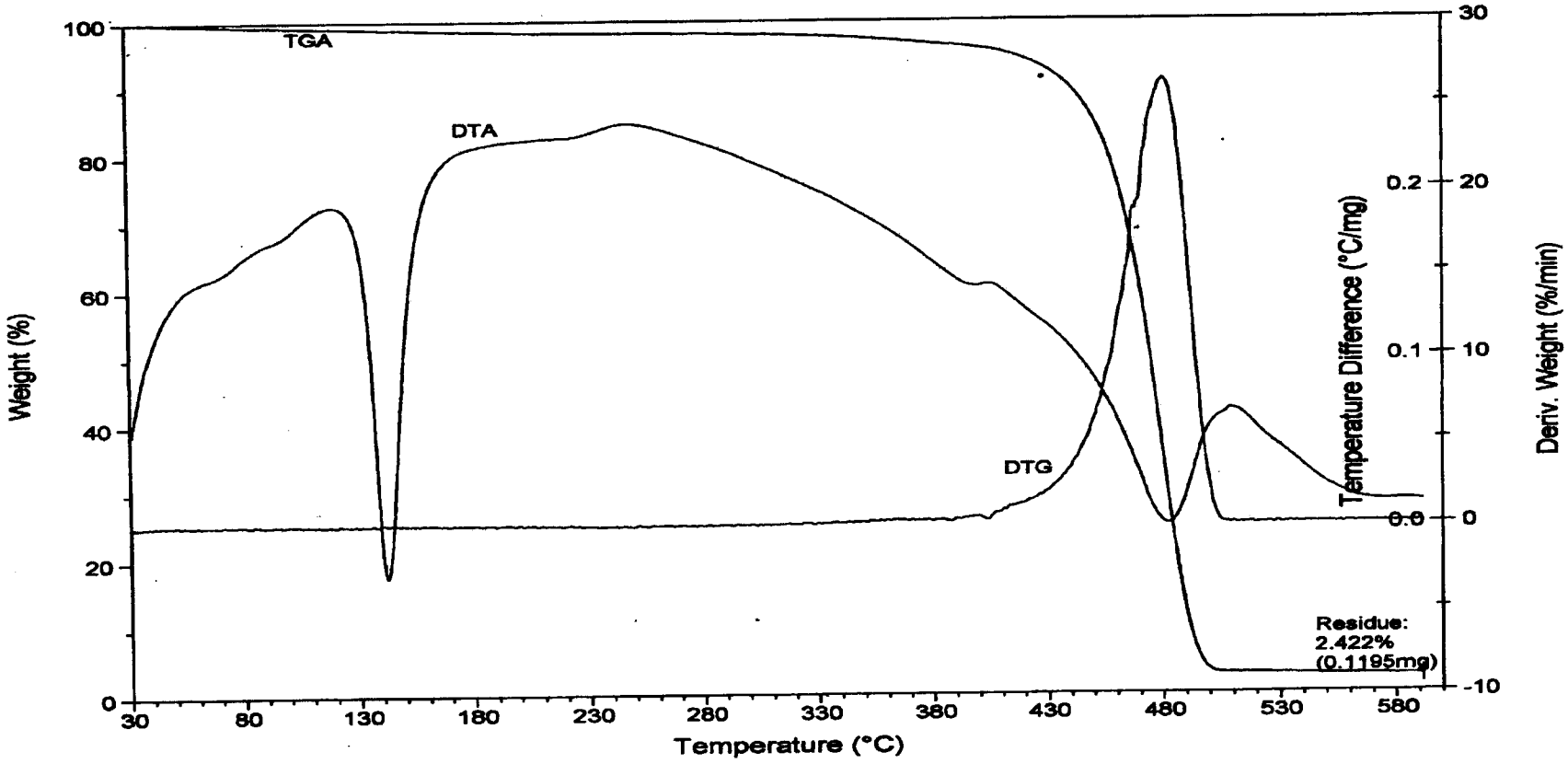

Figure 3.6: TGA-DTA thermogram of polyethylene produced at 25 °C using **1**

3.3.1.3 The effect of pressure on ethylene polymerization by 1

The results of ethylene polymerization experiments conducted at different ethylene pressure between 1-30 atm at 25 °C are summarised in Table 3.3 and depicted graphically in Fig. 3.7. These experiments were performed to gain insight into the influence of pressure on catalyst activity and the microstructure of the polyethylene produced. It is evident from the results in Table 3.3 that the activity is very low at 1 atm (12.41 kg/mol Ni h, entry 15) and it increases to 76.92 kg/mol Ni h at 2 atm (entry 16). As pressure increased through 5, 10, 25 and 30 atm, the amount of polyethylene produced increases. Monomer mass transport limitation at 1 atm is due to the high activity of this catalyst even under conditions of high dilution and low catalyst loading. This results in very rapid consumption of the monomer and the catalyst becomes starved of monomer. The amount of ethylene is low at 1 atm and the catalyst converts the monomer rapidly till there is no more ethylene to be converted. Monomer mass transport does not present problems when ethylene pressure is increased to 2 atm and above.

The temperature of 25 °C was chosen as a standard temperature, since the catalyst was found to be active at this temperature. One of the observations is the high evolution of heat during the polymerization at 10, 25, 30 atm, compared to 5 atm and below. This may be due to high rate of reaction at these elevated pressures and amount of monomer concentration in the reaction vessel. There was no significant change in activity when the pressure was increased from 5 atm to 10 atm. When

pressure was increased from 10 atm to 30 atm the activity increased from 1095.95 kg/mol Ni h to 3441.17 kg/ mol Ni h (entry 20 and 22, Table 3.3), which means that activity is tripled at 30 atm. There was a significant increase in activity when pressure was increased from 25 atm to 30 atm, from 2741.12 kg/mol Ni h (entry 21) to 3441.17 kg/mol Ni h (entry 22). In general there was an increase in activity as the pressure was increased, due to the high amount of monomer molecules at high pressures. It can be seen in the graph in Fig.3.6 that the activity increases steadily at pressures below 10 atm, and a rapid increase is observed when the pressure is increased to 25 atm.

Table 3.3: Effect of pressure on ethylene polymerization by catalyst **1**

Entry	Pressure. (atm)	TON[a]	($M_w \times 10^6$)[b]	M_w/M_n[c]	T_m[d] (°C)
15	1	12.41	3.86	2.32	136.42
16	2	76.92	4.02	2.57	136.51
17	3	104.37	4.06	2.23	136.60
18	4	161.74	3.89	2.51	136.01
19	5	249.48	1.44	2.43	136.76
20	10	1095.29	1.27	3.08	132.25
21	25	2741.12	0.65	1.92	131.97
22	30	3441.17	0.84	2.04	130.50

Reaction conditions: [Ni] = 4.5×10^{-5} M, toluene = 150 ml, Ni:Al = 1:1000 polymerization time = 3 h

[a]TON = kg/mol Ni h

[b]Determined by GPC, 1,3,5-trichlorobenzene

[c]Polydispersity by GPC, 1,3,5-trichlorobenzene

[d]Melting point determined by DSC

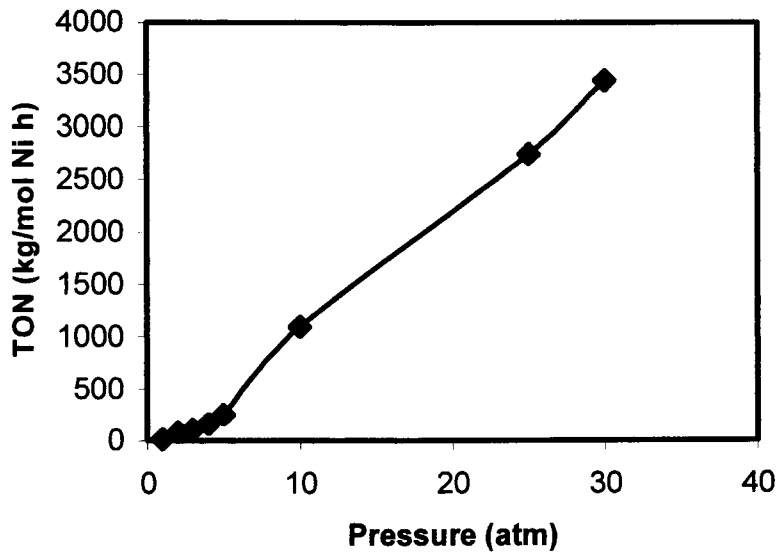

Figure 3.7: A graph showing effect of pressure on ethylene polymerization using **1**

An opposite effect of pressure was observed by De Souza and coworkers[25] using $[Ni(\eta^3\text{-}2\text{-}MeC_3H_4)\{ArN{=}C(H)C(H){=}NAr\}]PF_6$, Ar = 2,6-$C_6H_3{}^iPr$/ diethylaluminium chloride (DEAC) catalyst system. There was no change in activity when pressure was increased from 1 atm to 15 atm. But the molecular weight of the polyethylene produced by their nickel catalyst is low at 15 atm compared to the one produced at 1 atm. This observation of low molecular weight at high pressures was also observable for the polyethylene produced by catalyst **1** (Table 3.3). The molecular weight starts to decrease at 5 atm. The molecular weight at 1 atm is 3.86×10^6 g/mol and it decreases to 0.84×10^6 g/mol at 30 atm.

Melting points for these polymers produced in pressure variation experiments were measured using DSC and the decomposition pathway of the polymer was studied by TGA-DTA. The melting points of the polymer produced from 1 atm to 5 atm are all around 136 °C , which is typical of a linear polyethylene. Selected DSC data is listed in Table 3.3. It is interesting to note that at 10 atm and above, the melting point is around 130 °C (see Table 3.3), this a sign that the polyethylene produced has short branches. A TGA-DTA thermogram of the polymer (Figure 3.8) represents the decomposition of polyethylene produced at 1 atm.

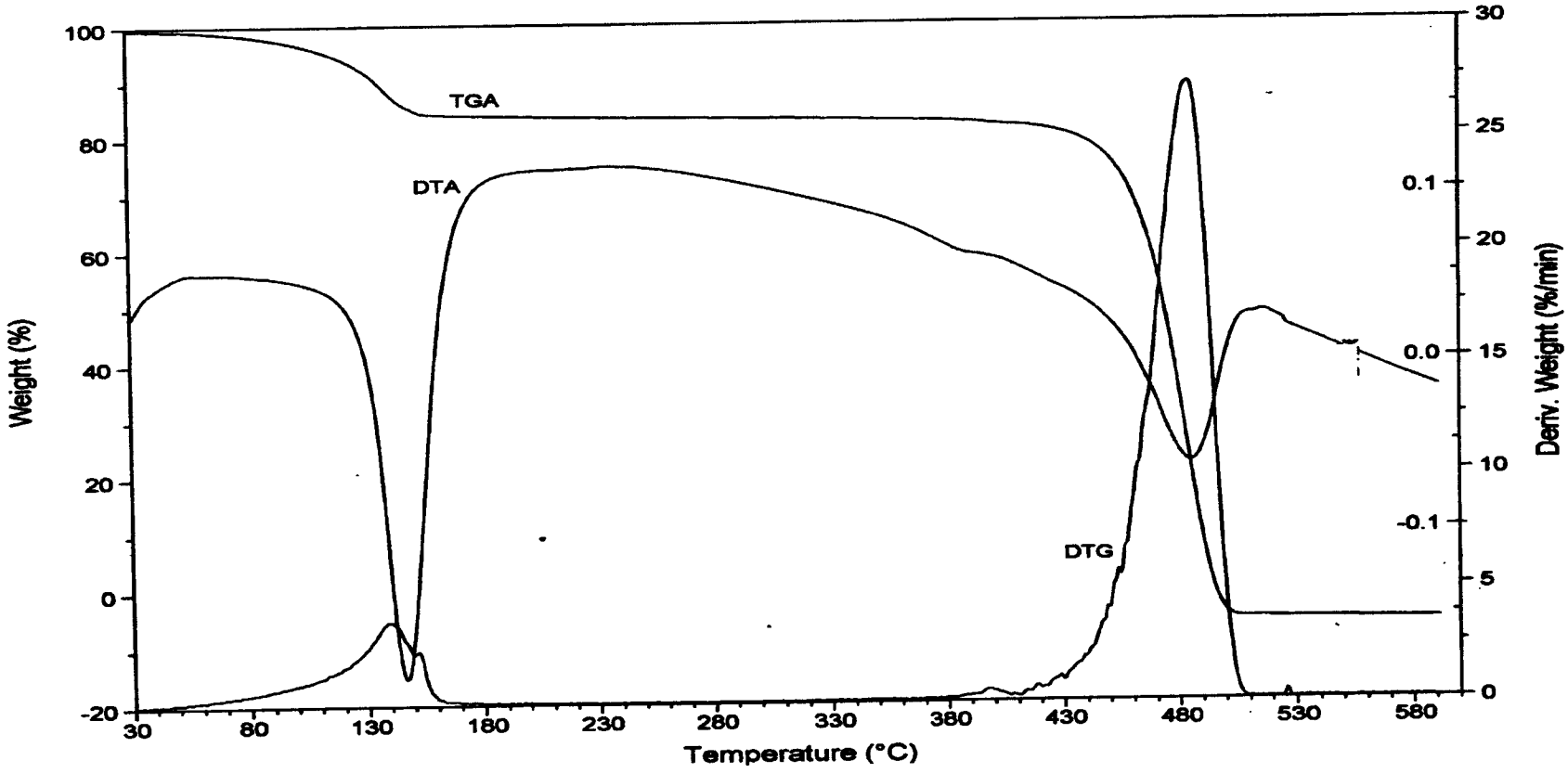

Figure 3.8: TGA-DTA thermogram of polyethylene produced at 1 atm using **1**

3.3.2 Polymerization results for the pyrazolyl palladium catalyst

The palladium pyrazolyl complexes with 1,3-benzenedicarbonyl (**3**) and 1,3,5-benzenetricarbonyl (**4**) linkers (Fig. 3.9), have been reported previously by Li and co-workers, and their preliminary catalytic ability in ethylene polymerization was investigated.[26] The key feature of these catalysts is the carbonyl group in the linker, which is electron withdrawing and believed to make the metal centre more electrophilic. This high electrophilic nature of the metal centre is very important in ethylene polymerization, because it increases the rate of olefin coordination and insertion into the metal alkyl bond. The ethylene polymerization studies undertaken here were done under conditions that were not investigated by Li and co-workers.[26] This section explores the role of temperature and MAO concentration on the ethylene polymerization by catalyst **4**. The previously reported polymerization data as well as new data will be presented for comparison purposes. The ethylene polymerization data for this catalyst is summarized in Table 3.4. Li and coworkers[26] observed that catalyst **3** was more active than catalyst **4** under similar reaction conditions. The lower activity of **4** is believed to be due to the non-coordinating pyrazoyl unit in the ligand, which could be competing with the palladium metal centre for the co-catalyst MAO. It is possible that the non-coordinating pyrazolyl unit coordinates to the aluminium of the co-catalyst. This is not unusual since aluminium complexes with pyrazole ligands $[Al(1,3,5\text{-}Me_2Pz)]$[27] and $[Tp_2Al][AlCl_4)]$[28] are known.

In this section the lower activity of catalyst **4** compared to **3** will be discussed extensively.

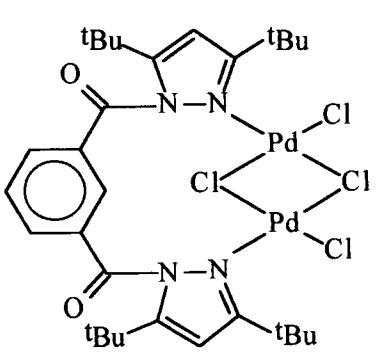

3

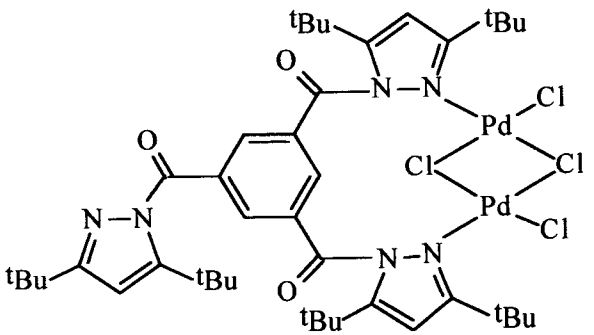

4

Figure 3.9: Palladium pyrazolyl catalysts (**3** and **4**)

Table 3.4: Ethylene polymerization data and conditions[a] for catalyst **4**

Entry	Al:Pd ratio	Reaction Time (h)	Temp. (°C)	TON[b]	$M_w(\times 10^6)$[c]	M_w/M_n[d]	T_m[e] (°C)
23	1000	2	30	440.10	2.27	2.33	136.53
24	2000	2	30	646.71	1.62	1.42	138.00
25	3000	2	30	985.33	0.79	1.38	136.51
26	4000	2	30	306.13	0.89	1.62	136.72
27	1000	1	50	1299.52	1.40	3.30	138.16
28	1000	1	70	2497.73	0.76	3.16	138.58

[a]Reaction conditions: [Pd] = 12.5×10^{-6} M, toluene = 150ml, pressure = 5 atm
[b]TON = kg/mol Ni h
[c]Determined by GPC, 1,3,5-trichlorobenzene
[d]Polydispersity determined by GPC
[e]Melting points determined by DSC

In order to investigate this possibility, polymerization reactions at higher MAO concentrations and longer reaction periods than the ones previously reported, were

performed. The MAO concentrations were increased to Al:Pd ratios of more than 1000:1 with a belief that, if there is a high amount of MAO in the system, this catalyst might be more active. The reaction times were increased to ensure the simultaneous complexation of the pyrazolyl unit to the aluminium centre in the co-catalyst and activation of the palladium metal centre by the co-catalyst. There was an increase in catalyst activity when co-catalyst to catalyst ratio was increased to 2000:1 (entry 24) and 3000:1 (entry 25). The interesting feature of increasing co-catalyst concentration, is that Al:Pd ratio of 3000:1 seem to be an optimal concentration for these catalyst, that means catalyst activity drops when MAO concentration is increased beyond this amount (Figure 3.10). The catalyst activity increased when MAO concentration was increased from 2000 to 3000, and it dropped drastically at 4000 (entry 26). This increase in catalyst activity with increasing co-catalyst concentration is a sign that for this catalyst to be highly active, a high enough concentration of MAO is required. This also supported our belief that the non-coordinating pyrazolyl unit in the ligand binds to the aluminium centre of the co-catalyst. The decrease in catalyst activity beyond the co-catalyst to catalyst ration of 3000:1 shows that there is a limit in the amount of MAO concentration that can activate this catalyst system. High amounts of the co-catalyst may poison the catalyst. Temperature effects on polymerization were also investigated, reactions at 50 °C (entry 27) and at 70 °C (entry 28) at Al:Pd ratio of 1000:1 were performed. The catalyst activity at 30 °C is 440 kg/mol Pd h which is very low compared to the activity at 70 °C (entry 28, 2497.73 kg/mol Pd h). The activity at 70 °C is comparable to the activity of catalyst **3** at 30 °C, which is 2591.40 kg/mol Pd h.[26]

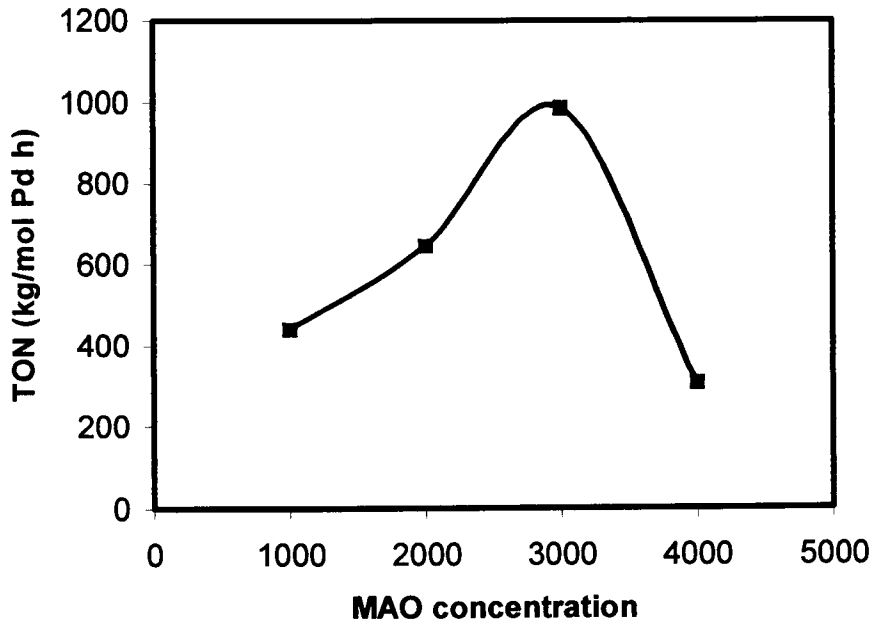

Figure 3.10: Effect of MAO concentration on catalytic activity of **4**

This increase in catalyst activity at high temperatures has been observed for other late transition metal catalysts. As in reported work on unbridged pyrazole palladium catalyst, activity increases with increasing temperature.[12] The high activity of this palladium catalyst at high temperatures also resembles the behavior observed for substituted pyrazole nickel catalysts discussed in section 3.3.1 of this Chapter. The above studies show that the presence of a carbonyl moiety has a remarkable influence on the activity of this catalyst. The polymers produced by this catalyst were characterized by high temperature GPC and thermal analysis and the data is summarized in Table 3.4. The molecular weights of the polymer obtained were between (0.79×10^6 g/mol and 2.27×10^6 g/mol, entries 23-26). The molecular weight

of the polymer obtained at 70 °C is low (0.76×10^6 g/mol) compared to that obtained at 50°C (1.38×10^6 g/mol). This observation is due to the high rate of β-hydride elimination at high temperatures as was the case with the pyrazole nickel complexes reported earlier sections of this Chapter. The polymers produced using catalyst **4** were found to have the melting points between 136-138 °C, which are typical of high-density polyethylene (HDPE). The melting points of these polymers were the same at both high and low temperatures.

Summary

The pyrazole nickel complexes prepared in this project have proven to be highly active catalyst precursors for ethylene polymerization. These complexes become active catalysts after activation with methylaluminoxane (MAO). Catalyst **2** was found to be more active than catalyst **1**, since the coordination of ethylene to the metal centre is easier in this catalyst. This nickel catalyst **(2)** show activity even at low co-catalyst to catalyst ratio (Al:Ni = 250:1. High molecular weight (*ca.*1.4×10^6 g/mol) polyethylenes were obtained using catalyst **1**. Molecular weights tend to low at high temperatures and high pressures due to high rate of β-hydride elimination and chain transfer.

Catalyst **4** previously reported by Li and co-workers[26] was also used as a catalyst for ethylene polymerization in this project. This catalyst was reported to be less active than catalyst **3**, due to the complexation of the free pyrazolyl unit of this catalyst to the aluminum of the MAO. This study has shown that this catalyst becomes highly

active when the co-catalyst to catalyst ratio (Al:Pd) is increased to 3000:1 which means this Al:Pd ratio is the optimal MAO concentration for this catalyst. Polymers obtained were found to have high molecular weight by GPC.

References

1. Ittel S. D., Johnson L. K., Brookhart M., *Chem. Rev.* 2000, **100**, 1169.

2. Maldanis R. J., Wood J. S., Chandrasekaran A., Rausch M. D., Chien J. C. W., *J. Organomet. Chem.* 2002, **645**, 158.

3. Papparaldo D., Mazzeo M., Antinucci S., Pellecchia C., *Macromolecules* 2000, **33**, 9483.

4. Soula R., Broyer J. P., Llauro M. F., Tomov A., Spitz R., Claverie J., Drujon X., Malinge J., Saudemont T., *Macromolecules* 2001, **34**, 2348.

5. Brintzinger H. H., Fischer D., Mülhapt R., Rieger B., Waymouth R. M., *Angew. Chem. Int. Ed. Engl.* 1995, **34**, 1143.

6. Kaminsky W., *J. Chem. Soc., Dalton Trans.* 1998, 1413.

8. Wilmes G. M., Polse J. L., Waymouth R. M., *Macromolecules* 2002, **35**, 6766.

9. Johnson L. K., Killian C. M., Brookhart M., *J. Am. Chem. Soc.* 1995, **117**, 6414.

10. Connor E. F., Younkin T. R., Henderson J. I., Hwang S., Grubbs R. H., Roberts W. P., Litzau J. J., *J. Polym. Sci: Part A: Polym. Chem.* 2002, **40**, 2842.

11. Chen E. Y., Marks T. J, *Chem. Rev.* 2000, **100**, 1391.

12. Li K., Darkwa J., Guzei I. A., Mapolie S. F., *J. Organomet. Chem.* 2002, **660**, 108.

13. Poddar S. N., *Sci. Cult.* 1969, **35**, 28.

14. Reimann C. W., Santoro A., Mighell A. D., *Acta Cryst.* 1969, **B26**, 595. (b) Reimann C. W., Mighell A. D., Mauer F. A., *Acta Cryst.* 1967, **23**, 135.

15. Strömberg S., Svensson M., Zetterberg K., *Organometallics* 1997, **16**, 3165.

16. Laine T. V., Piironen U., Lappalainen K., Klinga M., Aitola E., Leskela M., *J. Organomet. Chem.* 2000, **606**, 112.

17. Simon L. C., Williams C. P., Soares J. P. B., De Souza R. F., *J. Mol. Catal. A.: Chem.* 2001, **165**, 55.

18. Simon L. C., Williams C. P., Soares J. P. B., De Souza R. F., *Chem. Eng. Sci.* 2001, **56**, 4181.

19. Helldörfer M., Backhaus J., Milius W., Alt H. G., *J. Mol. Catal. A: Chem.* 2003, **193**, 59.

20. Wang C., Friedrich S., Younkin T. R., Li R. T., Grubbs R. H., Bansleben D. A., Day M. W., *Organometallics* 1998, **17**, 3149.

21. Yang H., Wang Q., Fan Z., Lou W., Feng L., *Eur. Polym. J.* 2003, **39**, 275.

22. Gates D. P., Svejda S.A., Oñate E., Killian C. M., Johnson L. K., White P. S., Brookhart M., *Macromolecules* 2000, **33**, 2320.

23. Guan Z., Cotts P. M., McCord E. F., McLain S. J., *Science*, 1999, **283**, 2059.

24. Feldman D., Barbalata A., *SYNTHETIC POLYMERS, Technology, properties, applications, 1st Ed., Chapman and Hall, London 1996.*

25. Escher F. F. N., Mauler R. S., De Souza R. F., *J. Braz. Chem. Soc.* 2001, **12**, 47.

26. Li K., Guzei I. A., Bikzhanova G. A., Darkwa J., Mapolie S. F., *Dalton Trans.* 2003, 715.

27. Romm I. P., Zayakino T. A., Sheinker V. N., Guryanova E. N., Garnovskii A. D., Osipov O., *Zh. Obshch. Khim.* 1976, **46**, 2279.

28. Trofimenko S., *Chem. Rev.* 1993, **93**, 943.

CHAPTER 4

CONCLUSION

The synthesis of four coordinate $(3,5\text{-}Me_2pz)_2NiBr_2$ **(1);** $(3,5\text{-}^tBu_2pz)_2NiBr_2$ **(4)** and six coordinate $(5\text{-}Mepz)_4NiBr_2$ **(2);** $(3,5\text{-}Me_2pz)_2NiBr_2$ **(3)** pyrazole nickel complexes was successfully carried out and the products were isolated in moderate to good yields. These complexes were characterized by a combination of NMR spectroscopy, IR spectroscopy and elemental analysis. Two of the complexes **1** and **2**, were further characterized by single crystal X-ray crystallography. Complex **1** has a distorted tetrahedral geometry and **2** has a distorted octahedral geometry. All these complexes were found to be paramagnetic, as evident by broad peaks on their ^1H NMR spectra. Complexes **2** and **3** are envisaged to have different structures in solid-state and in solution. These complexes have an octahedral geometry in the solid state, which converts to tetrahedral geometry in solution. That explains why their ^1H NMR spectra were found to be broad and indicative of paramagnetic behaviour. Complex **4** was found to be highly unstable when exposed to air for a long period of time. This instability can be attributed to the steric bulk of the tertiarybutyl substituents in the pyrazole ring which crowds the nickel centre.

Another aspect of this study involved the synthesis of new substituted α,ω-bis(3,5-R_2pyrazolyl)alkane-α,ω-dione ligands **(A1, A2, A3** and **A4)**. These ligands were obtained in moderate yields and were fully characterized by standard spectroscopic

techniques (IR and NMR) and elemental analysis. When these ligands were reacted with $(CH_3CN)_2PdCl_2$, hydrolysis of the linker was observed leading to the formation of the unlinked pyrazole palladium complexes. In some cases a mixture of the expected product and the unlinked pyrazole palladium complex was isolated as confirmed by ^1H NMR spectroscopy. After many attempts 1,5-bis(3,5-dimethylpyrazolyl)pentane-1,5-dione palladium chloride complex was isolated and characterized by ^1H NMR. This was achieved after extremely dry solvent conditions were used. When this synthetic approach was applied to other α,ω-bis(3,5-R_2pyrazolyl)alkane-α,ω-dione ligands, such as 1,2-bis(3,5-dimethylpyrazolyl)ethane-1,2-dione, no pure products were obtained. The reason for the resistance of these ligands to form palladium complexes is not clear at this stage.

The polymerization of ethylene was performed successfully using pyrazole nickel complexes **(1, 3)** prepared in Chapter 2, activated with methylaluminoxane (MAO). Complex **3** was found to have high catalytic activity compared to complex **1**. The difference in catalytic activity between these two complexes is due to steric bulk of the substituents. Complex **3** has less bulky substituents than complex **1**, which make the metal centre more accessible to the coordination of ethylene. It was also observed that the activity of these catalysts increases with increasing pressure. This observation is attributed to the fast insertion of ethylene into the metal alkyl bond at elevated pressures. The activities of these pyrazole nickel catalysts were lower compared to the activities obtained using analogous pyrazole palladium catalysts. The reason for the difference in activities between nickel and palladium catalysts is

that nickel catalysts have a tetrahedral geometry and palladium catalysts have square planar geometry which is suitable for easy access of the ethylene to the metal centre. The polymers obtained were characterized by high temperature ^{1}H NMR spectroscopy, high temperature GPC and thermal analysis. There was one peak observed in the ^{1}H NMR spectra of these polymers, which is indicative of a linear polyethylene. The linear character of these polymers was confirmed by DSC (melting point = 130-136 °C) typical of high density polyethylene (HDPE). High molecular weight polymers (between 0.84×10^6 and 3.85×10^6) were obtained with these catalysts. The molecular weights of the polymers isolated were found to decrease with increasing temperature. A sign that the rate of chain termination over chain propagation is high at elevated temperatures. The molecular weights of the polymers obtained at high pressures was low compared to the molecular weights of the polymers obtained at low pressures.

The palladium complex {1-[3,5-bis(1H-3,5-dibutylpyrazolyl-1-ylcarbonyl)benzoyl)]-1H-3,5-dibutylpyrazole}Pd_2Cl_4 prepared by Li and coworkers was also used as a catalyst for ethylene polymerization in this project. This complex was found have a lower activity compared to the analogous complex with two bonded pyrazolyl ligands. The low activity of this catalyst is suspected to be due to the free pyrazolyl moiety in this catalyst, which reacts the aluminium in MAO retarding the activation process. The influence of MAO was investigated for this catalyst, and a ratio of Al:Pd of 3000:1 was found to be an optimal ratio. In general these linked pyrazolyl palladium catalysts are more active than the unlinked ones. This is due to the

electron withdrawing carbonyl group in these ligands, which make the metal centre more electrophilic, resulting in high rate of ethylene insertion and subsequent insertion to the metal alkyl bond.

Future work will include the investigation of the mechanism for the hydrolysis of α,ω-bis(3,5-R_2pyrazolyl)alkane-α,ω-dione ligands on complexation, this entails improving reaction conditions. These ligands will also be reacted with nickel bromide to see if the same hydrolytic behavior will be observed. The pyrazole nickel complexes and pyrazolyl palladium complexes will be used as catalysts for co-polymerization of ethylene with higher olefins. This will also be extended to the co-polymerization of ethylene with polar monomers such as methyl acrylate.